BIOANALYTICAL APPLICATIONS OF MICROFLUIDIC DEVICES

BY

HUAIBIN ZHANG

DISSERTATION

Submitted in partial fulfillment of the requirements
for the degree of Doctor of Philosophy in Chemistry
in the Graduate College of the
University of Illinois at Urbana-Champaign, 2010

Urbana, Illinois

Doctoral Committee:

Professor Ralph G. Nuzzo, Chair
Professor Ryan C. Bailey
Professor Andrew A. Gewirth
Professor Jonathan V. Sweedler

ABSTRACT

The first part of the thesis describes a new patterning technique--microfluidic contact printing--that combines several of the desirable aspects of microcontact printing and microfluidic patterning and addresses some of their important limitations through the integration of a track-etched polycarbonate (PCTE) membrane. Using this technique, biomolecules (e.g., peptides, polysaccharides, and proteins) were printed in high fidelity on a receptor modified polyacrylamide hydrogel substrate. The patterns obtained can be controlled through modifications of channel design and secondary programming via selective membrane wetting. The protocols support the printing of multiple reagents without registration steps and fast recycle times.

The second part describes a non-enzymatic, isothermal method to discriminate single nucleotide polymorphisms (SNPs). SNP discrimination using alkaline dehybridization has long been neglected because the pH range in which thermodynamic discrimination can be done is quite narrow. We found, however, that SNPs can be discriminated by the kinetic differences exhibited in the dehybridization of PM and MM DNA duplexes in an alkaline solution using fluorescence microscopy. We combined this method with multifunctional encoded hydrogel particle array (fabricated by stop-flow lithography) to achieve fast kinetics and high versatility. This approach may serve as an effective alternative to temperature-based method for analyzing unamplified genomic DNA in point-of-care diagnostic.

ACKNOWLEDGEMENT

First and foremost, I would express my upmost gratitude to my advisor, Professor Ralph Nuzzo, for his invaluable guidance, support, and motivation throughout my PhD years. His outstanding scientific intuition, ingenuity, efficiency and effectiveness will continue to have a guiding influence throughout my career. The trust and freedom that Ralph gave me and the high research standard that he held me to at the same time enormously helped me to mature and grow up to be an independent researcher.

I sincerely thank Professor Jonathan Sweedler, who offered me constructive and valuable suggestions that effectively helped conquer some important obstacles throughout the microfluidic contact printing project. I am also grateful to Professor Andrew Gewirth for his career advice and insightful guidance in electrochemistry.

I heartedly appreciate the friendly group dynamics of the Nuzzo group, our close collaboration, and diverse group interaction, all of which have helped me with every aspect of my work and life at the University of Illinois and made the time enjoyable. Most notably, I would express my thanks to William Childs, Svetlana Mitrovski, Matthew Stewart, Rui Dong, Joo Kang, Jennifer Hanson Shepherd, Jimin Yao, Lanfang Li, An-Phone Lee, Mike Motala, Luke Thompson, Audrey Bowen, and Jason Goldman. My special thanks go to Jennifer, Svetlana, and Matthew for their friendly help and moral support in and out of lab.

During my work I have collaborated with many brilliant colleagues for whom I have

great regard. I wish to extend my warmest thanks to all those who have helped me and made this work possible, especially Adam DeConinck and Scott C. Slimmer.

I am grateful to the secretaries in the Chemistry Department and Material Research Laboratory, for assisting me in many different ways. Dawn Somers, Connie Knight, and Theresa Struss deserve special mention.

I also owe my loving thanks to my parents, parents-in-law, and brother for their unconditional support, understanding, and encouragement.

Finally and most importantly, I want to thank my dearest wife and soul mate, Yan, for her support and love. Her understanding, encouragement, sacrifices and devotion were in the end what made this dissertation possible. I am thrilled by the marriage we have forged over the past nine years and the personal growth each of us has made. I really look forward to continuing our growth together for years to come.

Table of Contents

Chapter 1 Introduction

1.1. MICROFLUIDICS

Microfluidics is the science and technology of manipulating small volumes of liquid (< 10^{-6} litres) using submillimeter channels (10^{-6} - 10^{-3} meters).[1] Controlling liquids on this scale offers a number of important advantages and applications. For example, microfluidics has a wide range of applications in analysis, particularly bioanalysis.[2] Biological samples are usually difficult to obtain, challenging to store, potentially hazardous during disposal, typically available only in low concentrations, and complex in nature. Microfluidics involves small channel size, which reduces sample requirements, decreases reagent consumption and minimizes waste. Microfluidic devices are reported to have higher throughput (through parallel operations), lower levels of contamination (using disposable units) and offer better sensitivity (by virtue of having higher concentrations of analytes in smaller volumes) than is the case for traditional bench-top instruments. Microfluidics also offers the promise of near-patient (or point-of-care) diagnostics,[3] which is essential for use in environments with limited resources and infrastructure, such as battlefields and remote areas.[4] In addition, microfluidic technologies have proven to be useful new tools for biological studies and engineering.[2,5-7]

Microfluidics has been closely associated with two terms—miniaturization and biology.

The success of the microelectronics industry established the powerful paradigm of miniaturization. Making basic units (e.g., transistors) smaller allows more units to be integrated into a single chip, which yields higher device performance and lower fabrication costs. The power of miniaturization has been observed in molecular analysis. Microanalytical methods (e.g., high-pressure liquid chromatography and capillary electrophoresis) both improve sensitivity and decrease costs in comparison with its counterparts in traditional analysis (e.g., liquid chromatography and electrophoresis). Microfluidics began as an extension of microanalysis techniques and sought to develop a versatile and complete analytical system. Andrew Manz proposed a new chemical sensing concept around 1990, the micro total analytical system (μTAS), and predicted that this system would provide numerous benefits that included high efficiency, low consumption, faster analysis and parallel operation.[8-9] This concept was further expanded, and was vividly described as 'lab-on-a-chip,' which literally means integrating several laboratory functions (e. g., sample preparation, separation, and analysis) on a single chip. The majority of molecular analysis is performed using liquid forms, and both μTAS and lab-on-a-chip are microfluidic technologies.

The growing interest in biology required the emergence of new analytical methods and research tools such as microfluidics. Genetic information is linked to heritable diseases, susceptibility to disease, and individual responses to medicines. Large amounts of genetic information (> 13 billion nucleotide pairs in human genome) requires high-throughput,

high-sensitivity and low-cost analytical methods. Portable DNA analysis devices are useful for applications such as epidemic disease monitoring and the detection of biological weapons. Microfluidics has been used for DNA analysis since its inception, and has demonstrated its potential. In addition to genomics, the ability to manipulate living cells has also attracted a great deal of attention. Tissue engineering seeks to make use of these capabilities to develop artificial organs to help millions of patients who require organ transplants. Microfluidics offers an unprecedented ability to control cellular microenvironments, guide cellular growth and study the fundamental science of cellular interaction.

The rapid development of microfluidics during the past two decades is reflected in the proliferation of literature on this subject. The International Statistical Institute (ISI) Web of Science database is used to count publications that contain "microfluidics" and closely associated terms (i.e., lab-on-a-chip and μTAS) in their titles and abstracts (Figure 1.1). Between 1990 and 1996, the number of indexed publications on this subject was quite limited (fewer than ten). During this period, microfluidic devices typically involved devices that were fabricated with silicon and glass using traditional microfabrication methods such as photolithography, micromachining, and etching. These fabrication methods require routine access to expensive facilities (e.g., clean rooms) and special equipment, which presents a barrier for general researchers in chemistry and biology seeking to create microfluidic devices. Microfluidics began to experience exponential

growth starting in 1997. The number of annual publications grew to more than 100 in 2000, 1000 in 2004, and close to 3,000 in 2009. One reason for this rapid growth was the development of polymer-based fabrication technique, or soft lithography, a technique which dramatically reduced the barriers to entry in the field of microfluidics.

1.2. SOFT LITHOGRAPHY AND PDMS

Soft lithography consists of a set of polymer-based microfabrication techniques. These techniques were developed by George Whitesides and his coworkers in order to complement photolithography.[10-11] The core concept of soft lithography is the replication of microstructures made by photolithography or other techniques onto a soft polymer stamp, followed by the use of the stamp as a patterning tool or for the purpose of making a channel system. A common method of making an elastic stamp is illustrated in Figure 1.2(a). Pre-polymer solution is cast on a patterned (silicon) master, cured and peeled off. The resulting stamp bears a surface relief structure that is the negative of what is on the master. The microcontact printing technique (Figure 1.2(b)) uses the relief pattern on the stamp to form ink patterns on the surface of substrates by means of contact. Self-assembled monolayers (SAMs)[12] constitutes an excellent ink for this purpose due to its crystalline-like structure and nanometer thickness. The SAMs patterns formed by thiol/thiolate or silane on gold or silicon surface can serve as an etching mask for further patterning. In addition to patterning, the elastic stamp can also seal with other substrates

to form microfluidic channel systems (Figure 1.2(c)). Once a microstructured master has been made using photolithography or other techniques, soft lithography can be used to create numerous polymer replicas quickly and easily in ambient laboratory environments without the use of specialized equipment, which produces a significant decrease in fabrication cost and lowers barriers to enter.

Polydimethylsiloxane (PDMS) is the polymer most commonly used to make microfluidic devices. Several properties of PDMS make it a particularly suitable material for biological applications. PDMS is transparent down to ~ 300 nm and low in background fluorescence, which makes PDMS-based microfluidic devices compatible with optical and fluorescence microscopy. PDMS is inert in water and is biocompatible, which makes it useful for cell studies. Another useful property is that biologically important gases (e.g., O_2, CO_2) can pass PDMS easily, which makes on-chip cell growth possible.

PDMS can form reversible or irreversible bonding with many substrates that are used to make microfluidic devices. Glass, polystyrene, and silicon are widely used in biology, and PDMS can reversibly bond with these materials. The reversible bonding between PDMS and these materials is driven by van der Waals's force, which is strong enough to withstand 5 psi pressure. PDMS can also be used to form irreversible bonding with numerous materials (e.g., clean glass, silicon, and polystyrene) when its surface is

activated by oxygen plasma,[13] UV/Ozone,[14-15] or Corona[16]. These treatments generate -OH groups on the PDMS surface, which can form covalent bonding with other materials. In some cases, PDMS needs to bond with porous membranes (e. g, polycarbonate membrane) in order to make multilayer channels. These hybrid channels are useful for making immunoassays,[17] making gateable nano- or micro-fluidic interconnections,[18-19] and for studying the flux of platelet agonists into flowing blood.[20] Special surface treatments are required for a permanent bonding between PDMS and polymer membranes. Methods such as applying a thin layer of epoxy or PDMS prepolymer glue should be conducted with great care in order to avoid microfluidic channels becoming blocked.[21] A recent study used a home-built initiated chemical vapor deposition instrument to coat PDMS and its bonding substrate with a layer of epoxy nano-adhesive.[22] Another study involved coating polymer membrane with 3-aminopropyltriethoxysilane and claimed that an irreversible bond with PDMA was formed.[23]

1.3. BIOLOGICAL APPLICATIONS OF MICROFLUIDICS

1.3.1. Tools for studying and manipulating cells

Microfluidic technologies provide unprecedented capabilities for controlling microenvironments for the purpose of studying and manipulating cells.[24-28] Channel size

of microfluidics is comparable to the intrinsic dimension of prokaryotic and eukaryotic cells. These cells are sensitive to environmental factors such as topology, substrate stiffness, surface chemistry, soluble gradients, etc.[29-31] Controlling these factors allows cell growth to be manipulated for biomedical applications such as wound healing and the development of artificial organs for transplantation.[32-34]

Microfluidic technologies have proved to be useful for patterning biomolecules.[35] Patterns of molecules in solution, or on the surface, have important effects on *in vivo* forms of cellular behavior such as chemotaxis,[36] axon extension[37-38] and differentiation.[39] Studies of these types of behavior were usually limited by the capabilities for patterning biomolecules. For example, a common Boyden chamber can only generate simple and unstable gradients.[40] Microfluidics can generate complex and stable gradients by taking advantage of a unique characteristic of hydrodynamics found on this scale, meaning laminar flow. Streams of miscible liquids flow side-by-side in microfluidics, and mass transfer between these streams is limited at the interface through diffusion.[5] The liquid-liquid interface, therefore, is usually clearly identified when two streams meet, and becomes a gradient as liquids diffuse into each other. The former (i.e., clear interface) has been used to deliver reagent to sub-cellular regions by placing cells at the interface of two streams.[41] The latter has been used to study chemotaxis, such as how sperm moves towards ovary extracts.[42] More complex gradients have been generated using a microdiluter channel design (Figure 1.3(a)),[43-44] which splits, combines and mixes fluids

several times in order to form a stable gradient that is orthogonal to the flow rate. This setup has been used to guide neuron growth (Figure 1.3(b))[44] and study how neutrophiles move towards interleukin-8 polypeptide.[45] A drawback of this method is that the gradient needs to be maintained by a constant liquid flow, which may exert shear force on living cells and alter their behavior.[46]

Microfluidics patterning has also been used to generate surface gradients. In one study, PDMS stamp is reversibly sealed with substrates (e.g., glass or PDMS) that need to be patterned.[47] Flows of avidin protein and PBS buffer are established in a microdiluter, and a gradient of avidin protein is generated at an outlet. Avidin protein is non-specifically adsorbed on the glass to form a surface-bound gradient.[47] The immobilized gradient avidin can then translated to gradients of other biotinylated biomolecules. Another way to capture soluble gradient is through polymerization.[48] For example, once a gradient of RGDS peptide dissolved in a prepolymer solution is formed in a microfluidic channel, the prepolymer solution is then exposed to UV light to initiate a photo-polymerization. The soluble peptide gradient is immobilized in the resulted hydrogel, which can be used to guide endothelial cell attachment. Another simple method to make surface-bound protein gradient is by taking advantage of depletion effects. When a protein solution fills a microfluidics channel, protein adsorbs to the surface and depleted from the solution.[49] Using this method, a simple microfluidic channel could generate a protein gradient with an intensity ranging from near-saturation to near-zero.

Microcontact printing has been widely used to form surface-bound biomolecules patterns.[50] For example, microcontact printing has been used to pattern a gold substrate with methyl- and tri(ethylene glycol)- terminated SAMs.[51] When the substrate is exposed to a fibronectin solution, the protein adsorbs only to SAMS with hydrophobic tail group (e.g., methyl-). The formed protein pattern is then used to control the attachment of endothelial cells. Microcontact printing has been used to pattern protein ink directly (Figure 1.4).[52] The surface of PDMS is treated by plasma or UV/Ozone to be hydrophilic first. A thin layer of protein solution is applied and carefully dried on the PDMS surface. The coated PDMS stamp could then transfer the protein pattern to other substrates in order to control cell growth.[50] This method has recently been used to pattern hydrogel substrates.[53-54]

1.3.2. DNA analysis

Microfluidics has attracted broad interest given its potential to help in the building of a fully integrated DNA analysis system, which is ideal for point-of-care (POC) diagnostics.[3-4] Microfluidics has demonstrated that it is capable of performing functions that are necessary for a sample-in-answer-out diagnostic device. These functions include cell sorting, cell lysis, DNA extraction and purification, DNA amplification, and DNA detection (e.g., sequencing and genotyping).[55 56 57-58] The DNA detection methods used in these studies usually are miniaturized versions of technologies used in bench-top

instruments. Some of these technologies may not fulfill the unique requirements that are needed for use in point-of-care applications. For example, point-of-care device require greater stringency regarding the stability of reagents due to the lack of air-conditioned storage and operating environments. It is also ideal for POC devices that need to be energy-efficient and versatile in order to decrease the need to carry extra batteries and equipment.

Single Nucleotide Polymorphism (SNP) is a DNA sequence variation that involves a single change in a single nucleotide.[59] SNPs are the most common type of human genetic variation,[60-61] and SNPs have attracted considerable interest as the targets of disease diagnostics,[62-64] as well as for being gene markers.[65-67] SNPs are usually discriminated using either temperature-based or enzyme-based methods. Allele-specific oligonucleotide hybridization (ASOH) is a typical temperature-based method.[59,68] In this method, thermal stability between a perfectly matched and mismatched DNA probe and its target is used to distinguish between the SNP alleles. ASOH requires an intensive assay optimization so that a single stringency condition (e.g., temperature, ion strength) can discriminate among all of the SNPs on the assay. SNPs can be scored easily by taking a fluorescence image after discrimination has been completed. A method called Dynamic allele-specific hybridization (DASH) uses a dynamic heating process and monitors the DNA dehybridization process.[69-70] DASH uses standard reaction conditions, and does not require assay optimization. The scoring of SNPs in this method is not as straightforward

as is the case for ASHO. On the other hand, enzyme-based genotyping methods use polymerases or ligases to discriminate among SNPs.[59] These methods offer high accuracy and specificity, and have become increasingly common in centralized facilities. Enzyme-based methods may not be ideal due to limited shelf-life, expensive reagents and stringent reaction conditions (e.g., 37^{o}C to ensure optimal enzyme activity).

In addition to discrimination methods, assay format is another important consideration for POC devices. Particle-based systems have several advantages over microarray-based systems for POC applications. Microarray is the most commonly used type of assay among bench-top instruments.[67] It is usually made using light-directed chemistry to immobilize sequence specific DNA probes onto a designated location within the parameters of a small chip. Although microarray has very high assay density, hybridization kinetics of planar microarray is generally slow, and requires hours to perform a sample hybridization step. Particle-based systems have higher surface/area ratios and higher kinetics. For example, micrometer-scale beads coated with ssDNA probe have been utilized to capture target ssDNA.[71-73] In these systems, the necessary hybridization time was decreased dramatically—from the period of hours required in the case of a planar surface microarray to as little as a few seconds.[73-75] In addition, particles that are encoded with identification information serve as a flexible assay format for POC applications.[76] Unlike microarray, encoded particle probe-sets can be changed rapidly on the spot to fulfill various types of diagnostic demands. Stop-flow lithography is a

recently-developed method that uses a strategy similar to photolithography to fabricate hydrogel particles.[77] This method combines particle synthesis, encoding and probe incorporation into a single process.

1.4. THESIS OVERVIEW

The purpose of this dissertation is to utilize PDMS-based microfluidic devices on bioanalytical applications, such as cells manipulation and DNA analysis. Chapter 2 describes a high-throughput, reusable printing platform for patterning biomolecular inks on soft material substrates. Hydrogels imprinted with biomolecules, (e.g., proteins, or peptides) have wide application in bioanalytical applications such as diagnostics and studies of cells in culture. Currently used micropatterning techniques, such as microcontact printing and microfluidic patterning, have some important limitations when used on soft substrates. The platform described here draws inspiration from both microcontact printing and microfluidic patterning techniques and extends them further through the utilization of a membrane-based microfluidic device design. A track-etched polycarbonate membrane is used to seal a PDMS microfluidic channel device to form a printer head. Model 'inks'—solutions of biotin-labeled biomolecular targets—are constantly replenished via perfusion of solution through the membrane and captured on a streptavidin-incorporating polyacrylamide hydrogel-coated substrate placed in conformal contact with the print head. Resulting patterns on the hydrogel substrate can be controlled

via channel design and selective membrane wetting. Multiple channel designs are used to pattern three model classes of biomolecules (i.e., peptides, polysaccharides, and proteins), and to demonstrate versatility of this method. Polylysine patterned hydrogel substrates were used to highlight a potential application of this patterning platform, as substrates for directed growth of hippocampal neurons. The short cycle time and reproducibility of this patterning technique are demonstrated in the end of this chapter.

Chapter 3 describes a novel, and often neglected, process—alkaline dehybridization—for DNA analysis. Alkaline solutions (e.g., 1M NaOH) have been widely used to dehybridize genomic DNAs, but alkaline dehybridization has not been reported to be able to discriminate SNPs. An integrated microfluidic (μ-fl) device was used to effect separations that discriminate single nucleotide polymorphisms (SNP) based on kinetic differences in the lability of perfectly matched (PM) and mismatched (MM) DNA duplexes during alkaline dehybridization. For this purpose, a 21-base single-stranded DNA (ssDNA) probe sequence was immobilized on agarose-coated magnetic beads, which in turn can be localized within the channels of a poly(dimethylsiloxane) microfluidic device using an embedded magnetic separator. The PM and MM ssDNA targets were hybridized with the probe to form a mixture of PM and MM DNA duplexes using standard protocols. The hydroxide ions necessary for mediating the dehybridization were generated electrochemically *in-situ* by performing the oxygen reduction reaction (ORR) using O_2 that passively permeates the device at a Pt

working electrode (Pt-WE) embedded within the microfluidic channel system. The alkaline DNA dehybridization process was followed using fluorescence microscopy. The results of this study show that the two duplexes exhibit different kinetics of dehybridization, rate profiles that can be manipulated as a function of both the amount of the hydroxide ions generated and the mass transfer characteristics of their transport within the device. This system is shown to function as a durable platform for effecting hybridization/dehybridization cycles using a non-thermal, electrochemical actuation mechanism, one that may enable new designs for lab-on-a-chip devices used in DNA analysis.

Chapter 4 describes a non-enzymatic, isothermal, versatile, and potentially high-throughput genotyping approach that uses an alkaline discrimination method acting on a multiplexed particle array. The kinetic difference of PM and MM duplexes dehybridization under alkaline conditions is effectively measured by the difference in fluorescence retention ratio, the peak value of which can serve as a simple metric for genotyping. A pH gradient is used to discriminate target DNA sequences with different SNP insertion points over a range of temperatures, reducing optimization requirements. This technique is combined with the use of SFL-fabricated multifunctional encoded hydrogel particles to achieve high versatility. This approach may serve as a new route for analyzing unamplified genomic DNA.

1.5. FIGURES

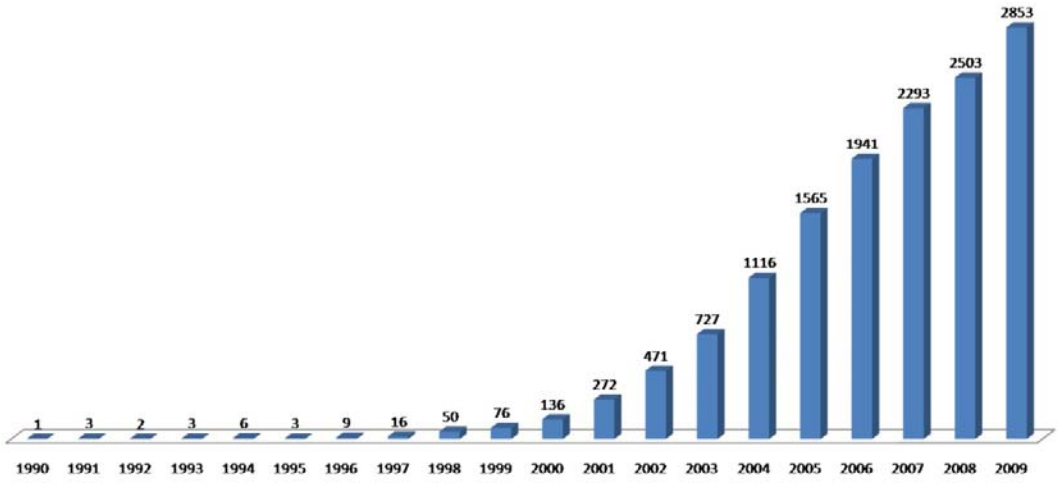

Figure 1.1. Annual publications related to microfluidics across all journals that are indexed by ISI Web of Science Database.

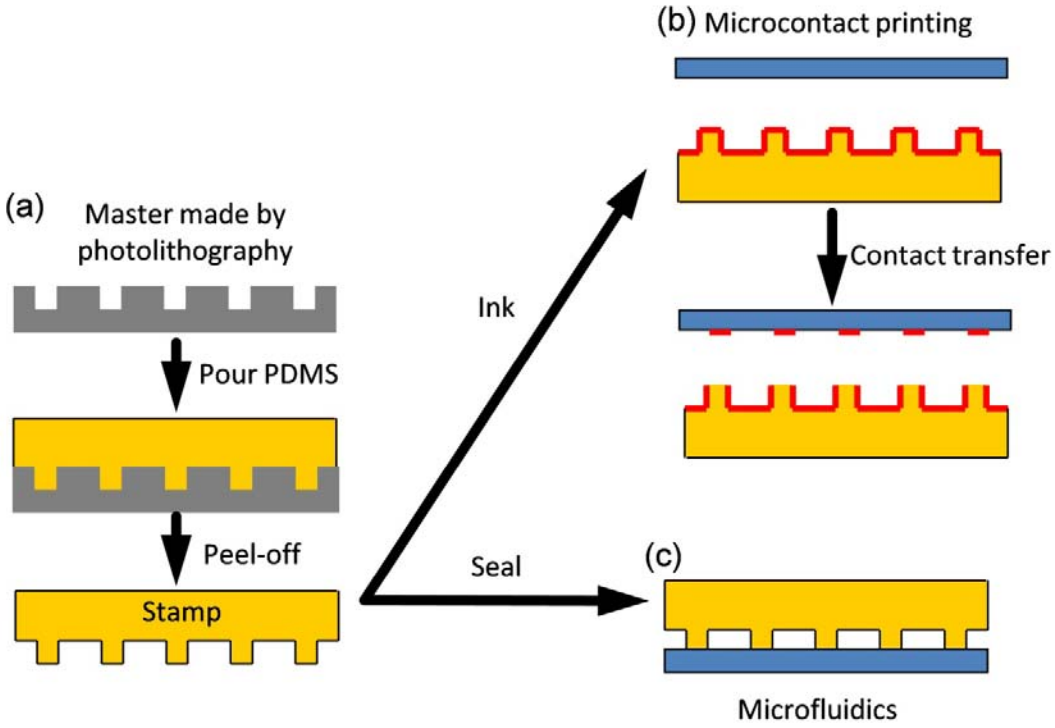

Figure 1.2: A schematic illustrating the fabrication of a PDMS stamp (a), which can be used to pattern molecular 'ink' through Microcontact Printing (b) or sealed with a given substrate to form a microfluidic channel system (c).

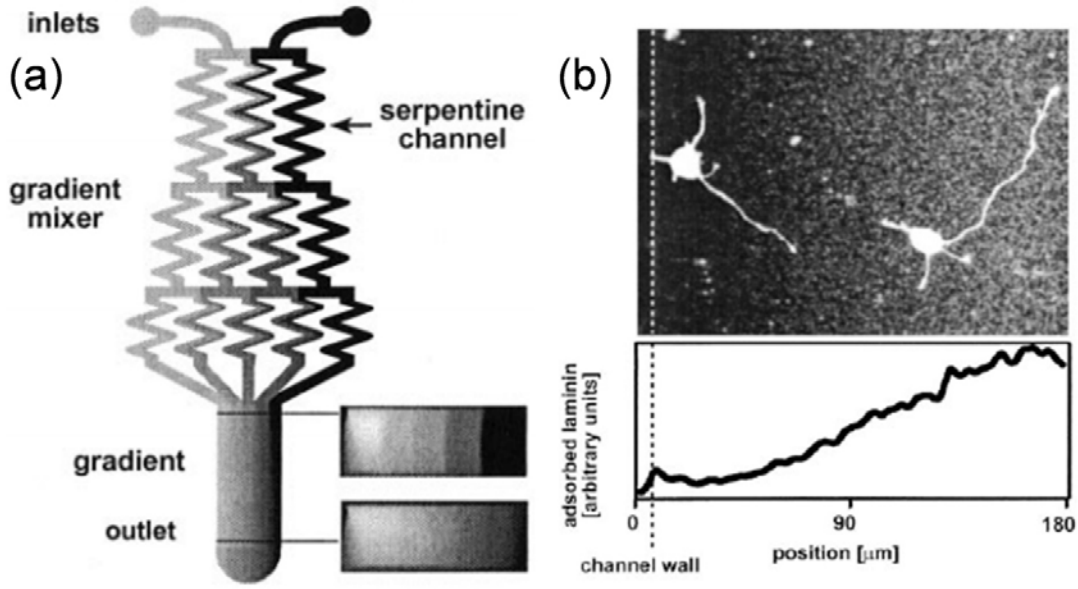

Figure 1.3: (a) A schematic drawing of a microfluidic diluter design that is used for the fabrication of immobilized laminin gradient for guiding Rat hippocampal neuron growth (b). (Reproduced with permission from Dertinger, S. K. W.; Jiang, X.; Li, Z.; Murthy, V. N.; Whitesides, G. M. *Proc. Natl. Acad. Sci. U. S. A.*, **2002**, 99, 12542. Copyright (2002) National Academy of Sciences, U.S.A.)

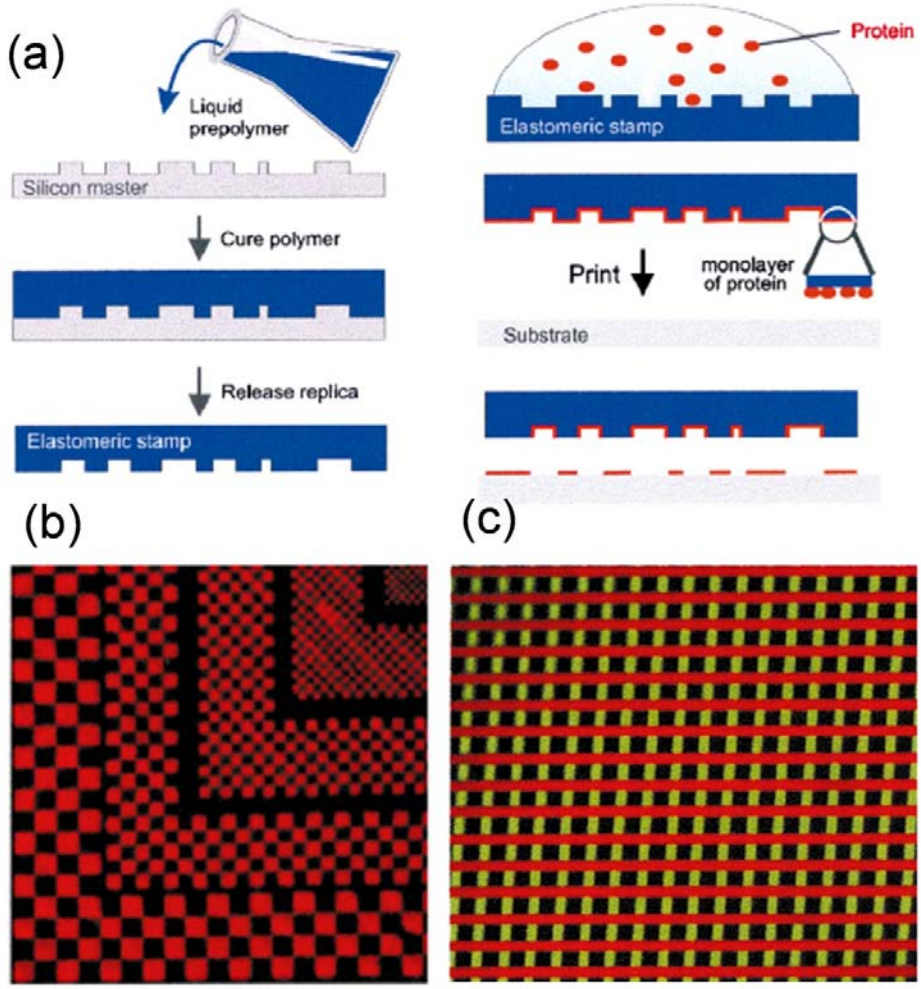

Figure 1.4: (a) Scheme of patterning protein with Microcontact Printing; (b) fluorescence images of rhodamine-labeled antibodies patterned on a glass slide; (c) Three different proteins printed on a glass slide by a flat stamp. (Reproduced with permission from A. Bernard, J. P. Renault, B. Michel, H. R. Bosshard, E. Delamarche, Advanced Material (Weinheim, Ger.), 2000, 12, 1067. Copyright Wiley-VCH Verlag GmbH & Co. KGaA.)

1.6. REFERENCES

(1) Whitesides, G. M. "The origins and the future of microfluidics"; *Nature* **2006**, *442*, 368.

(2) Sia, S. K.; Whitesides, G. M. "Microfluidic devices fabricated in poly(dimethylsiloxane) for biological studies"; *Electrophoresis* **2003**, *24*, 3563.

(3) Sia, S. K.; Kricka, L. J. "Microfluidics and point-of-care testing"; *Lab Chip* **2008**, *8*, 1982.

(4) Yager, P.; Edwards, T.; Fu, E.; Helton, K.; Nelson, K. *et al* "Microfluidic diagnostic technologies for global public health"; *Nature* **2006**, *442*, 412.

(5) Beebe, D. J.; Mensing, G. A.; Walker, G. M. "Physics and applications of microfluidics in biology"; *Annu. Rev. Biomed. Eng.* **2002**, *4*, 261.

(6) Weibel, D. B.; Whitesides, G. M. "Applications of microfluidics in chemical biology"; *Curr. Opin. Chem. Biol.* **2006**, *10*, 584.

(7) Khademhosseini, A.; Langer, R.; Borenstein, J.; Vacanti, J. P. "Microscale technologies for tissue engineering and biology"; *Proc. Natl. Acad. Sci. U. S. A.* **2006**, *103*, 2480.

(8) Manz, A.; Graber, N.; Widmer, H. M. "Miniaturized total chemical analysis systems: A novel concept for chemical sensing"; *Sensor Actua. B-Chem.* **1990**, *1*, 244.

(9) Reyes, D. R.; Iossifidis, D.; Auroux, P.-A.; Manz, A. "Micro Total Analysis Systems. 1. Introduction, Theory, and Technology"; *Anal. Chem.* **2002**, *74*, 2623.

(10) Xia, Y.; Whitesides, G. M. "Soft lithography"; *Angew. Chem. Int. Edit.* **1998**, *37*, 550.

(11) Xia, Y.; whitesides, G. M. "Soft Lithography"; *Annu. Rev. Mater. Sci.* **1998**, *28*, 153.

(12) Bain, C. D.; Troughton, E. B.; Tao, Y. T.; Evall, J.; Whitesides, G. M. *et al* "Formation of monolayer films by the spontaneous assembly of organic thiols from solution onto gold"; *J. Am. Chem. Soc.* **1989**, *111*, 321.

(13) Bhattacharya, S.; Datta, A.; Berg, J. M.; Gangopadhyay, S. "Studies on surface wettability of poly(dimethyl) siloxane (PDMS) and glass under oxygen-plasma treatment and correlation with bond strength"; *J. Microelectromech. S.* **2005**, *14*, 590.

(14) Efimenko, K.; Wallace, W. E.; Genzer, J. "Surface Modification of Sylgard-184 Poly(dimethyl siloxane) Networks by Ultraviolet and Ultraviolet/Ozone Treatment"; *J. Colloid. Interf. Sci.* **2002**, *254*, 306.

(15) Berdichevsky, Y.; Khandurina, J.; Guttman, A.; Lo, Y.-H. "UV/ozone modification of poly(dimethylsiloxane) microfluidic channels"; *Sensor Actua. B-Chem.* **2004**, *97*, 402.

(16) Haubert, K.; Drier, T.; Beebe, D. J. "PDMS bonding by means of a portable, low-cost corona system"; *Lab Chip* **2007**.

(17) Ismagilov, R. F.; Ng, J. M. K.; Kenis, P. J. A.; Whitesides, G. M. "Microfluidic Arrays of Fluid-Fluid Diffusional Contacts as Detection Elements and Combinatorial Tools"; *Anal. Chem.* **2001**, *73*, 5207.

(18) Kuo, T.-C.; M, D.; Cannon, J.; Chen, Y.; Tulock, J. J. *et al* "Gateable Nanofluidic Interconnects for Multilayered Microfluidic Separation Systems"; *Anal. Chem.* **2003**, *75*, 1861.

(19) Kuo, T.-C.; Cannon, J., D.M.; Shannon, M. A.; Sweedler, J. V.; Bohn, P. W. "Hybrid three-dimensional nanofluidic/microfluidic devices using molecular gates"; *Sensor Actuator* **2003**, *102*, 223.

(20) Neeves, K. B.; Diamond, S. L. "A membrane-based microfluidic device for controlling the flux of platelet agonists into flowing blood"; *Lab Chip* **2008**, *8*, 701.

(21) Chueh, B.; Huh, D.; Kyrtsos, C. R.; Houssin, T.; Futai, N. *et al* "Leakage-Free Bonding of Porous Membranes into Layered Microfluidic Array Systems"; *Anal. Chem.* **2007**, *79*, 3504.

(22) Im, S. G.; Bong, K. W.; Lee, C.-H.; Doyle, P. S.; Gleason, K. K. "A conformal nano-adhesive via initiated chemical vapor deposition for microfluidic devices"; *Lab*

Chip **2009**, *9*, 411.

(23) Aran, K.; Sasso, L. A.; Kamdar, N.; Zahn, J. D. "Irreversible, direct bonding of nanoporous polymer membranes to PDMS or glass microdevices"; *Lab Chip* **2010**, *10*, 548.

(24) El-Ali, J.; Sorger, P. K.; Jensen, K. F. "Cells on chips"; *Nature* **2006**, *442*, 403.

(25) Yi, C. Q.; Li, C. W.; Ji, S. L.; Yang, M. S. "Microfluidics technology for manipulation and analysis of biological cells"; *Anal. Chim. Acta* **2006**, *560*, 1.

(26) Shim, J.; Bersano-Begey, T. F.; Zhu, X. Y.; Tkaczyk, A. H.; Linderman, J. J. *et al* "Micro- and nanotechnologies for studying cellular function"; *Curr. Top. Med. Chem.* **2003**, *3*, 687.

(27) Hung, P. J.; Lee, P. J.; Sabounchi, P.; Lin, R.; Lee, L. P. "Continuous perfusion microfluidic cell culture array for high-throughput cell-based assays"; *Biotechnol. Bioeng.* **2005**, *89*, 1.

(28) Pearce, T. M.; Williams, J. C. "Microtechnology: Meet neurobiology"; *Lab Chip* **2006**.

(29) Lim, J. Y.; Donahue, H. J. "Cell Sensing and Response to Micro- and Nanostructured Surfaces Produced by Chemical and Topographic Patterning"; *Tissue Eng.* **2007**, *13*, 1879.

(30) Falconnet, D.; Csucs, G.; Michelle Grandin, H.; Textor, M. "Surface engineering approaches to micropattern surfaces for cell-based assays"; *Biomaterials* **2006**, *27*, 3044.

(31) Discher, D. E.; Janmey, P.; Wang, Y. L. "Tissue cells feel and respond to the stiffness of their substrate"; *Science* **2005**, *310*, 1139.

(32) Whitesides, G. M.; Ostuni, E.; Takayama, S.; Jiang, X.; Ingber, D. E. "Soft Lithography in Biology and Biochemistry"; *Annu. Rev. Biomed. Eng.* **2001**, *3*, 335.

(33) Wang, J.; Ren, L.; Li, L.; Liu, W.; Zhou, J. *et al* "Microfluidics: A new cosset for neurobiology"; *Lab Chip* **2009**, *9*, 644.

(34) Grayson, A. C. R.; Shawgo, R. S.; Johnson, A. M.; Flynn, N. T.; Li, Y. *et al* "A

bioMEMS review: MEMS technology for physiologically integrated devices"; *Proceedings of the IEEE* **2004**, *92*, 6.

(35) Khademhosseini, A.; Langer, R. "Nanobiotechnology: drug delivery and tissue engineering"; *Chem. Eng. Prog.* **2006**, *102*, 38.

(36) Adler, J. "Chemotaxis in bacteria"; *Science* **1966**, *153*, 708.

(37) Baier, H.; Bonhoeffer, F. "Axon Guidance By Gradients Of A Target-Derived Component"; *Science* **1992**, *255*, 472.

(38) Song, H.-J.; Poo, M.-M. "Signal transduction underlying growth cone guidance by diffusible factors"; *Curr. Opin. Neurobiol.* **1999**, *9*, 355.

(39) Engler, A. J.; Sen, S.; Sweeney, H. L.; Discher, D. E. "Matrix Elasticity Directs Stem Cell Lineage Specification"; *Cell* **2006**, *126*, 677.

(40) Boyden, S. "The chemotactic effect of mixtures of antibody and antigen on polymorphonuclear leucocytes"; *J. Exp. Med.* **1962**, *115*, 453.

(41) Takayama, S.; Ostuni, E.; LeDuc, P.; Naruse, K.; Ingber, D. E. *et al* "Laminar flows-Subcellular positioning of small molecules"; *Nature* **2001**, *411*, 1016.

(42) Koyama, S.; Amarie, D.; Soini, H. A.; Novotny, M. V.; Jacobson, S. C. "Chemotaxis Assays of Mouse Sperm on Microfluidic Devices"; *Anal. Chem.* **2006**, *78*, 3354.

(43) Dertinger, S. K. W.; Chiu, D. T.; Jeon, N. L.; Whitesides, G. M. "Generation of Gradients Having Complex Shapes Using Microfluidic Networks"; *Anal. Chem.* **2001**, *73*, 1240.

(44) Dertinger, S. K. W.; Jiang, X.; Li, Z.; Murthy, V. N.; Whitesides, G. M. "Gradients of substrate-bound laminin orient axonal specification of neurons"; *Proc. Natl. Acad. Sci. U. S. A.* **2002**, *99*, 12542.

(45) Jeon, N. L.; Baskaran, H.; Dertinger, S. K. W.; Whitesides, G. M.; Van De Water, L. *et al* "Neutrophil chemotaxis in linear and complex gradients of interleukin-8 formed in a microfabricated device"; *Nat. Biotechnol.* **2002**, *20*, 826.

(46) Hsu, S.; Thakar, R.; Liepmann, D.; Li, S. "Effects of shear stress on endothelial cell haptotaxis on micropatterned surfaces"; *Biochem. Biophys. Res. Commun.* **2005**, *337*, 401.

(47) Jiang, X. Y.; Xu, Q. B.; Dertinger, S. K. W.; Stroock, A. D.; Fu, T. M. *et al* "A general method for patterning gradients of biomolecules on surfaces using microfluidic networks"; *Anal. Chem.* **2005**, *77*, 2338.

(48) Burdick, J. A.; Khademhosseini, A.; Langer, R. "Fabrication of Gradient Hydrogels Using a Microfluidics/Photopolymerization Process"; *Langmuir* **2004**, *20*, 5153.

(49) Fosser, K. A.; Nuzzo, R. G. "Fabrication of Patterned Multicomponent Protein Gradients and Gradient Arrays Using Microfluidic Depletion"; *Anal. Chem.* **2003**, *75*, 5775.

(50) Kane, R. S.; Takayama, S.; Ostuni, E.; Ingber, D. E.; Whitesides, G. M. "Patterning proteins and cells using soft lithography"; *Biomaterials* **1999**, *20*, 2363.

(51) Mrksich, M.; Chen, C. S.; Xia, Y.; Dike, L. E.; Ingber, D. E. *et al* "Controlling cell attachment on contoured surfaces with self-assembled monolayers of alkanethiolates on gold"; *Proc. Natl. Acad. Sci. USA* **1996**, *93*, 10775.

(52) Bernard, A.; Renault, J. P.; Michel, B.; Bosshard, H. R.; Delamarche, E. "Microcontact Printing of Proteins"; *Adv. Mater. (Weinheim, Ger.)* **2000**, *12*, 1067.

(53) Hynd, M. R.; Frampton, J. P.; Dowell-Mesfin, N.; Turner, J. N.; Shain, W. "Directed cell growth on protein-functionalized hydrogel surfaces"; *J. Neurosci. Meth.* **2007**, *162*, 255.

(54) Hynd, M. R.; Frampton, J. P.; Burnham, M.-R.; Martin, D. L.; Dowell-Mesfin, N. M. *et al* "Functionalized hydrogel surfaces for the patterning of multiple biomolecules"; *J. Biomed. Mater. Res., Part A* **2007**, *81A*, 347.

(55) Sun, Y.; Kwok, Y. C. "Polymeric microfluidic system for DNA analysis"; *Anal. Chim. Acta* **2006**, *556*, 80.

(56) Auroux, P. A.; Koc, Y.; de Mello, A.; Manz, A.; Day, P. J. R. "Miniaturised nucleic acid analysis"; *Lab Chip* **2004**, *4*, 534.

(57) Di Carlo, D.; Ionescu-Zanetti, C.; Zhang, Y.; Hung, P.; Lee, L. P. "On-chip cell lysis by local hydroxide generation"; *Lab Chip* **2005**, *5*, 171.

(58) Burns, M. A.; Johnson, B. N.; Brahmasandra, S. N.; Handique, K.; Webster, J. R. *et al* "An integrated nanoliter DNA analysis device"; *Science* **1998**, *282*, 484.

(59) Syvanen, A.-C. "Accessing genetic variation: genotyping single nucleotide polymorphisms"; *Nat. Rev. Genet.* **2001**, *2*, 930.

(60) Sachidanandam, R.; Weissman, D.; Schmidt, S. C.; Kakol, J. M.; Stein, L. D. *et al* "A map of human genome sequence variation containing 1.42 million single nucleotide polymorphisms"; *Nature* **2001**, *409*, 928.

(61) Wang, D. G.; Fan, J.-B.; Siao, C.-J.; Berno, A.; Young, P. *et al* "Large-Scale Identification, Mapping, and Genotyping of Single-Nucleotide Polymorphisms in the Human Genome"; *Science* **1998**, *280*, 1077.

(62) Kruglyak, L. "Prospects for whole-genome linkage disequilibrium mapping of common disease genes"; *Nat. Genet.* **1999**, *22*, 139.

(63) McCarthy, J. J.; Hilfiker, R. "The use of single-nucleotide polymorphism maps in pharmacogenomics"; *Nat. Biotechnol.* **2000**, *18*, 505.

(64) Kassam, S.; Meyer, P.; Corfield, A.; Mikuz, G.; Sergi, C. "Single nucleotide polymorphisms (SNPs): History, biotechnological outlook and practical applications"; *Curr. Pharmacogenomics* **2005**, *3*, 237.

(65) Stoneking, M. "Single nucleotide polymorphisms: From the evolutionary past"; *Nature* **2001**, *409*, 821.

(66) Kruglyak, L. "The use of a genetic map of biallelic markers in linkage studies"; *Nat. Genet.* **1997**, *17*, 21.

(67) Hacia, J. G.; Fan, J. B.; Ryder, O.; Jin, L.; Edgemon, K. *et al* "Determination of ancestral alleles for human single-nucleotide polymorphisms using high-density

oligonucleotide arrays"; *Nat. Genet.* **1999**, *22*, 164.

(68) Stoneking, M.; Hedgecock, D.; Higuchi, R. G.; Vigilant, L.; Erlich, H. A. "Population variation of human MTDNA control region sequences detected by enzymatic amplification and sequence-specific oligonucleotide probes"; *Am. J. Hum. Genet.* **1991**, *48*, 370.

(69) Howell, W. M.; Job, M.; Gyllensten, U.; Brookes, A. J. "Dynamic allele-specific hybridization"; *Nat. Biotechnol.* **1999**, *17*, 87.

(70) Jobs, M.; Howell, W. M.; Stroemqvist, L.; Mayr, T.; Brookes, A. J. "DASH-2: Flexible, low-cost, and high-throughput SNP genotyping by dynamic allele-specific hybridization on membrane arrays"; *Genome Res.* **2003**, *13*, 916.

(71) Verpoorte, E. "Beads and chips: New recipes for analysis"; *Lab Chip* **2003**, *3*, 60N.

(72) Seong, G. H.; Zhan, W.; Crooks, R. M. "Fabrication of microchambers defined by photopolymerized hydrogels and weirs within microfluidic systems: Application to DNA hybridization"; *Anal. Chem.* **2002**, *74*, 3372.

(73) Kim, J.; Heo, J.; Crooks, R. M. "Hybridization of DNA to Bead-Immobilized Probes Confined within a Microfluidic Channel"; *Langmuir* **2006**, *22*, 10130.

(74) Fan, Z. H.; Mangru, S.; Granzow, R.; Heaney, P.; Ho, W. *et al* "Dynamic DNA hybridization on a chip using paramagnetic beads"; *Anal. Chem.* **1999**, *71*, 4851.

(75) Kohara, Y.; Noda, H.; Okano, K.; Kambara, H. "DNA probes on beads arrayed in a capillary, 'Bead-array', exhibited high hybridization performance"; *Nucl. Acids Res.* **2002**, *30*, e87.

(76) Nolan, J. P.; Sklar, L. A. "Suspension array technology: evolution of the flat-array paradigm"; *Trends Biotechnol.* **2002**, *20*, 9.

(77) Pregibon, D. C.; Toner, M.; Doyle, P. S. "Multifunctional Encoded Particles for High-Throughput Biomolecule Analysis"; *Science* **2007**, *315*, 1393.

Chapter 2 Patterning Biomolecules on Hydrogel Substrates Using Microfluidic Contact Printing

Note: The majority of the text comes from Huaibin Zhang, Jennifer N. Hanson Shepherd, and Ralph G. Nuzzo, "Microfluidic Contact Printing: a Versatile Printing Platform for Patterning Biomolecules on Hydrogel Substrates", Soft Matter **2010**, 6, 2238-2245.

The images included in 2.6 and 2.7 were taken by Dr. Jennifer N Hanson Shepherd.

2.1. INTRODUCTION

Methods for patterning biomolecules are of broad utility, with exemplary applications that include diagnostics,[1] chemical sensing,[2] and platforms for studying cellular behaviors.[3-4] The present report addresses this latter interest, highlighting the development of a protocol for patterning soft substrate materials in ways that complement those currently used to pattern hard substrates such as glass, silicon, or plastic. The patterning of the latter hard surfaces for use in biomolecular analysis has been intensively reported in the literature, with notable applications that include their use to direct neuronal growth,[5-7] study synaptogenesis,[8] and improve cellular attachment via modification with cell recognition molecules such as laminin.[9-10] Controlled biomolecular gradients have also been used to study important cellular processes, such as chemotaxis,[11] haptotaxis,[12] angiogenesis,[13] morphogenesis[14] and axon guidance.[15-16] Interest in performing similar cellular studies on soft materials is growing as it is now becoming well understood that substrate modulus can play a significant role in mediating

the morphological and physiological development of cells.[17-18] In this context, soft materials, specifically hydrogels, are more suitable substrates for cellular studies because their mechanical properties can be easily tailored to better mimic *in vivo* conditions.[19-20]

Micropatterning technologies, including microcontact printing (μCP) and microfluidic patterning, are a logical choice for generating patterns and gradients of this type as they allow the manipulation of small volumes of solution with precise control over its temporal and spatial delivery.[4] Microcontact printing, first described by the Whitesides group in the 1990's,[21-22] can be used to create complex but useful patterns of alkanethiol (and alkyl silane) self-assembled monolayers (SAMs) on gold (and glass) surfaces, via a physical 'stamping'-based transfer technique. These SAMs can be used as both a resist and a platform that enables subsequent modification via covalent attachment. Proteins, for example, can be attached to an appropriately patterned SAM either via non-specific adsorption[23] or through specific functionalized end groups on the thiols.[24-25] James *et al.* later modified the technique to make it amenable to and compatible with the direct printing of proteins.[26] In the latter study, hydrophobic polydimethylsiloxane (PDMS) stamps made via replica molding were modified with an oxygen plasma to render them hydrophilic. This modification in turn allowed the direct printing of a positively charged protein (polylysine) over a 4 cm^2 glass substrate. A few recent studies have extended μCP to pattern biomolecules on soft substrates. [27-28] A study conducted by Hynd *et al.* utilized an acrylamide-based hydrogel substrate that was photopolymerized in

the presence of a streptavidin-incorporating monomer. The resulting gel film was capable of binding biotinylated extracellular matrix proteins (ECM) transferred in patterned form via μCP.[27] A following study by the same authors examined cellular responses to these and found a preference for them to adhere in ECM modified regions.[29]

Microfluidic patterning is the most commonly used method to generate fluid-based gradients sustained by laminar flow,[30-32] but has also been used to create surface-bound patterns via adsorption.[9,33-34] In the latter case, a PDMS channel system is reversibly bound via a compliant soft-contact to a hard substrate such as glass or silicon. A solution containing a biomolecular adsorbate (e.g., a protein) is pushed through the channels and bonded to the surface in spatial registration either through specific or non-specific interactions with the substrate. The channel system is then removed from the substrate and the resulting patterned surface, or even the PDMS stamp itself, used for biological studies. Applications made using this approach have been reported in the literature with notable examples including axon guidance,[9,34] haptotaxis,[35] and directed cellular migration.[36]

While powerful, microfluidic patterning and μCP techniques both have important limitations in particular regarding their capacities for efficiently and reproducibly generating multi-component biomolecular gradients or discrete chemical patterns imprinted on soft substrates. It is inherently difficult to use microfluidic methods to

pattern soft materials, for example, due to the complexity involved in promoting close conformal contact with a hydrogel, which is necessary to prevent leakage. Furthermore, the reusability of the microfluidic patterning technique is usually low because the flow is disrupted when the substrate is separated from the channel after each printing step. This disturbance necessitates an extended preparation time and can result in a loss of precious reagents (e.g., a specific protein target for an assay). The limitations of μCP techniques in the latter context lie in the innate difficulty associated with rigorously controlling the amount of material transferred when using a complex macromolecular ink, which is essential for generating gradients of useful species such as proteins.[9,33,37] In addition, when patterning multiple biomolecular inks using μCP, difficult alignment steps are usually required. To address this limitation, Bernard *et al.* combined μCP and microfluidics to enable the printing of multiple biomolecules, without the need for a registration step.[38] In this study, a microfluidic channel was reversibly sealed to a planar PDMS stamp (i.e., a slab without surface relief). Protein solution flowing through the microfluidic channel adsorbed to the surface of the PDMS slab and in this way defined the "inking" areas. This protocol was used to print 16 different proteins to a plastic substrate at the same time. The one drawback of this method, however, is that the stamp is not reusable and does not usefully enable the patterning of soft substrates. There therefore remains a need and opportunity to provide further improvements to these techniques, especially in terms of the scope of both the inks and substrates that can be patterned.

The work described here draws inspiration from both microcontact printing and microfluidic patterning techniques and extends them further through utilization of a membrane-based microfluidic device design.[39] This system, presented schematically in Figure 2.1 (steps I-IV), creates a 'microfluidic contact printing' tool by using microfluidic channels fabricated via typical soft lithography methods[37,40-42] that are irreversibly sealed to a modified polycarbonate track-etched (PCTE) membrane. PCTE membranes have been incorporated into microfluidic devices to make gateable nano- or micro-fluidic interconnects in multilayered separation systems[43-45] and in the fabrication of stacked microfluidic devices used to study the flux of platelet agonists into flowing blood.[46] Previous studies that incorporated PCTE membrane into their devices used adhesives (e.g, epoxy or PDMS prepolymer) to interface the membranes with the PDMS microchannels.[45,47-48] Applying an ultra-thin layer of the adhesives is necessary and challenging because excess glue on the membrane can block membrane pores and, possibly, even neighboring microfluidic channels. The device reported here is fabricated using vapor deposited thin-film adhesion layers that obviate this latter requirement, thus simplifying fabrication.

In this study, the printing tool was used to pattern a single biomolecular ink solution via complex single channel designs; multiple biomolecular ink solutions were also patterned simultaneously using a multi-channel design. The system's capabilities for generating gradients using multiple channel designs also are demonstrated. We

specifically demonstrate capabilities for patterning model biomolecular ink compositions including those based on small chain-length peptides, polysaccharides, and proteins.

2.2. RESULTS AND DISCUSSION

2.2.1. Device design and general observations

The schematic presentation in Figure 2.1 I-IV highlights the process flow used to fabricate the printing device. A significant feature of the design is the durable integration of a PCTE membrane with an open feature microfluidic device to create a flexible, reusable patterning tool. As noted above, this strategy addresses some important limitations of microfluidic patterning and μCP techniques, specifically in regards to patterning soft materials, simultaneous printing of multiple biomolecules, and long cycle time. The integration of the PCTE membrane into a microfluidic device not only facilitates conformal contact with the hydrogel substrates but also shields the laminar flow field from disturbance when the gel-bearing substrate is removed. A single device is therefore able to pattern multiple hydrogel coated slides with a very short cycle time. Despite recent efforts[38] to address registration issues related to μCP, there are at present no reports that describe its use to print biomolecules directly on hydrogels in either a gradient or registered multiple printing-level form. As we show in the data below, specific features of the method described here allow gradients and multiple biomolecular patterns to be printed in a single step.

The printing procedure involves two components of actuation: (a) transudation of a biomolecular 'ink' through a PCTE membrane; and (b) the subsequent capture of this 'ink' by an affinity modified hydrogel. The quantitative aspects of the transferred pattern (feature width, depth, shape, and contour; concentration of imprinted biomolecular ink; gradient profiles; and hierarchy) can be tailored by manipulation of simple mass-transfer responsive system features. For example, the location of the 'ink' supplied can be controlled through combination of the underlying channel design and the use of a secondary selective membrane wetting protocol (see below). The amount of 'ink' supplied also can be dynamically modulated by such factors as the flow rate/backing pressure and contact time between the hydrogel and the device. 'Ink' capture is the result of a competition between diffusive zone spreading within the hydrogel and the kinetics of the coupling reaction, which in the current model involve a non-covalent binding between the biotinylated 'ink' and streptavidin-incorporating gel. The printing resolution, therefore, is directly affected by intrinsic 'ink' characteristics (e.g., the molecular weight or charge distribution) as well as the probe concentration in the hydrogel. These modifiable and controllable system parameters allow a versatile and dynamic patterning capability for soft substrates, as illustrated in the following sections.

2.2.2. Interfacing PCTE membranes with PDMS microchannels

Creating a strong bond between the PCTE membrane and PDMS microchannel support is a critical design requirement for this microfluidic device. To do so (Figure 2.1(a)),

the PCTE membranes are first modified with a thin layer of vapor-deposited titanium (an adhesion layer), followed by silicon dioxide, which substantially improves bonding between the PDMS microchannels and the membrane. This adhesion layer does not cause any obvious deformation of the PCTE membrane (Figure 2.1(b)) but decreases the pore size by approximately 14 nm at these mass coverages (Figure 2.2). We believe that the SiO_2 coating gives the PCTE membrane a glass-like surface, which is able to form strong chemical bonds with PDMS after surface activation using a corona discharge.[49] The latter treatment in fact provides fully irreversible adhesive bonding. [50] We note that interfacing of the channel to the modified membrane is significantly improved when the cast PDMS channels are soft or slightly under-cured (procedure described in the ESI).[51]

The PCTE membrane used was large enough to cover and seal the entire underlying channel system (including the inlet and outlet) to circumvent the possibility of leaking.[44,46,48] To accommodate this design, a syringe needle was inserted through the PDMS sidewall into the inlet reservoir and then sealed to the PDMS using epoxy, as is schematically depicted in Figure 2.1(c). The optical micrograph in Figure 2.1(d) shows the underlying microchannel system of a completed printing device (white areas).

2.2.3. Channel designs and versatile patterning of biomolecular inks

Small chain peptide patterned using single-channel designs.

We used the IKVAV (Ile-Lys-Val-Ala-Val) sequence as a model small chain peptide.

The IKVAV sequence is a small peptide derived from the large glycoprotein laminin, which plays an important role in various cellular processes including migration, differentiation, attachment, and neurite extension.[52-54] It more importantly has been identified as the active recognition site in laminin and used in model form for controlling cellular adhesion and neurite extension.[55] To immobilize this sequence, the IKVAV was modified with biotin on one end for attachment to the streptavidin-incorporating polyacrylamide hydrogel and fluorescein isothiocyanate (FITC) on the other end for visualization purposes.

Examples of two single channel designs and the corresponding peptide patterns transferred to the hydrogel are presented in Figure 2.3. As can be seen from the fluorescence micrographs, IKVAV is easily transferred to the hydrogel substrate in a registry directly corresponding to the underlying channel design. In these images, the concentration of streptavidin in the hydrogel was ~ 50 μg/ml which most likely explains the halo effect seen around the transferred channel edges. When the streptavidin concentration was increased 20 times, however, a pattern that not only had improved resolution, but also smaller features was generated (Figure 2.3(e)) as expected for a reaction-diffusion based capture system.[56] A specific quantitative comparison of the relationship between streptavidin concentration and printing resolution can be found in example presented in Figure 2.4.

It is worth noting that the peptide-patterned hydrogels, when stored at 4°C for several weeks, did not experience significant reduction in fluorescence intensity or diffusive spreading of the bound peptide. This affirms that the stability of the biotin-streptavidin affinity system permits the generation of patterned peptide substrates in advance, a feature we found to be useful in studies of guided cell growth mediated by immobilized peptide sequences.[57] This aspect of the work is discussed below.

Polysaccharides patterned using multi-channel designs.

To further explore the printing capabilities of the system, two multi-channel designs were tested using fluorescein and rhodamine labeled biotinylated dextrans (MW = 10 kDa) as model polysaccharides. Dextran is a hydrophilic polysaccharide that has a high water solubility, is commonly used as both an anterograde and retrograde tracer in neurons,[58] and has been variously used as a drug delivery vehicle.[59] In the results presented in Figure 2.5, fluorescein and rhodamine labeled biotinylated dextrans were injected into each individual channel. The printed pattern is directly related to the underlying channel design, as well as the specific ink moved through the corresponding microchannel. A proven channel design[30] (Figure 2.5(d)) for generating complex gradients (a mixing tree), was incorporated into the system. The two labeled dextrans were injected into the channel system at points where the solutions are split, combined, and mixed, to create co-localized gradients which were then transferred to the hydrogel (Figure 2.5(e)). These data demonstrate that parallel printing of multiple substances can

be accomplished in a single patterning cycle. This provides a useful point of comparison to classical μCP methods, where the patterning of multiple biomolecular inks requires sequential inking and printing steps along with effective means of registration. The printing platform is for this reason one we believe could be useful for creating substrates for use in high-throughput screening methods.

Large-area protein gradients generated using a single-channel design.

A serpentine single-channel gradient generator was used to transfer a FITC and biotin labeled polylsyine (MW = 15-30 kDa) to the hydrogel substrate (Figure 2.6). Polylysine is commonly used to treat substrates for tissue culture to improve cell adhesion and viability, as well as in patterned form to guide neuronal growth on planar substrates.[60-62] A single channel design with an incrementally increasing channel spacing (Figure 2.6(a)) was used to create the printed concentration gradient shown in Figure 2.6(b), one quantitatively analyzed in the data given in Figure 2.6(c). The chemical gradient formed results from both the incremented spacing as well as the pressure drop that occurs as the solution moves farther from the channel inlet.[63] Using a single channel to pattern a single component gradient in this way may be preferred for reasons of ease of implementation over other more complex designs, such as the mixing-tree[30] based device shown in Figure 2.5(d). While the latter is well suited to printing multicomponent gradients, the simpler single channel design serves as a convenient way to create well defined grayscale patterns for chemotactic[64] or haptotactic[65] cell migration assays.

Orthogonal patterning via secondary protein exposure.

A secondary protein exposure does not overwrite the first protein pattern. The patterns are bound stably to the gel substrates via the biotin-streptavidin linkage, which allows a secondary patterning step to be carried out using a different biomolecular ink. This is illustrated by the example shown in the micrograph presented in Figure 2.6(e), which shows an initially printed pattern of FITC-polylysine-biotin. The image presented in Figure 2.6(f) illustrates the results of a secondary exposure, an orthogonal patterning, of rhodamine-Bovine Serum Albumin (BSA)-biotin on the same substrate. As is clearly seen in this latter image, the secondary exposure does not fully overwrite the initial patterning but in fact shows a significant orthogonality in the relative uptake of the BSA. We further quantify this phenomenon showing it in a plot that highlights the blockage (of BSA), Figure 2.7. This capability allows the substrate to be easily modified with a second biotinylated target to provide better control of the surface properties.

Protein patterned gel substrates for neuronal guidance.

Hydrogels patterned with polylysine using the channel design presented in Figure 2.6(d) were used to guide the growth of hippocampal neurons. The neurons can detect and respond in accordance (Figure 2.6(g)) with the underlying polylysine pattern. As illustrated in the contrast enhanced image in Figure 2.6(g), the neuronal processes (red) are seen to follow along the edge of the protein pattern (green), connecting with other cell soma (blue) as they navigate the substrate. The images reveal a general tendency for the

cell soma to attach near the transition boundary of the polylysine domain and propagate dense projections of processes into it. The highlighted phenomenon is similar to the findings presented in previous studies of neuronal guidance on polylysine patterned on hard substrates.[5,60-62] We do find that soft substrates based on polyacrylamide hydrogels are more challenging to use given the substantial cytotoxicity of residual monomer. We are currently developing significantly more biologically compliant gel chemistries that will remove this sensitivity (see below).

2.2.4. Discrete features patterned using selective membrane wetting

A selective membrane wetting method can be used to advantageously extend the patterning of discrete features using the microfluidic contact printing tool. As received or post-modification with Ti/SiO_2, PCTE membranes are hydrophobic so pores in the membrane must be 'wetted' with a low surface tension solvent,[25] such as isopropyl alcohol (IPA), to initiate solution penetration. In the previous sections, the membrane covering the channel system was wet extensively by IPA using a cotton swab (Figure 2.8), which in turn created patterns determined explicitly by the channel design. The 'writing' method described here uses a capillary tube to precisely deliver the IPA wetting agent (Figure 2.9 and Figure 2.10) to distinct membrane regions to create a secondary degree of control on the pattern generation that operates in hierarchy with the channel design (Figure 2.11(a, b)). We found that it is only in these selectively wetted regions where biotinylated solutions transude through the membrane to be captured subsequently by the

streptavidin-incorporating hydrogel (Figure 2.11(c)). The micrograph presented in Figure 2.11(d) shows a 'UIUC' pattern that was 'drawn' on the PCTE membrane-sealed channel system, while Figure 2.11(e) and f show the resulting transudation of a biotinylated FITC solution through these wetted regions along with the corresponding pattern of the FITC-biotin captured in the gel. These exemplary results suggest this method is a versatile way to pattern substrates in the form factor of multiplexed arrays without the requirement for a 3D integrated microfluidic delivery system.

2.2.5. Reusability and reproducibility

The plot in Figure 2.12 illustrates the recycle capability of the system and the pattern transfer reproducibility between consecutively printed gels. The analysis was done using fluorescein-labeled dextran with the channel design shown in Figure 2.1(d). In order to determine an appropriate testing time, the fluorescence intensity and diameter of the transferred patterns in relation to printing time were also investigated and found to increase linearly as the stamping time was incremented from 0.5 to 10 minutes (Figure 2.13). This follows in accordance with a diffusive broadening of the target flux in the gel over time. Based on these data, a 5-minute stamping time was adopted to test the reusability and reproducibility of the printing technique. As seen from the plot given in Figure 2.12, with inset micrographs displaying printing results from the same device at different time points over several days, the intensity of the transferred patterns was essentially constant over multiple printing cycles. These data affirm a broader

capability for the generation of uniformly patterned substrates with short cycle time and useful copy numbers.

2.2.6. Further system modifications

The system reported in this work has significant potential to be modified, whether by altering the channel design, membrane material selection, method of membrane wetting, the incorporated affinity binding system, or hydrogel system used as a receiving substrate. In our continuing work, for example, we are exploring printing platforms that are modified to use binding schemes exploiting complementary strands of ss-DNA as well as antibody/antigen recognition methods. The more important modification, however, centers on new gel chemistries to replace the bench-mark polyacrylamide system used here, ones that will significantly enhance biocompatibility in cell-based studies. We will report on progress in this area shortly. Finally, we would like to stress the challenges related to printing large biomolecules like proteins, which are known to have biofouling issues caused by denaturization and agglomeration. These challenges are closely related to the intrinsic characteristics of the inks, which in turn need to be reflected in the optimization of system parameters like membrane selection, modification of the pore surface chemistry, sample preparation, and flow rate control.

2.3. CONCLUSION

Microfluidic contact printing, a new patterning technique described here, combines

several of the desirable aspects of μCP and microfluidic patterning techniques, and addresses some of their important limitations through the integration of a PCTE membrane. Using this technique, biomolecules (e.g., peptides, polysaccharides, and proteins) were printed in high fidelity on a receptor modified polyacrylamide hydrogel substrate. The transferred pattern is primarily dictated by the design rules of the underlying microfluidic channel system, coupled with diffusive zone spreading. The application of a selective membrane wetting protocol, allows a versatile secondary patterning capability. The protocols support the printing of multiple reagents without registration steps and fast recycle times.

2.4. EXPERIMENTAL

2.4.1. Fabrication

Device fabrication

Polyvinylpyrrolidone (PVP) or PVP-free (PVPF) PCTE membranes (0.22 μm pore, GE Osmonics Labstore, Minnetonka, MN) were carefully placed in conformal contact with 1 mm thick PDMS slabs, which act as sacrificial support layers during surface modification. Care was taken to minimize scratches and deformation on the membranes throughout every step of the modification procedure, as small scratches detrimentally affect future patterning attempts. A 50 Å adhesion layer of titanium, followed by 100 Å of SiO_2 were evaporated onto the surface of the membranes, at a rate of approximately

0.1 Å/s to provide a uniform surface coverage (Temescal FC-1800 electron beam evaporator). This coverage, given the ballistic nature of the deposition method, is not conformal to the high aspect ratio pore interiors, which remain hydrophobic. Scanning electron microscopy (JEOL 6060LV General Purpose SEM, Tokyo, Japan) was used to image the membrane before and after deposition. Membrane pore sizes were measured using Image Pro Express (Media Cybernetics, Inc., Bethesda, MD) and analyzed by Microsoft Excel (Figure 2.2).

Silicon masters were generated using the following standard photolithography techniques.[66-67] Silicon wafers were scored into desired sizes, cleaned with piranha solution, rinsed with deionized water (Milli-Q, Millipore, Billerica, MA) and then blown dry with nitrogen. SU8-50 (MicroChem Corp., Newton, MA) was spun-coated onto the wafer pieces at 2900 rpm, with a ramping of 100 rpm/sec, for 30 seconds. The wafers were pre-baked for 5 minutes at 120 ºC and patterned by exposing to UV (MJB3 Mask Aligner, Suss Microtech, Garching, Germany) for 45 seconds. Exposed wafers were then post-baked for 5 minutes at 120 ºC and cooled, before being developed with SU8 developer (Microchem Corp.). All patterned wafers were treated with tridecafluoro-1,1,2,2-tetrahydrooctyl trichlorosilane (Sigma Aldrich, St. Louis, MO) for two hours in a dessicator under vacuum, to prevent adhesion of PDMS to the fabricated masters.

The silicon master was covered with degassed PDMS (10:1 ratio, Sylgard® 184).

Samples were heated at 70 ºC until PDMS was softly cured (~20 minutes), which significantly improves irreversible interfacing between the PDMS microchannels and supporting substrate. In the fabrication process described here, the PDMS is cured long enough to be removed from the master, but can still be deformed when gently manipulated with a tweezers (i.e. a small indent on the surface can be seen versus fully cured PDMS, which cannot be deformed in such a manner). To quantitatively characterize the experimental condition of the soft-cure, the curing ratio first proposed by Go and Shoji was used.[51] The curing ratio, R, is defined as $R= t_s/t_f$, where t_s is the soft cure time and t_f is the full cure time. The full cure time, in minutes, can be calculated based on the experimental equation $\log10(t_f)= 3.4710 - 0.0158T_s$, where T_s is the soft cure temperature in degrees Celsius. For this system, samples were cured for 22 minutes at 70 °C, which gives a curing ratio, R, of 0.1. It should be noted that the soft cure time depends on the amount of PDMS being cured, so longer soft cure times may be required for larger samples.

The softly cured PDMS mold replicas were removed from the masters, and holes were punched at the channel inlets and outlets using biopsy punches. The backside (or unpatterned side) of the PDMS stamp and a microscope slide were permanently bonded together, after both surfaces were treated by Corona discharge (BD-20AC with power line filter, Electro-Mechanics, Ravenswood, IL, starting voltage 45 KV) for 40 seconds.[49] The previously Ti/SiO_2 modified PCTE membranes were exposed for 2 minutes to

Corona discharge, while the open PDMS channels (previously attached to the supporting glass microscope slide) were exposed to Corona discharge for 40 seconds. The two activated components were carefully placed into contact and then placed in a 70 ºC oven to cure for at least one hour. Once curing was complete, a syringe needle (26 gauge) that had been removed from its plastic housing, was inserted into the inlet hole (from the sidewall of the device) and sealed with 5-minute epoxy. The device was then placed in 70 ºC oven for at least one hour to ensure that the epoxy was fully cured.

Hydrogel preparation

Microscope slides were cut into 25 mm x 10 mm pieces to serve as supports for the hydrogel substrates. The glass pieces were cleaned with piranha solution for 20 minutes, rinsed with Milli-Q water and dried with nitrogen. To promote adhesion between the cleaned glass slides and the hydrogel substrate, each slide was treated with 100 µl of 3-(trimethoxysilyl)-propyl acrylate : glacial acetic acid: H_2O (1:2:2, v/v) for 1hr and then rinsed with water and then ethanol.[29] The silane treated glass slides were generally used within a few days.

Prepolymer solution was prepared containing 10% acrylamide, 0.26% N,N-methylene-bis-acrylamid (Bis) and 0.05% N,N,N',N'-Tetramethylethylenediamine (TEMED). A 5mg/ml solution of Streptavidin acrylamide (Invitrogen, Carlsbad, CA) in PBS was added to the prepolymer solution in a 1:100 ratio for regular patterning experiments or in

a 1:5 ratio for biological studies and small feature size/high resolution patterning. A 10 wt % aqueous solution of ammonium peroxydisulfate initiator was added in a 1:50 ratio. The pre-polymer solution was quickly distributed to the previously silane-treated glass slides, which were placed on a PDMS slab to prevent liquid overflow. The pre-polymer solution was covered by a glass microscope slide, with one or three #1 coverslips used as spacers, to allow for full gelation. As prepared, the hydrogel slabs were approximately 50 μm thick (one coverslip as a spacer) or 150 μm thick (three coverslips as a spacer). Thicker gels were used for general patterning experiments, while thinner gels were used for cell culture studies. Once gelation was complete, typically 20 minutes, the glass supported gels were removed from the PDMS slab, separated from the microscope slides and stored at 4 ^{o}C in deionized water until needed.

Membrane wetting

As received and following surface modification, the PCTE membranes are hydrophobic so must be exposed to IPA to allow solution to penetrate through the pores. The microfluidic contact printing device was for this reason exposed to solvent in two ways. In the first method, a cotton swab soaked in IPA was used to wet channel regions where solution perfusion was desired (Figure 2.8) and then was immediately submerged in water to prevent solvent evaporation. This technique was most commonly used to wet devices used in patterning experiments. We note that, when using this wetting technique, the best printing results were attained using PVP modified membranes.

In the second method, a 'pen' was created to 'write' solvent in discrete places across the channel system covered by the PCTE membrane. As highlighted in Figure 2.9, the 'pen' in this setup was made by connecting fused silica capillary tubing (D_{inner} = 50 μm, D_{outer} = 150 μm, Polymicro Technologies, Phoenix, AZ) to a syringe (1 ml Norm-Ject® Luer syringes, Henke Sass Wolf, Germany) loaded into a syringe pump (PHD 2000 programmable pump, Harvard Apparatus, Holliston, Massachusetts) using polyethylene tubing (PE-20, Intramedic Clay Adams® Brand, Diagnostic Systems, Sparks, MD). The capillary tubing was housed inside an empty Sharpie marker (Sharpie®, Oak Brook, IL) shaft to facilitate handling. Prior to use, the syringe was filled with isopropyl alcohol (IPA), which served as the 'ink'. A PDMS channel device, fabricated as described above, was submerged in a petri dish of deionized water. Submerging the device in water while 'writing' allows for a greater working time to pattern the device, as the 'ink' will quickly evaporate when exposed to air. The submerged device was placed on a sample stage that can be precisely controlled laterally and vertically. A stereoscope (SZX7, Olympus, Melville, NY) mounted on an articulating arm boom stand was used to observe the writing process. Before the writing process, the syringe pump was set to 1 μl/min, while flow was allowed to stabilize. The stage was slowly brought up until the water covered the tip of the capillary tubing. At this point, the stereoscope was used to observe the progress of IPA through the 'pen' tip. When the IPA reached a steady perfusion state through the tip, a change in the refractive index between the IPA and the water can be observed. At this time, the dish was slowly brought up further, until an

interface formed between the surface of the device and tip. It is important that the capillary tip not touch the top of device, as it will tear and/or deform the membrane as it rasters along the surface. Once the interface has formed, the desired pattern can be written on the PDMS device, by carefully moving the stage in the x- and y-directions. After drawing is complete, devices are submerged in deionized water. A sequence of images that demonstrates this process can be seen in Figure 2.10.

Prior to use, and after being 'wet' with IPA, the microfluidic devices were degassed for at least 20 minutes in a vacuum oven, submerged in deionized water, using the channel outgas technique (COT) described previously.[68] After degassing, devices were stored submerged in deionized water until needed.

2.4.2. Patterning and imaging

Peptide patterning.

Biotin-Ile.Lys.Val.Ala.Val. Lys (FITC)-NH_2 (Biotin-IKVAV-FITC) was synthesized by the Biotechnology Center at the University of Illinois at Urbana-Champaign. A 100 μM stock solution of this peptide was prepared using Milli-Q water and stored at 4 °C until needed. The peptide solution was loaded into a syringe, connected to a single-channel microfluidic device via PE-20 polyethylene tubing, and then loaded into a syringe pump (1 μl/min, Harvard Apparatus, Holliston, MA). To prevent solvent evaporation, a drop of water was placed on the membrane and covered with a cover slip. The progression of

the fluorescently labeled peptide through the microchannel system was tracked using a fluorescence microscope (Epifluorescent Microscope Olympus, AX-70 with a CCD camera Optronic MagnaFire, Melville, NY). Once flow of the labeled peptide could be observed through the wetted channel regions (typically 5-10 minutes), the coverslip was removed, the membrane surface was rinsed briefly with water and then blotted dry. A streptavidin-incorporating hydrogel was placed on the channel system, after excess water was removed, and held in place with a small weight to ensure conformal contact. Care should be taken to avoid trapping air at the interface as this will detract from successful patterning. Peptide pattern transfer was typically complete after 2.5 minutes. Once the patterning was complete, the gel was removed from the device, rinsed with deionized water and then imaged via fluorescent microscopy. All fluorescent images were background corrected using the method described in the ESI.

Dextran patterning.

Biotinylated dextran (MW = 10 kDa) labeled with either a tetramethylrhodamine (mini-ruby) or fluorescein (mini-emerald) (Invitrogen) were used. A 20 μM stock solution of each labeled dextran was prepared using Milli-Q water and stored at room temperature until needed. The dextran solutions were interfaced with the microfluidic devices and visualized in the same way as described previously for the peptide solution.

Contact times of ~ 5 minutes typically gave high fidelity pattern transfer. Individual

images of the mini-ruby and mini-emerald components of the patternwere captured using appropriate filter sets and then combined using Adobe PhotoShop (Adobe, San Jose, CA).

Protein patterning

Biotin-polylysine (MW = 15-30 kDa) was purchased from Nanocs (New York, NY) and labeled with FITC using the EZ-Label Fluorescein Isothiocynate Protein Labeling Kit (Pierce Biotechnology, Rockford, IL) according to the included instructions. Typical dialysis methods were used to remove the excess FITC reagent. Biotinylated Bovine Serum Albumin (BSA) was purchased from Pierce Biotechnology and functionalized with NHS-rhodamine (Pierce Biotechnology) as per the included instructions. Once the labeling was complete and the excess dye had been removed, the protein solutions were stored at 4 ºC until needed.

Polylysine solution, 2 mg/ml in Milli-Q water, was prepared and then degassed in a vacuum oven. After the solution had been degassed, it was interfaced with the microfluidic device in the same way as described above. For these patterning attempts, the flow rate was set to either 0.5 or 1 µl/min depending on the channel design. It was found that higher flow rates were better for creating gradients as the printed pattern resolution decreased with an increasing flow rate. For printing discrete features, lower flow rates are desirable (less than or equal to 0.5 µl/min). Printing protein patterns typically require longer contact time (15-30 minutes) depending on channel design.

Patterned gels were stored in PBS buffer overnight at 37 ºC to remove any unbound protein and then transferred to 4 ºC for further storage.

For the secondary patterning of BSA, approximately 100 µl of rhodamine and biotin labeled BSA (1mg/ml in Milli-Q water) was placed on top of the polylysine patterned gel and allowed to adsorb for 1 hour. The gel slab was rinsed with deionized water, placed in fresh deionized water at 37 ºC for several hours and then imaged.

Hippocampal neuron culture and imaging

Primary hippocampal neurons were used to highlight a potential application for patterned gels created using this platform—guided cell growth. The cell plating procedure and immunocytochemistry protocol used are similar to those published previously.[69]

Prior to use in culture, patterned polylysine gel slabs were sterilized by exposure to 0.1% Gentamicin (Invitrogen) PBS solution for 2 hours [29] before being transferred to a petri dish of fresh sterile PBS, where they were stored overnight at 4 ºC.

The cell plating procedure used is similar to one published previously.[69] Hippocampal neurons were isolated from post-natal day one (P1) Long-Evans rats. All experiments were conducted under protocols approved by the UIUC Institutional Animal

Care and Use Committee of the Vice Chancellor for Research, and under continuous supervision of the campus veterinarian staff. The gels were plated at an initial density of approximately 150 cells/mm^2. Neuronal samples were maintained in a humidified environment at 37 ºC with 5% CO_2 and supplemented with Neurobasal media twice weekly for one week.

After 7 days in culture, neuronal samples were prepared for fluorescent imaging using the same method presented previously.[69] Samples were treated with DAPI (Invitrogen) to stain the DNA in the nucleus blue, while rhodamine-phalloidin (Invitrogen) was used to stain the actin in the cytoskeleton red. All fluorescent microscopy was carried out using a Zeiss Axiovert 200M inverted research-grade microscope. A Dapi/Hoechts/AMCA filter (Chroma Technology, Rockingham, VT) was used for the DAPI imaging, a Special Yellow Rhodamine/Cy3/Texas Red filter (Chroma Technology) was used for the rhodamine imaging, and a Piston/GFP filter (Chroma Technology) was used to image the fluorescein.

Image background correction

All images used, either in the text or for image analysis, were background corrected in the following manner, modified from method described by Model *et al*.[70] A standard slide was created by placing 0.1 mM fluorescein solution between a coverslip and a microscope slide, which was subsequently imaged using fluorescence microscopy.

These images could then be used to highlight fluorescent intensity heterogeneity related to the microscope and camera. Matlab (The MathWorks, Natick, MA) was used to background correct the raw images. Using this software, RGB images were first converted to gray scale and then each was divided by an image of the reference; corrected images were then outputted with false coloring.

2.4.3. System characterization

Testing the device reusability and pattern reproducibility

The reusability of the device was demonstrated by patterning gels using the same device at different time points over several days. The device, in this case, was based on serpentine channel (width = 50 μm) that connected nine dots (diameter = 350 μm), forming a 3x3 array as shown in Figure 2.1(d). Fluorescein labeled biotinylated dextran (i.e., mini-emerald) was injected at 1 μl/min and the stamping time between the hydrogel and the device was held constant at 5 minutes. Using the same device, 11 patterned gels were created. The first 5 gels were printed on day 1, while the following 6 were printed three days later (day 4). In between printing cycles on day 1 and 4, the device was stored at 4 ºC in deionized water. Patterned gels were imaged, background corrected, and analyzed using Image Pro Express. For each image, the pixels in nine representative areas, corresponding to the nine dots patterned directly from the underlying channel design, were sampled. The mean intensity of pixels within each circular area was measured to represent the area intensity.

Typically, in a microfluidic channel, there is a drop in pressure as the distance from the channel inlet increases.[63] Thus, it might be expected that the intensity of a transferred pattern would be directly related to the underlying location in the microchannel. In an effort to address this phenomenon, the nine circular areas were analyzed separately by grouping corresponding areas of the 11 consecutively printed patterns together (so there were 9 groups in total). For each group, the mean intensity of the 11 circular areas was determined to attain a normalization factor. This factor was then used to generate a normalized mean intensity for the corresponding area of the pattern. The plot given in Figure 2.12 gives the normalized mean intensity for each of the 9 regions of the pattern; standard deviation of the intensity for each region was used to generate error bars.

Testing the time dependence relationship on transferred pattern intensity and size

The printed pattern fidelity, in terms of diameter in comparison to the original channel design, was investigated using the channel design (Figure 2.1(d)) and setup described in the pattern transfer reproducibility/device reusability section. In this analysis, the only parameter that was changed was the stamping time which ranged from 0.5 to 10 minutes. Specifically, the relationship between printing time and pattern intensity and diameter were considered. The AOI (Area of Interest) function was used to fit the 9 transferred dots. The normalization factor that was generated for the pattern reproducibility study (overall mean intensity for dots 1-9 printed at 5 minutes) was used as a baseline. The

5-minute overall intensity was used as a baseline, as this time was most often used for dextran patterning. The individual mean intensity for each dot was divided by this normalization factor, to allow for strict comparison between time and intensity. Using this ratio, the percent change from the baseline or the most typically used printing parameters can be visualized. This data is presented in Figure 2.13, with error bars representing the standard deviation. As shown by the highlighted plot, the intensity of the transferred pattern increases linearly with stamping time.

The dependence of time on the size of the resulting patterns (in relation to the original channel design) was investigated similarly. The AOI function was used to determine the area in pixels of each of the 9 dots. An optical image of the original channel design was loaded into Image Pro, the actual radius determined (~35 pixels) which was used to determine the area. The determined area was subsequently used as a normalization factor. Each individually measured area was divided by the normalization factor, to get a ratio of the actual dot size in relation to the transferred dot. These data are plotted in Figure 2.13, with error bars representing the standard deviation. We found that the diameter of the printed circles increased linearly with printing ranging from 0.5 to 10 minutes. For example, the diameter of the 10 minute transfer is almost twice as large as that of 5 minute transfer. The size of the transferred pattern depends on the diffusion kinetics of the dextran inside the gel, the capture efficiency of the streptavidin for the biotinylated dextran, as well as the size and conformation of the dextran itself.

2.5. ACKNOWLEDGEMENTS

This work was supported by the Wm. Keck Foundation and the National Science Foundation (grant CHE0704153). We used facilities of the Center for Microanalysis of Materials at UIUC supported by the U. S. Department of Energy, Division of Materials Sciences under Award No. DE-FG02-07ER46471. We would like to thank Karen Weis for her invaluable advice and guidance in regards to cell culture and Jon Ekman, Imaging Technology Group, UIUC, for his help with cell imaging.

2.6. FIGURES

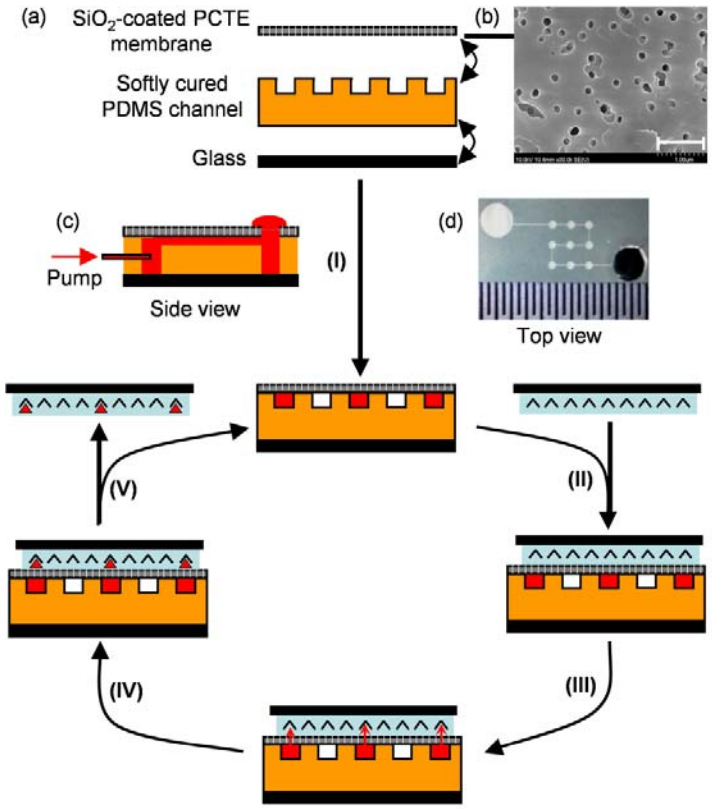

Figure 2.1: Device fabrication (I) and printing process flow (II-V) are schematically represented in (a). The polyacrylamide gel (with incorporated streptavidin) is placed on top of the sealed microchannels (II) where the biotinylated biomolecule solution can diffuse through the PCTE membrane into the gel (III) and be captured by the streptavidin protein (IV), to form long term gradients/patterns (V). The pore morphology after Ti/SiO_2 deposition is shown in the SEM image in (b). A schematic representation of the side view of the device is presented in (c), while the top view of a completed device is shown in the brightfield image in (d). Scale bar in (b) is 1 μm and the smallest ruler mark in (d) is 500 μm.

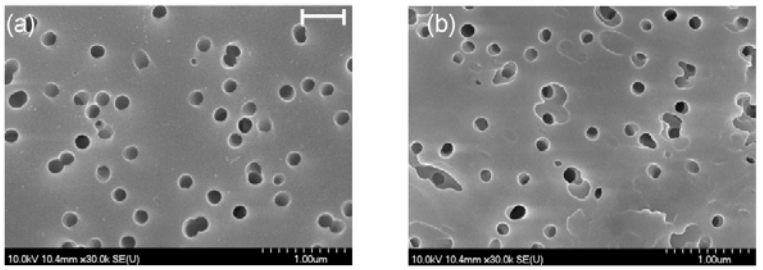

Statistic	Before Deposition	After Deposition
Min. diameter (nm)	76	96
Max. diameter (nm)	196	194
Mean diameter(nm)	154	140
Standard Deviation	13	11
Sample size	40	47

Figure 2.2: SEM micrographs of track-etched polycarbonate membrane before (a) and after (b) Ti/SiO_2 deposition. The table presents statistical information of the pore size analysis. The average diameter of the pore decreased about 14 nm after Ti/SiO_2 deposition. Scale bar is 500 nm.

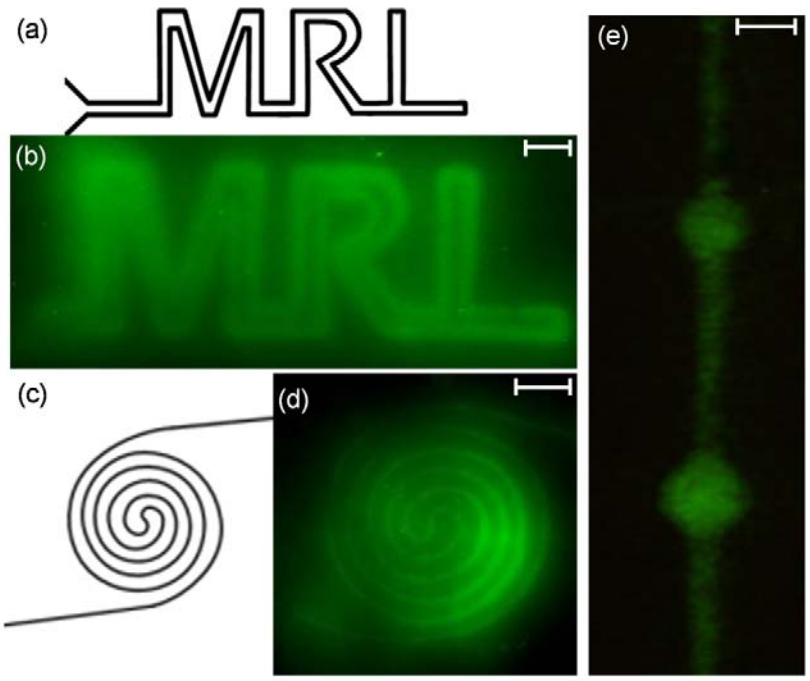

Figure 2.3: Patterning results for the IKVAV peptide for different channel designs (width = 50 μm) are shown in (a) and (c). The original channel design can be directly transferred to the gel (b), (d). In (e) two 75 μm diameter dots, on a 20 μm wide channel, were transferred to the gel to highlight printing resolution capabilities. Scale bar is 250 μm in (b), 500 μm in (d) and 50 μm in (e).

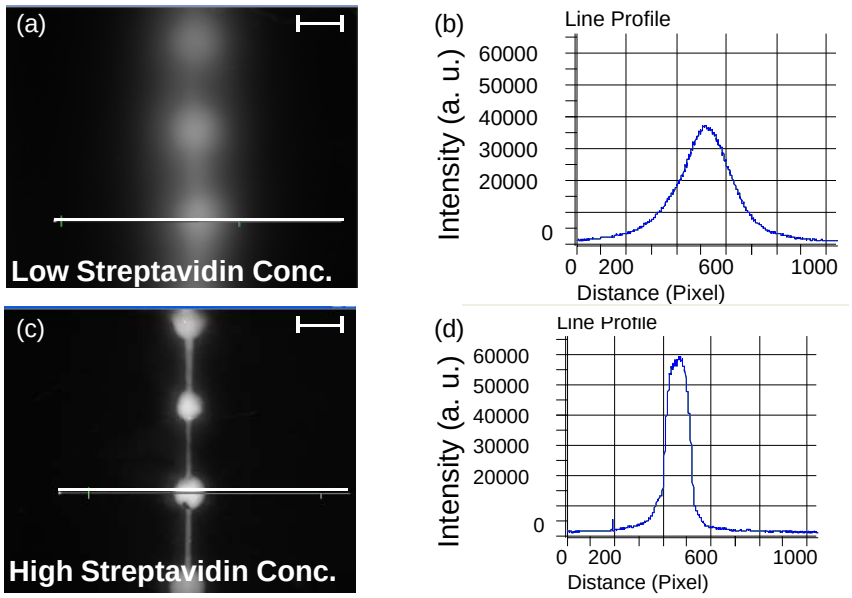

Figure 2.4: Initial printing results for biotin-polylysine-FITC on polyacrylamide hydrogels. Hydrogels in (a) and (c) were made with prepolymer solution containing 50 μg/ml and 1mg/ml streptavidin acrylamide, respectively. Line scans in (b), (d) highlight differences in pattern resolution related to streptavidin concentration. Scale bars are 500 μm.

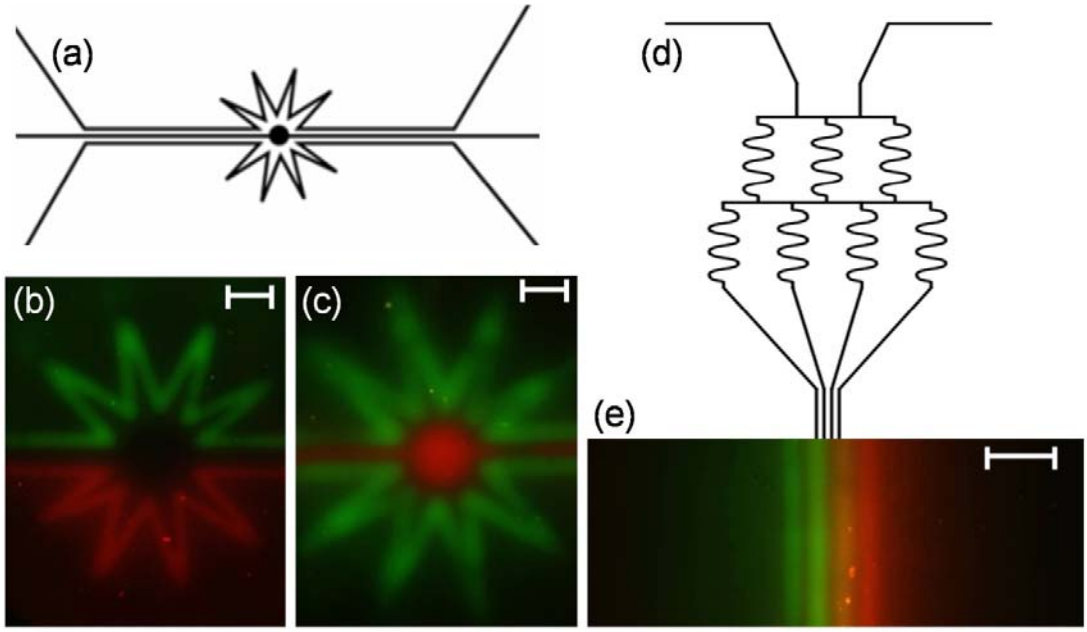

Figure 2.5: Patterning results for the fluorescein and rhodamine labeled dextran solutions for the multi-channel designs highlighted in (a) and (d). The fluorescent micrographs in (b) and (c) show that multiple biomolecules can be patterned onto the gel in one printing attempt, directly related to the underlying channel design. The complex mixing scheme in (d) can be used to create gradients of biomolecules like the one pictured in (e). Scale bars are 500 μm.

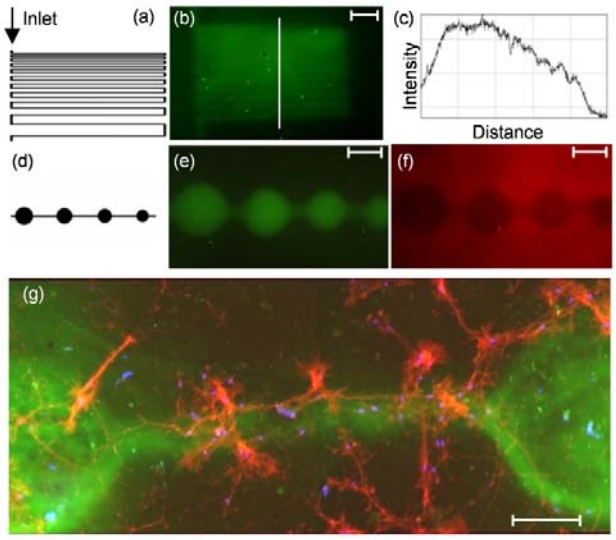

Figure 2.6: Patterning results for the direct printing of FITC-labeled polylysine and indirect patterning of rhodamine labeled BSA. The channel design shown in (a) can be used to create gradients of biomolecules using a simple single channel design, which has a fixed channel width (50 μm) and range of spacing between loops from 40 to 160 μm. The transferred gradient shown in (b) is quantitatively represented by the line scan across the sample, presented in (c). The single channel design in (d) was used to create a pattern of fluorescently labeled polylysine (e) and then the substrate was exposed to a secondary patterning of rhodamine labeled BSA (f); the secondary patterning does not 'overwrite' the first. Finally, the response of primary hippocampal neurons to polylysine patterns created with the channel design in (d) is presented in (g). In this image, the biotin-polylysine-FITC pattern appears green, while the cell nuclei (stained with DAPI) appear blue and the cell processes (stained with rhodamine-phalloidin) appear red. Scale bars are 500 μm in (b), (e) and (f), and 100 μm in (g).

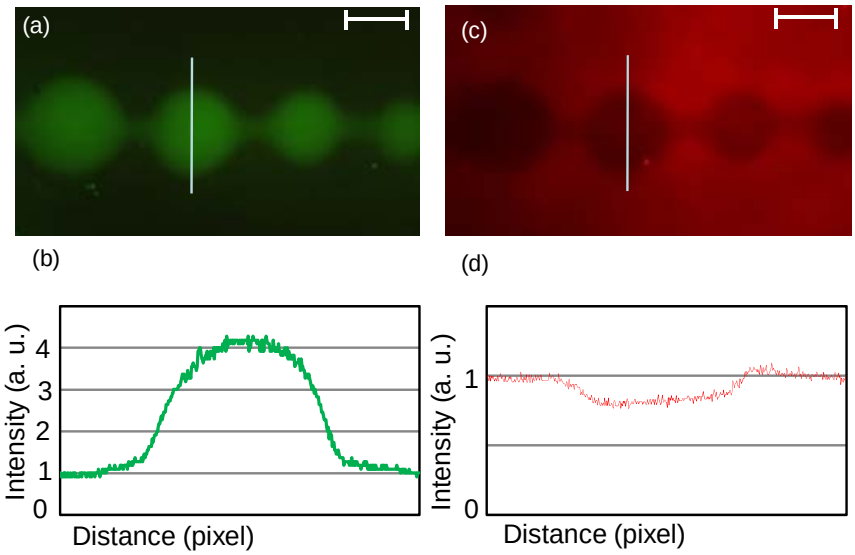

Figure 2.7: (a) Fluorescent micrograph highlights initial patterning of biotin-PDL-FITC, while (c) shows secondary exposure of biotin-BSA-Rhodamine. The line scans in (b) and (d) quantitatively describe the initial patterning and the orthogonal exposure, respectively. Scale bars are 500 μm.

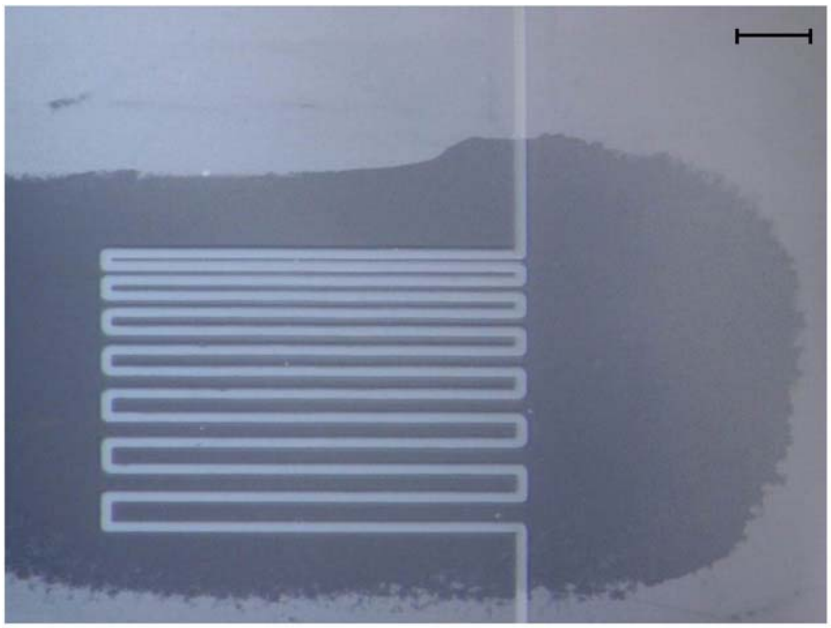

Figure 2.8: The underlying channel design was wetted with isopropyl alcohol using a cotton swab. The wetted device was immediately submerged in water to prevent solvent evaporation. The color of the PCTE membrane changed from white to translucent after wetting. Scale bar is 500 μm.

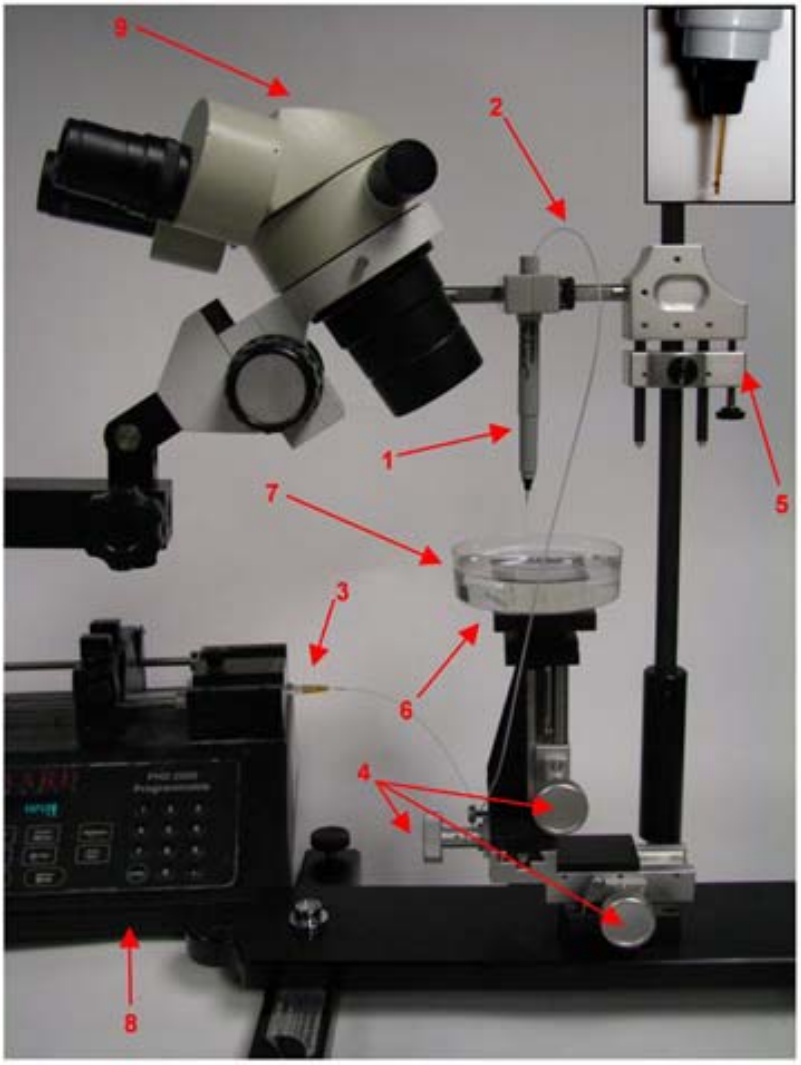

Figure 2.9: Experimental set-up of the writing station for selective membrane wetting. (1) "Pen", an empty Sharpie® marker shaft contains fused silica capillary tubing (D_{inner} = 50 μm, D_{outer} = 150 μm, see inset for an enlarged view); (2) PE-20 tubing; (3) 1 ml syringe, loaded with isopropyl alcohol; (4) Control of lateral, vertical movement of stage; (5) Adjustable clamp; (6) Sample stage; (7) Petri dish, with submerged device in water; (8) Syringe pump; (9) Stereoscope.

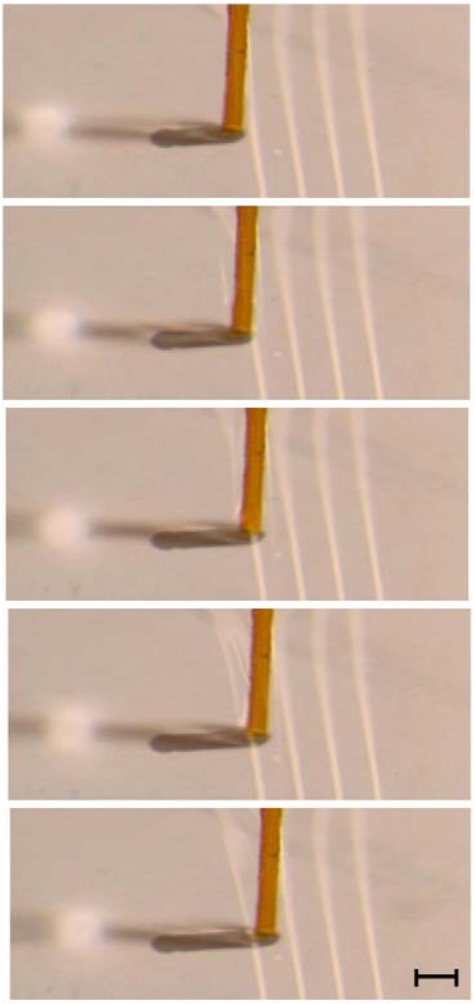

Figure 2.10: Image sequences highlights selective wetting of the PCTE membrane with isopropyl alcohol using a capillary ‘pen’, gently rastered across the membrane surface. Membrane color changes from white to translucent after IPA exposure. Scale bar is 300 μm.

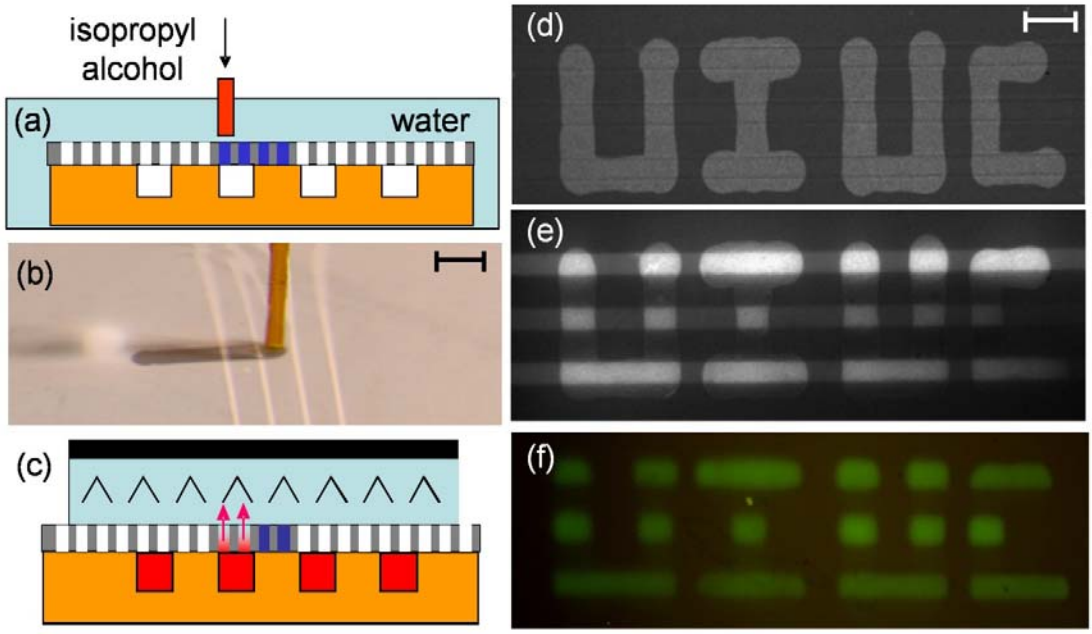

Figure 2.11: The secondary membrane wetting technique is schematically represented in (a), while an optical micrograph of the 'writing' process is presented in (b). Solution can diffuse out through the underlying microchannels only in the regions that have been wetted with solvent (c). The optical micrograph in (d) shows a pattern that was 'written' on the membrane, while the fluorescence image in (e) shows the diffusion of the FITC-biotin molecule through the wetted regions. The resulting pattern that was transferred to the gel is shown in (e). Scale bars are 300 μm.

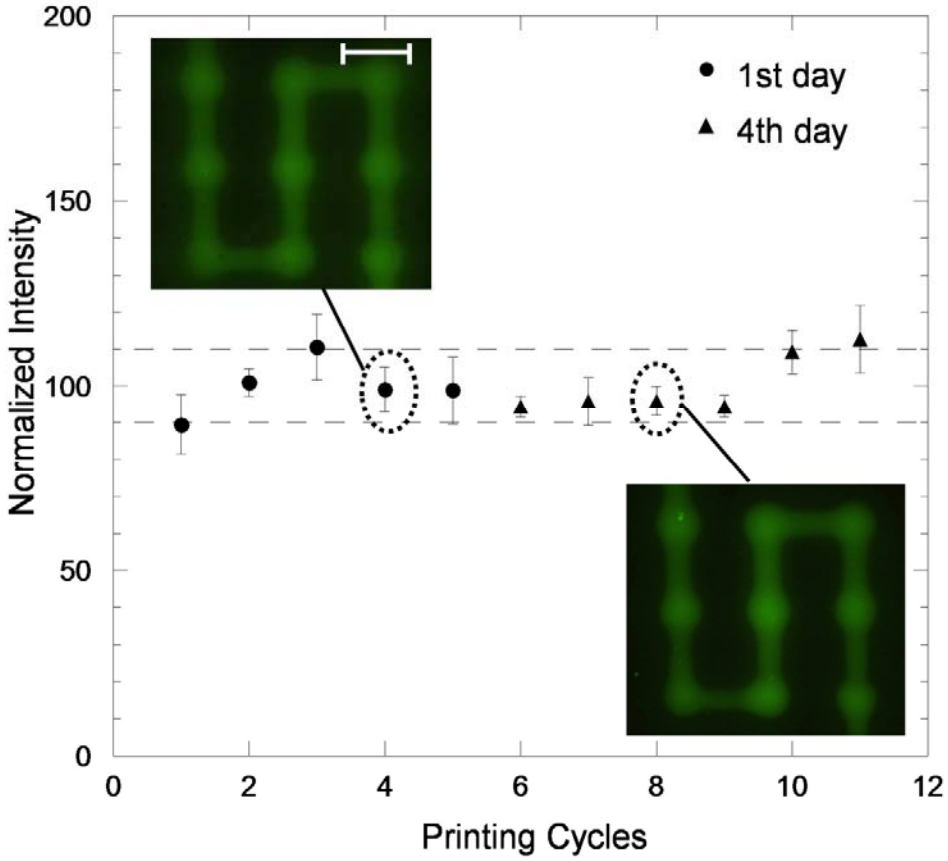

Figure 2.12: The plot presented here shows the system's high pattern transfer reproducibility over consecutive printing cycles. The first 5 data points represent printing attempts on day 1, while the last 6 data points represent printing attempts completed on day 4. The inset micrographs visually highlight the similarity in fluorescence intensity between individual printing cycles. Scale bar is 500 μm.

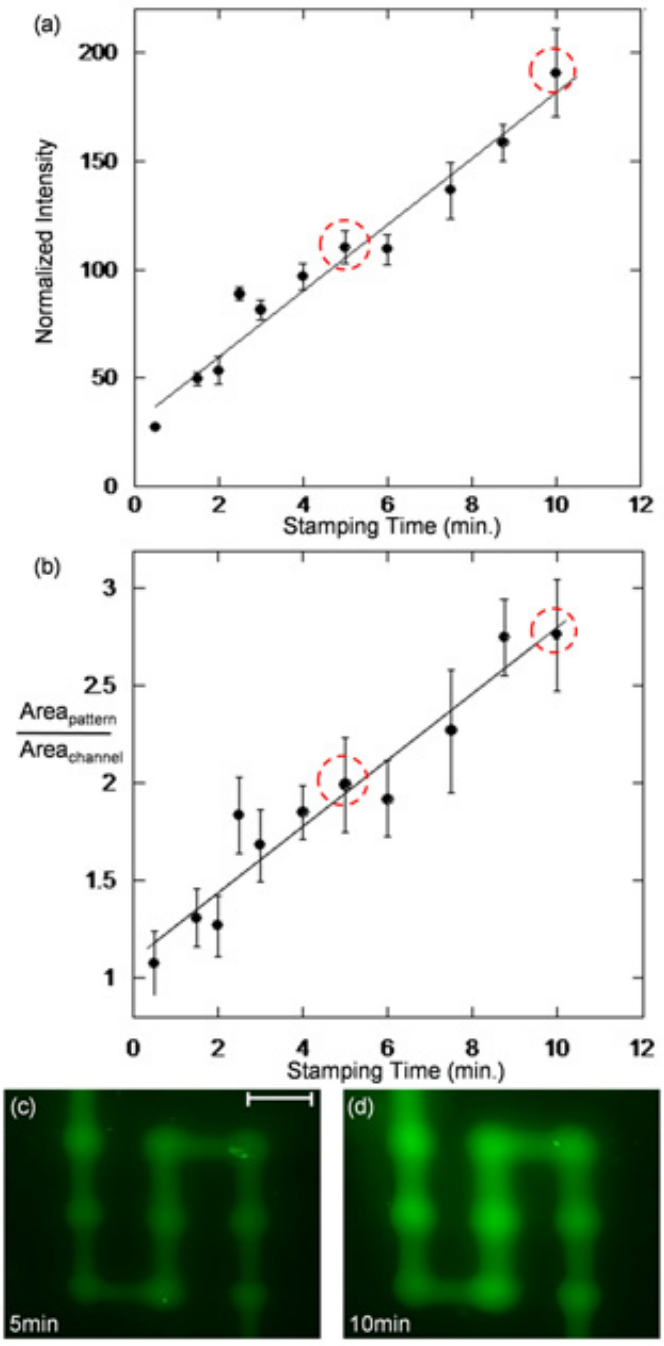

Figure 2.13: The fluorescence intensity (a) and diameter (b) of the printed pattern linearly increases, through a stamping time range of 0.5-10 minutes. In (c) a micrograph of the printed pattern at 5 minutes is given, while the printed pattern after 10min is given in (d). Scale bar is 500 μm.

2.7. REFERENCES

(1) Vo-Dinh, T.; Cullum, B. M.; Stokes, D. L. "Nanosensors and biochips: frontiers in biomolecular diagnostics"; *Sensor Actuat. B-Chem.* **2001**, *74*, 2.

(2) Haupt, K.; Mosbach, K. "Molecularly Imprinted Polymers and Their Use in Biomimetic Sensors"; *Chem. Rev.* **2000**, *100*, 2495.

(3) Offenhausser, A.; Bocker-Meffert, S.; Decker, T.; Helpenstein, R.; Gasteier, P. *et al* "Microcontact printing of proteins for neuronal cell guidance"; *Soft Matter* **2007**, *3*, 290.

(4) Kane, R. S.; Takayama, S.; Ostuni, E.; Ingber, D. E.; Whitesides, G. M. "Patterning proteins and cells using soft lithography"; *Biomaterials* **1999**, *20*, 2363.

(5) James, C. D.; Davis, R. C.; Meyer, M.; Turner, A.; Turner, S. *et al* "Aligned Microcontact Printing of Micrometer-Scale Poly-L-Lysine Structures for Controlled Growth of Cultured Neurons on Planar Microelectrode Arrays"; *IEEE T. Bio.-Med. Eng.* **2000**, *47*, 17.

(6) Oliva Jr., A. A.; James, C. D.; Kingman, C. E.; Craighead, H. G.; Banker, G. A. "Patterning Axonal Guidance Molecules Using a Novel Strategy for Microcontact Printing "; *Neurochem. Res.* **2003**, *28*, 1639.

(7) Ahn, D. J.; Jin, J. J.; Lee, G. S.; Kwon, G.; Pak, J. J. *et al* "Hippocampal neuronal network directed geometrically by sub-patterns of microcontact printing (uCP)"; *J. Ind. Eng. Chem.* **2003**, *9*, 25.

(8) Cornish, T.; Branch, D. W.; Wheeler, B. C.; Campanelli, J. T. "Microcontact Printing: A Versatile Technique for the Study of Synaptogenic Molecules "; *Mol. Cell Neurosci.* **2002**, *20*, 140.

(9) Dertinger, S. K. W.; Jiang, X.; Li, Z.; Murthy, V. N.; Whitesides, G. M. "Gradients of substrate-bound laminin orient axonal specification of neurons"; *P. Natl. Acad. Sci. USA* **2002**, *99*, 12542.

(10) Wang, D.-Y.; Huang, Y.-C.; Chiang, H.; Wo, A.-M.; Huang, Y.-Y. "Microcontact

printing of laminin on oxygen plasma activated substrates for the alignment and growth of Schwann cells"; *J. Biomed. Mater. Res. B* **2006**, *80B*, 447.

(11) Adler, J. "Chemotaxis in bacteria"; *Science* **1966**, *153*, 708.

(12) Carter, S. B. "Haptotaxis and the mechanism of cell motility"; *Nature* **1967**, *213*, 256.

(13) Carmeliet, P. "Mechanisms of angiogenesis and arteriogenesis"; *Nat. Med.* **2000**, *6*, 389.

(14) Turing, A. M. "The chemical basis of morphogenesis"; *B. Math. Biol.* **1990**, *52*, 153.

(15) Baier, H.; Bonhoeffer, F. "Axon guidance by gradients of target-derived component"; *Science* **1992**, *255*, 472.

(16) Song, H.-J.; Poo, M.-M. "Signal transduction underlying growth cone guidance by diffusible factors"; *Curr. Opin. Neurobiol.* **1999**, *9*, 355.

(17) Discher, D. E.; Janmey, P.; Wang, Y.-L. "Tissue cells feel and respond to the stiffness of their substrate"; *Science* **2005**, *18*, 1139.

(18) Engler, A. J.; Sen, S.; Sweeney, H. L.; Discher, D. E. "Matrix Elasticity Directs Stem Cell Lineage Specification"; *Cell* **2006**, *126*, 677.

(19) Cushing, M. C.; Anseth, K. S. "Hydrogel Cell Cultures"; *Science* **2007**, *316*, 1133.

(20) Hynd, M. R.; Turner, J. N.; Shain, W. "Applications of hydrogels for neural cell engineering"; *J. Biomat. Sci.-Polym E.* **2007**, *18*, 1223.

(21) Kumar, A.; Whitesides, G. M. "Features of gold having micrometer to centimeter dimensions can be formed through a combination of stamping with an elastomeric stamp and an alkanethiol ㅌink ㅓ followed by chemical etching"; *Appl, Phys. Lett.* **1993**, *63*, 2002.

(22) Kumar, A.; Biebuyck, H. A.; Whitesides, G. M. "Patterning Self-Assembled Monolayers: Applications in Materials Science"; *Langmuir* **1994**, *10*, 1498.

(23) Lopez, G. P.; Biebuyck, H. A.; Harter, R.; Kumar, A.; Whitesides, G. M. "Fabrication and imaging of two-dimensional patterns of proteins adsorbed on self-assembled monolayers by scanning electron microscopy"; *J. Am. Chem. Soc.* **1993**, *115*, 10774.

(24) Mrksich, M.; Grunwell, J. R.; Whitesides, G. M. "Biospecific Adsorption of Carbonic Anhydrase to Self-Assembled Monolayers of Alkanethiolates That Present Benzenesulfonamide Groups on Gold"; *J. Am. Chem. Soc.* **1995**, *117*, 12009.

(25) Garcia-Payo, M. C.; Izquierdo-Gil, M. A.; Fernandez-Pineda, C. "Wetting Study of Hydrophobic Membranes via Liquid Entry Pressure Measurements with Aqueous Alcohol Solutions"; *J. Colloid Interf. Sci.* **2000**, *230*, 420.

(26) James, C. D.; Davis, R. C.; Kam, L.; Craighead, H. G.; Isaacson, M. *et al* "Patterned Protein Layers on Solid Substrates by Thin Stamp Microcontact Printing"; *Langmuir* **1998**, *14*, 741.

(27) Hynd, M. R.; Frampton, J. P.; Burnham, M.-R.; Martin, D. L.; Dowell-Mesfin, N. M. *et al* "Functionalized hydrogel surfaces for the patterning of multiple biomolecules"; *J. Biomed. Mater. Res. A* **2007**, *81A*, 347.

(28) Burnham, M. R.; Turner, J. N.; Szarowski, D.; Martin, D. L. "Biological functionalization and surface micropatterning of polyacrylamide hydrogels"; *Biomaterials* **2006**, *27*, 5883.

(29) Hynd, M. R.; Frampton, J. P.; Dowell-Mesfin, N.; Turner, J. N.; Shain, W. "Directed cell growth on protein-functionalized hydrogel surfaces"; *J. Neurosci. Meth.* **2007**, *162*, 255.

(30) Dertinger, S. K. W.; Chiu, D. T.; Jeon, N. L.; Whitesides, G. M. "Generation of Gradients Having Complex Shapes Using Microfluidic Networks"; *Anal. Chem.* **2001**, *73*, 1240.

(31) Jeon, N. L.; Baskaran, H.; Dertinger, S. K. W.; Whitesides, G. M.; Van De Water, L. *et al* "Neutrophil chemotaxis in linear and complex gradients of interleukin-8 formed

in a microfabricated device"; *Nat. Biotechnol.* **2002**, *20*, 826.

(32) Chung, B. G.; Flanagan, L. A.; Rhee, S. W.; Schwartz, P. H.; Lee, A. P. *et al* "Human neural stem cell growth and differentiation in a gradient-generating microfluidic device"; *Lab Chip* **2005**, *5*, 401.

(33) Jiang, X. Y.; Xu, Q. B.; Dertinger, S. K. W.; Stroock, A. D.; Fu, T. M. *et al* "A general method for patterning gradients of biomolecules on surfaces using microfluidic networks"; *Anal. Chem.* **2005**, *77*, 2338.

(34) Romanova, E. V.; Fosser, K. A.; Rubakhin, S. S.; Nuzzo, R. G.; Sweedler, J. V. "Engineering the morphology and electrophysiological parameters of cultured neurons by microfluidic surface patterning "; *FASEB J.* **2004**, *18*, 1267.

(35) Rhoads, D. S.; Guan, J.-L. "Analysis of directional cell migration on defined FN gradients: Role of intracellular signaling molecules"; *Exp. Cell Res.* **2007**, *313*, 3859.

(36) Petty, R. T.; Li, H.-W.; Maduram, J. H.; Ismagilov, R.; Mrksich, M. "Attachment of Cells to Islands Presenting Gradients of Adhesion Ligands"; *J. Am. Chem. Soc.* **2007**, *129*, 8966.

(37) Whitesides, G. M.; Ostuni, E.; Takayama, S.; Jiang, X.; Ingber, D. E. "Soft Lithography in Biology and Biochemistry"; *Annu. Rev. Biomed. Eng.* **2001**, *3*, 335.

(38) Bernard, A.; Renault, J. P.; Michel, B.; Bosshard, H. R.; Delamarche, E. "Microcontact Printing of Proteins"; *Adv. Mater.* **2000**, *12*, 1067.

(39) Jong, J. d.; Lammertink, R. G. H.; Wessling, M. "Membranes and microfluidics: a review"; *Lab Chip* **2006**, *6*, 1125.

(40) Xia, Y.; Whitesides, G. M. "Soft Lithography"; *Polym. Mater. Sci. Eng.* **1997**, *77*, 596.

(41) Xia, Y.; Whitesides, G. M. "Soft Lithography"; *Angew. Chem. Int. Edit.* **1998**, *37*, 550.

(42) Rogers, J. A.; Nuzzo, R. G. "Recent Progress in Soft Lithography"; *Mater. Today* **2005**, *8*, 50.

(43) Kuo, T.-C.; Cannon, J., D.M.; Shannon, M. A.; Sweedler, J. V.; Bohn, P. W. "Hybrid three-dimensional nanofluidic/microfluidic devices using molecular gates"; *Sensor Actuat.* **2003**, *102*, 223.

(44) Kuo, T.-C.; Cannon, J. D. M.; Chen, Y.; Tulock, J. J.; Shannon, M. A. *et al* "Gateable Nanofluidic Interconnects for Multilayered Microfluidic Separation Systems"; *Anal. Chem.* **2003**, *75*, 1861.

(45) Flachsbart, B. R.; Wong, K.; Iannacone, J. M.; Abante, E. N.; Vlach, R. L. *et al* "Design and fabrication of a multilayered polymer microfluidic chip with nanofluidic interconnects via adhesive contact printing"; *Lab Chip* **2006**, *6*, 667.

(46) Neeves, K. B.; Diamond, S. L. "A membrane-based microfluidic device for controlling the flux of platelet agonists into flowing blood"; *Lab Chip* **2008**, *8*, 701.

(47) Hediger, S.; Fontannaz, J.; Sayah, A.; Hunziker, W.; Gijs, M. A. M. "Biosystem for the culture and characterisation of epithelial cell tissues"; *Sensor Actuat. B-Chem.* **2000**, *63*, 63.

(48) Chueh, B.; Huh, D.; Kyrtsos, C. R.; Houssin, T.; Futai, N. *et al* "Leakage-Free Bonding of Porous Membranes into Layered Microfluidic Array Systems"; *Anal. Chem.* **2007**, *79*, 3504.

(49) Haubert, K.; Drier, T.; Beebe, D. J. "PDMS bonding by means of a portable, low-cost corona system "; *Lab Chip* **2006**, *6*, 1548.

(50) Smith, P. J.; Owen, M. J.; Holm, P. H.; Toskey, G. A. In *Electrical Insulation and Dielectric Phenomena, 1992. Annual Report.* Victoria, BC, Canada, 1992, p 829.

(51) Go, J. S.; Shoji, S. "A disposable, dead volume-free and leak-free in-plane PDMS microvalve"; *Sensor Actuat. A-Phys.* **2004**, *114*, 438.

(52) Graf, J.; Iwamoto, Y.; Sasaki, M.; Martin, G. R.; Kleinman, H. K. *et al* "Identification of an amino acid sequence in laminin mediating cell attachment, chemotaxis, and receptor binding"; *Cell* **1987**, *48*, 989.

(53) Timpl, R.; Rohde, H.; Robey, P. G.; Rennard, S. I.; Foidart, J. M. *et al*

"Laminin--a glycoprotein from basement membranes"; *J. Bio. Chem.* **1979**, *254*, 9933.

(54) Ekblom, M.; Klein, G.; Mugrauer, G.; Fecker, L.; Deutzmann, R. *et al* "Transient and locally restricted expression of laminin a chain mRNA by developing epithelial cells during kidney organogenesis"; *Cell* **1990**, *60*, 337.

(55) Tashiro, K.; Sephel, G. C.; Weeks, B.; Sasakig, M.; Martinn, G. R. *et al* "A Synthetic Peptide Containing the IKVAV Sequence from the A Chain of Laminin Mediates Cell Attachment, Migration, and Neurite Outgrowth"; *J. Biol. Chem.* **1989**, *264*, 16174.

(56) Grzybowski, B. A.; Bishop, K. J. M.; Campbell, C. J.; Fialkowski, M.; Smoukov, S. K. "Micro- and nanotechnology via reaction-diffusion"; *Soft Matter* **2005**, *1*, 114.

(57) Hersel, U.; Dahmen, C.; Kessler, H. "RGD modified polymers: biomaterials for stimulated cell adhesion and beyond"; *Biomaterials* **2003**, *24*, 4385.

(58) Vercilli, A.; Repici, M.; Garbossa, D.; Grimaldi, A. "Recent techniques for tracing pathways in the central nervous system of developing and adult mammals"; *Brain Res. Bull.* **2000**, *51*, 11.

(59) Mehvar, R. "Dextrans for targeted and sustained delivery of therapeutic and imaging agents"; *J. Controlled Release* **2000**, *69*, 1.

(60) Branch, D. W.; Corey, J. M.; Weyhenmeyer, J. A.; Brewer, G. J.; Wheeler, B. C. "Microstamp patterns of biomolecules for high-resolution neuronal networks"; *Med. Biol. Eng. Comput* **1998**, *36*, 135.

(61) Branch, D. W.; Wheeler, B. C.; Brewer, G. J.; Leckband, D. E. "Long-term maintenance of patterns of hippocampal pyramidal cells on substrates of polyethylene glycol and microstamped polylysine"; *IEEE Trans. Biomed. Eng.* **2000**, *47*, 290.

(62) Chang, J. C.; Brewer, G. J.; Wheeler, B. C. "A modified microstamping technique enhances polylysine transfer and neuronal cell patterning"; *Biomaterials* **2003**, *24*, 2863.

(63) Sia, S. K.; Whitesides, G. M. "Microfluidic devices fabricated in

poly(dimethylsiloxane) for biological studies"; *Electrophoresis* **2003**, *24*, 3563.

(64) Nelson, R. D.; Quie, P. G.; Simmons, R. L. "Chemotaxis Under Agarose: A New and Simple Method for Measuring Chemotaxis and Spontaneous Migration of Human Polymorphonuclear Leukocytes and Monocytes"; *J. Immunol.* **1975**, *115*, 1650.

(65) Huttenlocher, A.; Ginsberg, M.; Horwitz, A. "Modulation of cell migration by integrin-mediated cytoskeletal linkages and ligand-binding affinity"; *J. Cell Biol.* **1996**, *134*, 1551.

(66) Rothschild, M. "Projection optical lithography"; *Mater. Today* **2005**, *8*, 18.

(67) Ronse, K. "Optical lithography-a historical perspective"; *C. R. Phys.* **2006**, *7*, 844.

(68) Monahan, J.; Gewirth, A. A.; Nuzzo, R. G. "A method for filling complex polymeric microfluidic devices and arrays"; *Anal. Chem.* **2001**, *73*, 3193.

(69) Hanson, J. N.; Motola, M. J.; Heien, M. L.; Gillette, M.; Sweedler, J. V. *et al* "Textural Guidance Cues for Controlling Process Outgrowth of Mammalian Neurons"; *Lab Chip* **2009**, *9*, 122.

(70) Model, M. A.; Burkhardt, J. K. "A standard for calibration and shading correction of a fluorescence microscope"; *Cytometry* **2001**, *44*, 309.

Chapter 3 Alkaline Dehybridization for the Discrimination of Single Nucleotide Polymorphisms

Note: The majority of the text comes from Huaibin Zhang, Svetlana M. Mitrovski, Ralph G. Nuzzo, "A Microfluidic Device for the Discrimination of Single Nucleotide Polymorphisms in DNA Oligomers Using Electrochemically Actuated Alkaline Dehybridization", *Anal. Chem.*, **2007**, 79, 9014-9021. Reproduced by permission of the American Chemical Society.

3.1. INTRODUCTION

Single Nucleotide Polymorphism (SNP) is a DNA sequence variation that involves one change in a single nucleotide. As the most common type of human genetic variation,[1-2] SNPs have attracted considerable interest as targets of disease diagnostics,[3-5] as well as gene markers.[6-8] Due to the abundance and importance of SNPs, many detection techniques[9-10] have been developed, most of which can be divided into two broad categories: scanning and diagnostic.[11] The scanning methods are able to separate wild- and mutant-type DNA based on their difference in mobility and/or stability. Typical SNP detection techniques that use the scanning strategy include single-strand conformation polymorphism (SSCP)[12], heteroduplex analysis (HA)[12], denaturing gradient gel electrophoresis (DGGE)[13], and denaturing high-performance liquid chromatography (DHPLC)[14]. The diagnostic methods, in contrast, require that the sequence of DNA be known prior to designing the primer. Examples of techniques using the latter diagnostic strategy include polymerase chain reactions (PCRs)[15], single-base extensions (SBE)[16],

and ligase detection reactions (LDR)[17]. Most of these SNP detection techniques, however, suffer from drawbacks associated with low throughput and (for some) high expense.[9]

Miniaturization provides a way to increase throughput at lower cost because small dimensions reduce reagent consumption while enabling an ability to do multiplex analyses. The best example demonstrating the cost-advantages that attend miniaturization and large scale integration is provided by the semiconductor industry, where advances in photolithography[18-19] have served to spur the progression of what is perhaps the most powerful and sophisticated manufacturing technology ever developed. The extension of these manufacturing methods (photolithography in particular) into the field of DNA analysis has enabled an effective, and highly versatile platform technology for microarray based systems.[20] These devices are usually made by using light-directed chemistry to immobilize thousands of sequence specific DNA probes onto a designated location within a small chip;[21] hundreds of SNP variations can be detected in parallel in this way.[22] The planar microarray format, however, engenders reaction kinetics that are diffusion-limited, requiring as much as several hours to complete a hybridization process.[23] The lithographic processes used to fabricate these devices also have an intrinsic step-sequence error rate that limits sequence homology within a "pixel", and for this reason the length of the sequences that can be analyzed.[24] These limitations provide one motivation to current research in the field that seeks to develop new analytical

platforms.[25]

Analytical methods based on microfluidic technologies have demonstrated their potential in a number of diversified areas of application including biology, medicine, chemical analysis, and missions for homeland security.[26-30] Microfluidic devices offer many distinct benefits including the ability to manipulate exceptionally small volumes of liquid, resulting in low reagent consumption, short analysis times, and improved sensitivity.[26] These systems, in addition, can be mass-fabricated at low cost, especially when polymer-based materials are used in their construction.[31] These advantages make microfluidics a particularly attractive platform for performing DNA analyses.[32-33]

This report considers a new integration and chemical actuation strategy for a μ-fl system that can be used to analyze oligo-DNA duplexes for the presence of SNPs. Many conventional SNP detection methods, such as SSCP[34], DGGE[35], LDR[36], and SBE[37], have already been successfully realized in microfluidic formats.[11] These microfluidic platforms provide new opportunities for improving the analytical figures of merit as well. For example, micrometer-scale beads coated with ssDNA probe have been utilized in microfluidic formats to capture target ssDNA.[38-40] In these systems, the necessary hybridization time was decreased dramatically—from the period of hours required in a planar surface microarray to as little as a few seconds.[40-42] Mass transfer impacts due to the high surface-to-volume ratio of the bead-based assay are central contributors to this

enhanced performance.[38,41] Bead-based microfluidic devices have also been used in SNP discrimination.[43-47] In an exemplary study reported by Liu *et al*,[43] a monolayer of ssDNA coated beads was assembled in a microfluidic device to dynamically enhance the capture of a target ssDNA; a subsequent treatment with formamide was then used to discriminate a SNP. Their results suggest that the presence of SNP sequences can be distinguished more effectively based on dehybridization than on capture/hybridization.[43] The present work follows a similar strategy using, though, a different chemical mechanism.

It is known in the literature that alkaline dehybridization is a reliable and convenient way to denature double-stranded DNA (dsDNA) via a mechanism involving the deprotonation of guanine and cytosine segments;[48-49] at high pH (e.g., pH > 13), essentially all such interactions are destroyed.[49] High-concentration alkaline solutions also are used to dehybridize long chain DNA sequences with high G/C content.[50-51] If the pH is held at a moderate range (e.g., pH = 11 - 13), the dehybridization process is less strongly driven and, in some cases, reversible.[48,52-53] The literature on this subject is limited and what data, however, exist suggests that pH provides an inefficient means through which to detect SNPs,[54] as the pH range in which an essentially thermodynamic discrimination can be made is quite narrow ($\Delta pH < 0.3$) and likely very sequence-length limited.

In a previous study, we described a microfluidic electrochemical actuator that is able to generate precise and highly localized fluxes of high pH within a microfluidic channel system.[55] In this work, we have utilized this capacity to drive an alkaline DNA dehybridization process and examined its capability for providing a kinetic discrimination of the presence of a model SNP. For this purpose we exploit an indiscriminate capture of oligonucleotide sequences by ssDNA-coated magnetic beads contained in a microfluidic device that integrates a magnetic separator and microelectrochemical cell. The latter is used to electrochemically generate a basic reagent with both temporal and spatial control by performing the oxygen reduction reaction (ORR) using gas that passively permeates the polymeric components of the device.[55] The functional design used here integrates a simplified device design that retains a capacity to electrochemically generate transient pH values that are high enough to dehybridize DNA. By controlling the duration of a potential pulse, and thereby the temporal/spatial profile of the OH^- concentration created by it, we were able to specifically release a single nucleotide mismatched (MM) DNA while retaining the majority of perfectly matched (PM) DNA on the bead. We show here that multiple hybridization/dehybridization cycles can be carried on a single chip with excellent recapture efficiency.

3.2. EXPERIMENTAL

3.2.1. Materials and reagents

A PDMS prepolymer (Sylgard 184, Dow Corning, Midland, MI, mixed in a 10:1 ratio with the curing agent) was used to fabricate the μ-fl device.[56] The cylindrical nickel-plated NdFeB magnet (d x h = 2 x 2 mm) was purchased from CMS Magnetics (Plano, TX). Magnetic core agarose beads (20-75 μm, 6 % agarose, cross-linked with epichlorohydrin) functionalized with glyoxal were obtained from Colloidal Science Solutions (West Warwick, RI). Aldehyde-functionalized glass slides (VALS, Vantage Aldehyde Slides) used in experiments described in the supplementary materials were purchased from CEL Associates (Pearland, TX). Phosphate Buffered Saline (PBS, pH = 7.4, $[H_2PO_4^-] + [HPO_4^{2-}] = 6.7$ mM) was purchased from HyClone (Logan, UT). Silver epoxy resin (EPO-TEK 4110) was obtained from Epoxy Technology (Billerica, MA). Silicone adhesive (AST-RTV 27806) was purchased from Anti-Seize Technology (Franklin Park, IL). All chemicals used were of analytical grade.

The DNA oligomers used in this study were obtained from Integrated DNA Technologies (Coralville, IA) and are listed in Table 3.1. The amine group used to immobilize the probe was linked to the 3' end through a 6 carbon chain. The 5' end of PM target DNA was labeled with a Cal Fluor® fluorophore (λ_{excite} = 598 nm, $\lambda_{emission}$ = 617 nm). For some experiments requiring a double label, the 5' end of MM target

DNAs was modified with an Oregon Green fluorophore (λ_{excite} = 494 nm, $\lambda_{emission}$ = 518 nm). All DNA oligomers were purified by HPLC by the manufacturer and used as received. A 100 μM stock solution of the Probe DNA was prepared in PBS buffer; 100 μM stock solutions of the PM and MM target DNAs were prepared in TE buffers (10 mM Tris, 1 mM EDTA, pH 7.5). All DNA solutions were stored in a freezer at -12 °C.

3.2.2. DNA immobilization on agarose beads

The procedure used to immobilize the Probe DNA on the beads was based on the protocol provided by the manufacturer. In this procedure, 50 mg of agarose beads were filtered from their aqueous suspension using a sintered glass filter and resuspended in 150 μl of a coupling solution of pH = 10 carbonate buffer containing 0.15 M NaCl and 50 mM $NaCNBH_3$. The suspension was shaken for 15 minutes after which 10 μL of a 100 μM Probe DNA solution in PBS was added and the mixture shaken for an additional 75 minutes. The suspension was held at room temperature overnight to complete the coupling step. The Probe-linked beads were then filtered and re-suspended in 100 μL of the coupling solution. After adding 240 μl of 0.4 % (v/v) ethanolamine aqueous solution, the mixture was vigorously shaken for 1 hour to block the unreacted aldehyde sites on the beads. The beads were then filtered, washed copiously with 18 MΩ milli-Q water, and resuspended in water (containing 0.03 % NaN_3 as a preservative).

3.2.3. Microfluidic device fabrication

The fabrication procedure for the microfluidic device used in this study is depicted schematically in Figure 3.1(a). In step (i), a nickel-plated NdFeB cylindrical magnet (the separator) was conformally attached to a flat PDMS membrane (previously cured for > 48 h). A Pt thin-film working electrode (WE) assembly, comprising a 100 nm thick Pt layer deposited on a 15 nm Ti adhesion layer that is supported in turn by a 1 mm thick quartz slide, was fabricated using standard photolithography lift-off procedures described elsewhere.[57] The WE array was placed onto the PDMS flat, Pt-side-down, at a distance of 5 mm from the magnet (measured from the center of the electrode to the center of the magnet). In step (ii), the PDMS prepolymer was poured over the setup and placed in a vacuum oven for 10 minutes to remove entrained air bubbles. The polymer was then cured at 70 °C for 2 hours. In step (iii), the entire "sandwich" was flipped over and the thin PDMS membrane was carefully peeled away to reveal the WE and magnet embedded within the PDMS. The latter assembly served as the bottom layer of the microfluidic device. The upper layer of the device (iv) consisted of a microfluidic channel (20 mm long, 0.94 mm wide, and 0.12 mm high) that was fabricated in PDMS using a rapid prototyping procedure.[56] The ends of the PDMS channel were opened using a 1.5 mm diameter biopsy punch to permit introduction of solution into the device as well as to serve as access points for a Ag-wire pseudo-reference (RE) and Pt-wire counter (CE) electrodes. The bottom and upper layers of the microfluidic device were

treated with UV/ozone for 5 min to promote adhesion.[58] The two layers were then sealed together irreversibly by placing them in conformal contact and heating the assembled structure in an oven at 70 °C for 2 hours. Electrical contact to the thin-film WE was made using silver-epoxy resin and a Pt-wire.

The microfluidic device was filled with electrolyte solution (PBS buffer) using the channel outgas technique.[59] The DNA coated magnetic beads were inserted into the channel by applying hydrodynamic flow, which was induced by keeping the solution levels at the ends of the channel at uneven heights. The latter procedure resulted in the formation of a plug of beads above the embedded magnet (which in turn could be dislodged by a steep, pulsatile increase of the flow rate or mechanically agitating the device). The Pt-wire CE and an Ag-wire pseudo-RE were inserted into the reservoirs and the entire assembly then placed into a box containing electrical contacts by which the WE, CE, and RE were connected to a potentiostat (650B, CH Instruments, Austin, TX). Figure 3.1(b) shows schematic representations of the top and side views of the assembled device.

3.2.4. On-chip DNA hybridization and dehybridization

The immobilization of the Probe DNA (Table 3.1) on the agarose beads was effected using the Schiff base coupling protocol schematically depicted in Figure 3.2.[60] The

terminal amine groups on the 3' end of the Probe were reacted with the aldehyde groups on the glyoxal-coated agarose beads to form a C=N bond (Schiff base reaction).[60] This linkage was reduced *in-situ* to a more stable C-N bond by $NaCNBH_3$. The unreacted aldehyde sites on the beads were then blocked using ethanolamine coupled in a manner similar to that used for the Probe DNA.

Dynamic DNA hybridizations were performed in the channel by flowing 20 μL of 1 μM PM target (Table 3.1) solution (20 pmol) over the beads at a linear displacement rate of 9×10^{-3} m/sec (corresponding to a 20 min contact time for DNA hybridization). The DNA solution that remained in the inlet reservoir was replaced with PBS buffer, which was allowed to pass through the channel for 20 minutes to rinse away any excess PM target in the channel. The magnetic separator served to concentrate the beads in this flow field in the region down stream of the WE (closest to the CE).

The dehybridization reaction of the captured PM duplex was performed using base electrochemically generated by the ORR.[55] These experiments were performed under potentiostatic control (at −0.6 V vs. Ag). The course of the dehybridization process was monitored by fluorescence microscopy using an epifluorescent microscope (Olympus, AX-70, Melville, NY) equipped with a CCD camera (Optronic MagnaFire). The images were analyzed using Image Pro software (Media Cybernetics, Silver Spring, MD).

3.2.5. Visualization of pH profile inside the channel

The pH change resulting from the ORR inside the channel was monitored *in situ* by fluorescence microscopy using fluorescein as a pH sensitive dye. The emission of the fluorescein probe is one for which the quantum yield (Φ) is strongly pH dependent. The value of Φ is 0.20–0.25 for the neutral molecule (pK_a = 2.2) and 0.25–0.35 for the monoanion (pK_a = 4.3), while the Φ of the dianion (pK_a = 6.7) is markedly larger (~ 0.93).[61]

The channel of a device depicted by Figure 3.1(c) was filled with electrolyte (0.1 M NaCl + 0.1 mM fluorescein, pH = 4). With the syringe pump stopped, a 34 second square wave potentiostatic pulse at ε = -0.6 V (Ag) was applied, conditions similar to that used to desorb a MM1 target DNA. A high emission plug was formed in the WE region during the pulse. The entire plug was forced from the region of the WE in the direction of the beads using a hydrodynamic flow driven by a syringe pump at a rate of 0.3 μl/sec. Time-lapse fluorescence images at the WE region were recorded using a fluorescence microscope in conjunction with a U-MWIB filter set. A sequence of representative micrographs is shown in Figure 3.6. The time that the syringe pump was actuated was set as time zero.

The number of electrons supplied by the 34 second pulse was 9.35 x 10^{-5} C yielding

9.69×10^{-10} mol OH^-, assuming that hydroxide ions were the sole product of the ORR. The volume of the high emission region formed in the vicinity of the WE is ~ 0.2 μl, corresponding to a calculated average pH in the imaged plug of ~ 11.7. Since the average pH of the plug is much larger than the pK_a of fluorescein dianion (i.e., 6.7), we did not observe any long-ranged intensity gradient along the plug.

When an external actuation was applied, the plug moved with some initial hysteresis along the channel with a linear translation velocity of 3×10^{-5} m/sec. This accords well with the value of 4×10^{-5} m/sec estimated using the volumetric delivery of the syringe pump for channels with these dimensions. It is worth noting that the edge shape of the plug becomes parabolic during the external actuation and that similar parabolic fronts are observed in Figure 3.3(e) and Figure A.1(c) in the Appendix A.

3.2.6. Procedure for SNP discrimination

PM and MM target ssDNAs were hybridized to the Probe ssDNA using an off-chip procedure as follows: 100 μl of the Probe-coated beads were mixed with 40 μl of 5 μM PM (or MM) target solution. The mixture was shaken vigorously for 20 minutes at room temperature. The beads were then separated by centrifugation, rinsed by shaking with fresh 300 μl PBS solution for 5 minutes, after which they were separated from the solution by centrifugation. The rinsing step was repeated three times.

Equal amounts of PM and MM duplex coated DNA beads were mixed together and injected into the channel hydrodynamically, concentrating them as an intimate mixture in the region of the magnetic separator. To complete the device, an Ag wire pseudo-RE was pierced through the PDMS sidewall into one of the extension reservoirs (Figure 3.1(c)). A second needle, connecting to a programmable syringe pump, was also incorporated at the location of the RE. A paste of silicone adhesive (AST-RTV 27806) was applied to the connection point of the Ag wire (or the needle) and the PDMS sidewall, and fastened at room temperature for 2 hours to seal any gap between the inserted object and the sidewall. The reservoir was covered with a thin PDMS slab. The syringe pump was used to affect a secondary external control of the fluid flow inside the channel. The Pt-wire CE was placed into the other extension reservoir.

Hydroxide ions were generated at the WE by a series of potentiostatically applied current pulses at E = −0.6 V, the duration of which was varied between 15 to 50 s. The plug of base generated in this way was passed through the channel in the direction of the duplex coated beads at a flow rate of 0.3 μL/min using a hydrodynamic flow of a pushing buffer that was actuated externally using the syringe pump.

The dehybridization of the duplex DNA was followed by fluorescence microscopy. The emission of the PM target was monitored using a XF102-2 filter set (λ_{excite} = 565 ± 30 nm, $\lambda_{emission}$ = 655 ± 45 nm) while the MM targets were observed using a U-MWIB

filter set (λ_{excite} = 475 ± 15 nm, $\lambda_{emission}$ > 515 nm). When required, both target types could be observed simultaneously using a XF101-2 filter set (λ_{excite} = 525 ± 25 nm, $\lambda_{emission}$ > 565 nm); this protocol, while convenient, is relatively inefficient at collecting intensity from the MM targets.

3.3. RESULTS AND DISCUSSION

Magnetic core agarose beads and a nickel-plated NdFeB magnetic separator were used in this model system because they provide an efficient and relatively simple microfluidic platform[62] for testing the non-thermal MEMS-based actuation of DNA hybridization and dehybridization processes of interest in this work. The magnetic core agarose gel beads, functionalized with an amine-terminated Probe ssDNA using a standard glutaraldehyde coupling protocol, have several critical functions in this device. First, they enable the efficient collection of non-hybridized DNA fragments present in the solution and their subsequent concentration in bound form at the region of the device where the electrochemically mediated sorting is carried out. Second, and most important, this configuration facilitates a chemokinetic approach to discriminate SNPs that we believe may possess broad utility. These aspects of the device design and operation are described below.

Figure 3.3(a) shows an image of the magnetic beads spreading uniformly through the

channel after their introduction into the device. Using flow to direct them to the region of the separator, the beads aggregate above the embedded magnet, leading to the formation of a dense plug as illustrated by the fluorescence micrograph of Figure 3.3(b). This image was obtained after capturing a fluorescently-labeled target ssDNA as described in next section.

The magnetic beads can be dislodged from the separation region and released to the channel using either external mechanical agitation or a pulsatile high flow rate of the buffer. In this design, the balance of the shear and magnetic forces is used to discriminate whether the beads are retained or washed away from the magnetic separator. This simple design complements a related approach described by others that employs a variable force magnetic separator.[63]

3.3.1. On-chip DNA hybridization

The capture of a fluorescently labeled, PM ss-target sequence (Table 3.1) by the bead-immobilized probe sequence proceeds efficiently in the μ-Fl device. Such capture strategies have been well studied and excellent discussions on this aspect are available in the literature.[40-41] As the image of Figure 3.3(b) shows, the plug of packed beads serves as an efficient platform for hybridization-based capture, and provides a signal level for the duplex relative to the background that is quite high (here for the capture of 20 pmol of

target ss-DNA by a factor of 23). These performance metrics are vastly superior to those obtained with this same microscope for a device integrating a planar functionalized glass surface to effect the DNA hybridization (device fabrication procedure and dehybridization images are in Appendix A). We also found that the on-chip hybridization performed using the supported bead device configuration yielded faster kinetics, a result likely due to its higher total surface area as compared to a planar glass surface assay.[41,64]

We should note here that the extent of nonspecific adsorption of the various DNAs on the agarose beads is insignificant as revealed by control experiments carried out using both on-chip and off-chip hybridization protocols. In both cases, the nonspecific adsorption of a 21-base sequence showing no sequence homology was significantly lower than the specific adsorption of a sequence with either a SNP or full complementarity (Figure 3.4). This is not a surprising result given the fact that agarose gels have been extensively used as inert matrices in electrophoresis[65-66] and chromatography[67] to separate various DNA[65,68], RNA[69] and protein analytes[67,70-71].

3.3.2. Alkaline dehybridization

The immobilized PM duplex was dehybridized successfully using a transient high concentration flux of OH^- that was generated electrochemically at the WE. In this

experiment, the Pt-WE was polarized cathodically by applying a potential step from the open circuit potential (OCP) to −0.6 V (corresponding to an ~ 3 μA ORR current)[55] and the course of the DNA dehybridization process followed by fluorescence microscopy. The micrographs presented in Figure 3.3(c-e) show images taken in the area of the beads (down stream of the WE) at times of 300, 330, and 400 s after the beginning of the potential step at the WE. In this experiment no external flow field is applied. In this mode of operation, the base generated at the WE spreads spontaneously through the channel, doing so at a rate that is faster in the direction of the CE. This intrinsic quality of the device's actuated flow dynamics follows from a balance of the directional flow that is driven by the Faradaic current (towards the CE) and diffusive transport as described in a previous report.[55] The sequence of images shown in Figure 3.3(c-e) reveals that dissociation of the target ssDNA, and its detachment from the beads, proceeds along the direction corresponding to the motion of the OH^- front generated at the Pt-WE. As the target DNA is swept from the magnetically entrained beads, a fluorescent stream is seen to move from the WE towards the CE compartment.

It should be noted that under these conditions the pH of the solution in the channel is quite high. Assuming that the value of the total electrical charge generated during a 5 min current pulse at E = −0.6 V is directly proportional to the amount of hydroxide ions generated at the WE, from the known volume element of the device lying between the WE and the magnet (0.94 mm x 0.12 mm x 5 mm = 0.56 μL), we estimate that the

average value of the pH within segment of the device is equal to a pH ~ 12 (we assume for this calculation that hydroxide ions were the sole product of the ORR, i.e. that the number of exchanged electrons per O_2 molecule is equal to 4[72]. We conducted several off-chip control experiments, using basic buffers of known pH, and found that the dehybridization reaction for duplexes of this size proceeded to completion as long as an alkaline buffer of pH = 11 or greater is used. We also found that the time needed to effect a complete dehybridization from the beads decreased with increasing the pH of the solution. In one particularly informative control experiment in which a PM duplex coated glass slide was immersed in a pH = 11 buffer, we found that it took 11 s for the fluorescence intensity to decrease (by loss of the labeled strand to and dilution in the bulk of the buffer) by 40 % of the initial value. When a more alkaline (pH = 13) buffer solution was used, however, the fluorescence intensity decreased to the background level nearly instantaneously (within a few seconds of its introduction into the basic solution). Additional experiments also suggested that these pH dependent rate sensitivities are also influenced by the sequence complementarity, specifically that the rate of displacement of a mismatched sequence were in fact faster—a feature exploited below as the basis for a protocol for SNP detection.

It should be pointed out that the PDMS used in the device serves as a passive source of O_2 for the embedded electrochemical cell. The efficiency of this device results from both the high solubility and diffusivity of O_2 in this material, which are higher in PDMS

than they are in water, as well as the design rules of the device being in a range where those beneficial aspects can be exploited. These issues, which have consequential impacts on device design, have been examined in detail and quantitatively discussed in an earlier report.[55]

The alkaline dehybridization performed in the way described above possesses a number of potential advantages. In contrast to the more commonly used method of so-called thermal melting, alkaline dehybridization does not require the integration of heating elements onto the chip, eliminates the necessity of precise thermal control and isolation, allows the use of heat sensitive reagents, and increases device power efficiency by obviating thermal dissipation. The passive reagent foundation of the method also eliminates the need for components that provide an external supply of the dehybridization reagent (hydroxide or formamide), making it particularly attractive for use in portable devices. Most importantly, though, the on-chip generation of hydroxide allows the base to be generated in a localized manner with a coupled ability to fine tune the temporal and spatial profiles of the hydroxide ions released using programmed current pulses in conjunction with an externally actuated device flow.

3.3.3. SNP discrimination via alkaline dehybridization

We used the alkaline dehybridization mechanism as a means to discriminate between

PM and MM DNA. To do so, the WE was subjected to a series of current pulses of varying durations at a potential sufficient to drive the ORR. The region of the magnetically held beads was monitored simultaneously by fluorescence microscopy. Figure 3.5(a) shows a plug formed by a mixture of MM1 (green) and PM (red) DNA duplex-coated beads before the application of the current pulse. The sequence of micrographs in Figure 3.5(a-d) illustrate that these two DNA complexes can be discriminated effectively using a sequence of current pulses of varying duration. The sample for this model demonstration was a mixture comprised of equal amounts of independently prepared PM (red) and MM1 (green) duplex-coated beads. The image of Figure 3.5(a) shows the collection of this mixture of beads from a flowing stream (an externally actuated linear displacement relocation of 9×10^{-3} m/sec) in the form of a closely packed plug in the region above the embedded magnet.

The system was then interrogated using a stop-flow program correlated with a series of cathodic pulses applied at the WE upstream of the bead bed. The response is illustrated in the series of images given in Figure 3.5(b-c). In these experiments, a plug of hydroxide ions (Figure 3.6) was generated by the application of the cathodic current pulse(s) at the WE (located outside of field of view on the left side of the frame in Figure 3.5(a-d)) with the flow stopped, after which the entire plug of base was forced from the region of the WE in the direction of the beads using a hydrodynamic flow of buffer (~ 4×10^{-5} m/sec) driven by a syringe pump. The image shown in Figure 3.5(b) is a

fluorescence micrograph taken after an alkaline plug generated by a 34 s square wave potentiostatic pulse at ε = -0.6 V (Ag) had passed the bead plug. One sees from this image that this exposure to base substantially depletes the MM1 DNA while only minimally affecting the red intensity that corresponds to PM DNA duplex.

The application of two additional potentiostatic current pulses leads to a nearly complete removal of the MM1 DNA; the red intensity, though diminished, evidences a selectivity favoring the retention of the PM-DNA (Figure 3.5(c)). The exhaustive desorption of the PM DNA requires a more extensive exposure to high pH. An intensity analysis of Figure 3.5(c) reveals that the sequence of three 34 s potentiostatic current pulses decreases the red intensity (and its correlated population of PM-DNA) to ~ 67 % of its initial value. The application of a fourth, slightly longer, pulse (36 s) led to a further reduction to ~ 17 % of the initial red intensity. One additional pulse lead to a nearly complete desorption of the PM DNA via the alkaline-mediated dehybridization, the measured red intensity being < 5 % of its initial value (Figure 3.5(d)).

The graph presented in Figure 3.5(e) treats the trends in the data described above more quantitatively. The composite figure shows plots of total intensity (red + green) as well as a ratio of red and green intensities as a function of the total charge generated by the potentiostatic pulses. The data used to construct these plots were measured in a separate set of experiments using excitation and collection protocols selective for the high

sensitivity detection of each duplex form, as the fluorescence intensities used to construct the composite images of Figure 3.5(a-d) are too low to quantify accurately.

The latter data (Figure 3.5(e)) reveal that the total (red + green) intensity decreases progressively with the increasing amount of cathodic charge passed in the cell via the ORR. This suggests that a progressive desorption of target DNA strands from the probe-conjugated beads (via alkaline dehybridization) occurs during the course of the experiment. The ratio of the red and green intensities, corresponding to the changing proportion of PM and MM1-bearing DNA duplexes in the bead plug increases dramatically—reaching a limiting value that is about 70 times that of the initial value. The subsequent decline noted in this ratio reflects the ultimate depletion of the PM-DNA (and the decay of the PM-intensity level to that of the background). Though far from optimized, these data demonstrate that alkaline dehybridization, driven in a pulsatile form, can effect a kinetic discrimination of a SNP—doing so here for a single-base mismatch in a 21-base-long sequence.

We tested the discrimination protocol on two additional ssDNA targets (MM2 and MM3, Table 3.1). Each forms a single mismatch with the probe ssDNA. The resulting SNPs, however, differ from the one formed by MM1 in terms of not only the type of the mismatched pair but also the location of the SNP. Compared to the C•T pair that was in the center of the MM1-probe duplex, MM2 resulted in a G•T mismatched pair that was

three-bases away from the 3' end, while MM3 formed an A•G mismatched pair localized at three-bases away from the 5' end. As illustrated by a sequence of fluorescence micrographs (Figure 3.7), the method is able to selectively dehybridize MM2 and MM3 from a mixture of mismatched and perfectly matched DNA duplex-beads.

3.3.4. Recapture efficiency of the beads

We examined the recapture efficiency of this system, and its stability, by performing repetitive hybridization/dehybridization cycles on a single plug of beads. In one representative experiment, six hybridization/dehybridization cycles were performed to test the recapture efficiency for a PM target ss-DNA and the processes monitored by fluorescence microscopy. These data are presented in Figure 3.8, which shows a plot of the fluorescence intensities measured after each capture (C1-C7) and release (R1-R6) step. The signal/background ratio measured over a common rectangular area at the leading edge of the plug (illustrated by the 0.4 x 0.75 mm box overlaying micrograph C1) was used to construct this plot. Representative fluorescence micrographs taken at different stages of the process are also shown. These results illustrate the reproducibility of the in-device DNA hybridization/dehybridization reactions over replicate capture and release cycles, demonstrating that multiple analyses can be carried out using a single set of agarose beads. We note that the slight variations seen in this experiment are likely due to a rearrangement of beads that is driven by the hydrodynamic

flow over the course of the experiment. Evidence of such rearrangements can be seen in the micrographs (C1 and C5) shown in Figure 3.8.

3.4. CONCLUSION

A hybrid-PDMS microfluidic device embedding a microelectrochemical reactor can be used to discriminate SNPs in a 21-base oligonucleotide via an electrochemically-actuated alkaline dehybridization process. The system exploits a passive reagent delivery design, using the O_2 that readily permeates the PDMS structures of the device as the precursor for OH^- generated via the ORR.

The SNP discrimination mechanism, as currently embodied in this device design, exploits the impacts of mass-transfer effects on the sequence-sensitive kinetics of alkaline dehybridization. At this point, the design of the device is far from optimized and one can envision several areas where subsequent improvements might be made. First, we used an arbitrary limit of ~ 1 hour to complete one cycle of the on-chip hybridization/dehybridization in the present work. This cycle time can be dramatically improved because of the rapid kinetics intrinsic to the bead-based systems employed here. Second, a relatively high concentration (10^{-6} M) of the target DNA was used in the hybridization step for convenience. We believe that the device should be able to detect concentrations that are orders of magnitude lower than this value. The sensitivity of the device is mainly limited by the efficiency of bead-based systems and the capabilities of

fluorescence microscopy, both of which has been well studied and known to be extremely sensitive. In addition, the sensitivity can be improved further by coupling the device with a DNA amplification module. Third, a purification factor of 70x was achieved by this simple design. The pulsatile release of the OH^- here uses a reagent that is generated at a single electrode, a design that we believe innately limits the nature of the pH profiles (temporal and spatial) that can be programmed. Alternatively, an array system integrating individually addressable electrodes should enable a more precise control over the kinetics of multiple base triggered reactions. Developing such designs, however, will require a deeper understanding of the dynamics and chemical sensitivities of the alkaline dehybridization of oligo-DNA duplexes. Such understandings, we believe, will lead to device design rules that can exploit this sensitivity in technologically useful ways.

3.5. ACKNOWLEDGEMENTS

This work was supported by the National Science Foundation (CHE0097096) and used facilities of the Center for Microanalysis of Materials at UIUC supported by the U.S. Department of Energy, Division of Materials Sciences under Award No. DEFG02-91-ER45439. The authors gratefully acknowledge useful discussion with Dr. William Childs during the early stages of this project.

3.6. FIGURES AND TABLE

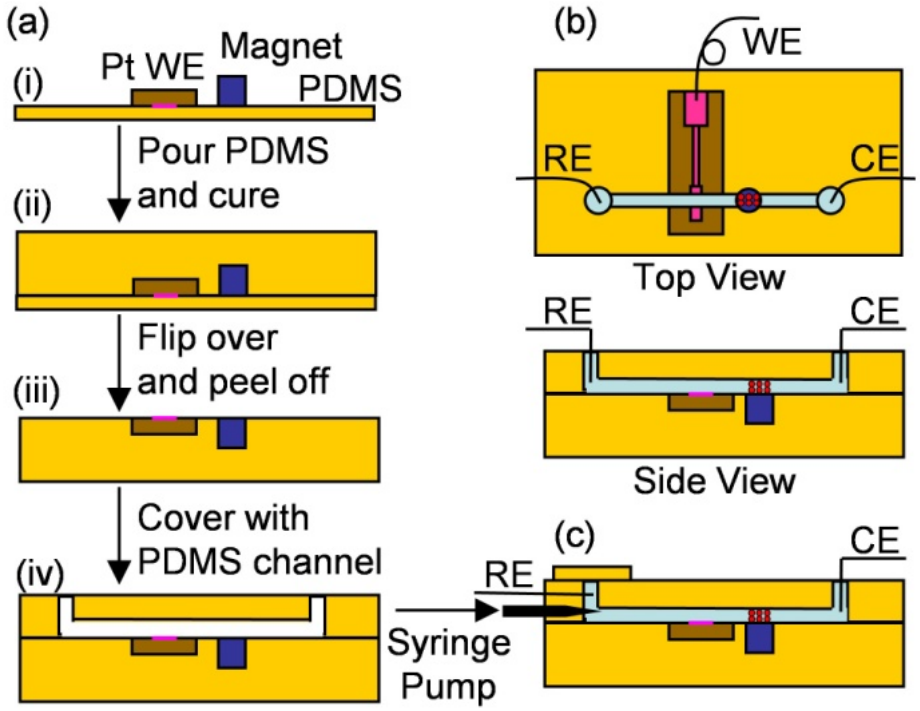

Figure 3.1: Schematic presentation of (a) the fabrication procedure, (b) the top and side views of the assembled device, and (c) the side view of an assembled device when a programmable syringe pump is incorporated to actuate flow.

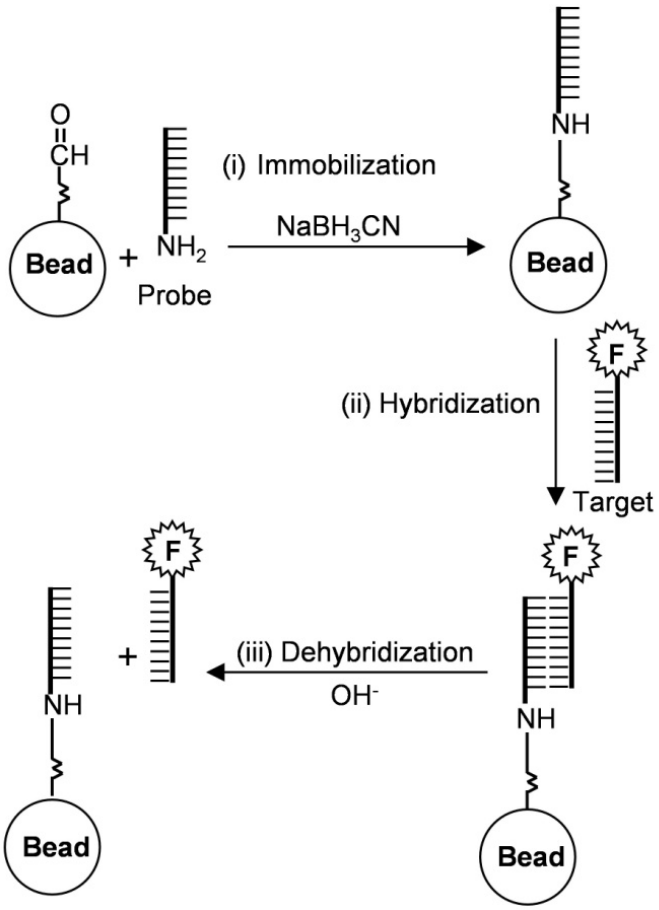

Figure 3.2: Schematic representations of the DNA (i) immobilization, (ii) hybridization, and (iii) dehybridization procedures.

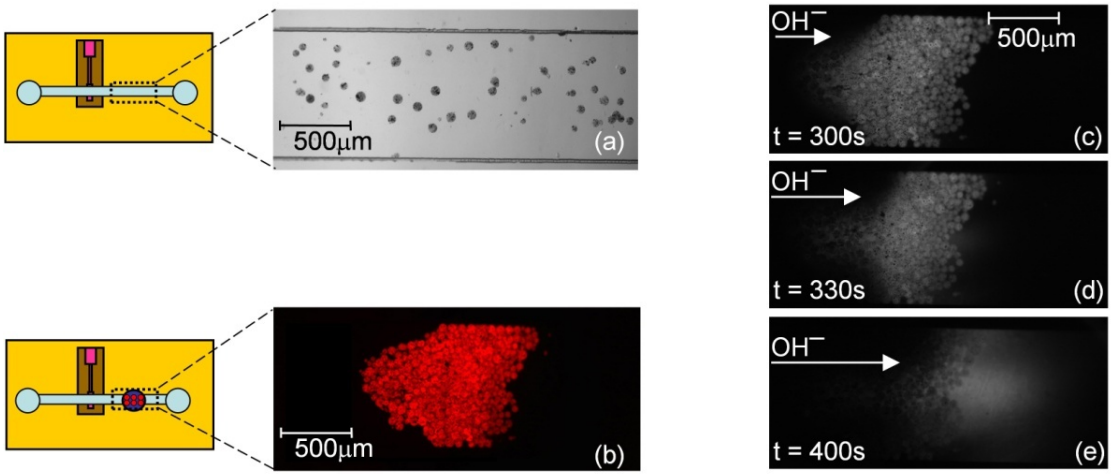

Figure 3.3: (a) An optical image of magnetic agarose beads inside the channel of a model device. (b) Fluorescence micrograph of a plug of PM duplex coated magnetic agarose beads positioned above the embedded magnet. The PM target was dynamically captured by the Probe using an on-chip protocol. (c-e) Fluorescence micrographs of the PM duplex coated agarose beads taken at 300 s (c), 330 s (d) and 400 s (e) after the beginning of the potential step at the WE.

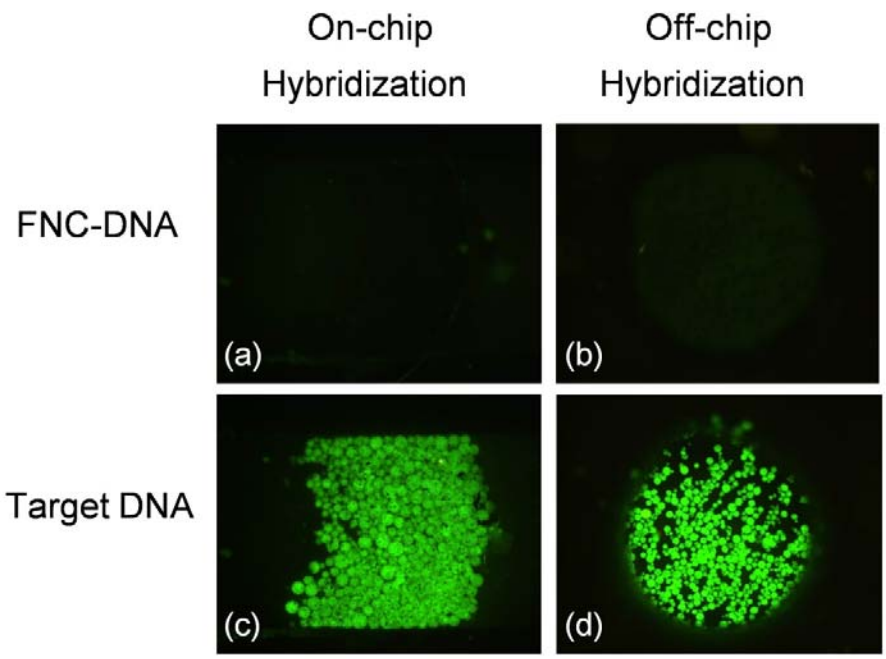

Figure 3.4: Fluorescence micrographs of control experiments examining the relative importance of nonspecific adsorption of various analytical DNA samples on probe conjugated beads, studies carrying out using both *in situ* and *ex situ* hybridization protocols as described in the experimental methods. In these experiments fluorescence micrographs were recorded after mixing the probe-conjugated agarose beads with either a fully noncomplementary DNA (FNC-DNA: (a) and (b) above) and Target DNA containing a SNP ((c) and (d) above). The fully noncomplementary DNA used here had the structure: 5'-Oregon Green 488-TCA GAG CAT ATA AAG TGA GGT -3'.

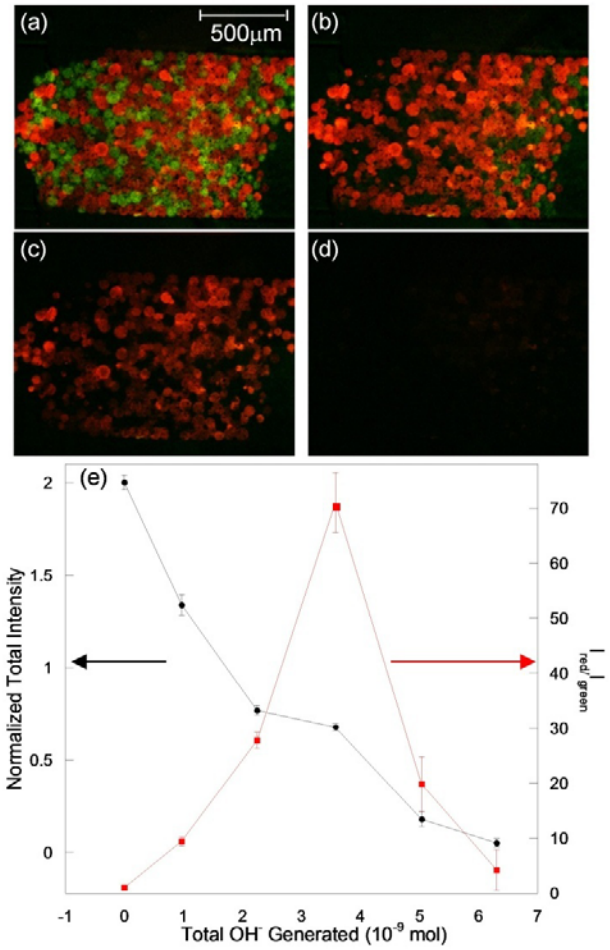

Figure 3.5: Fluorescence micrographs of a mixed plug of PM (red) and MM1 (green) conjugated magnetic core agarose beads bearing a covalently linked 21 base sequence. The image in (a) corresponds to the starting plug, one formed from the capture of an equal mixture of beads bearing PM and MM1 duplexes. The images in (b-c) show the progressive alkaline dehybridization and elution of the ss- MM1 and PM targets using pulsatile infusions of high pH generated by the ORR. The image in (d) illustrates the exhaustive desorption of the ss-PM target via an exposure to a slightly higher pH. The plots in (e) show the total intensity (red + green), and a ratio of red and green intensities as a function of the total OH^- generated by the potentiostatic pulses.

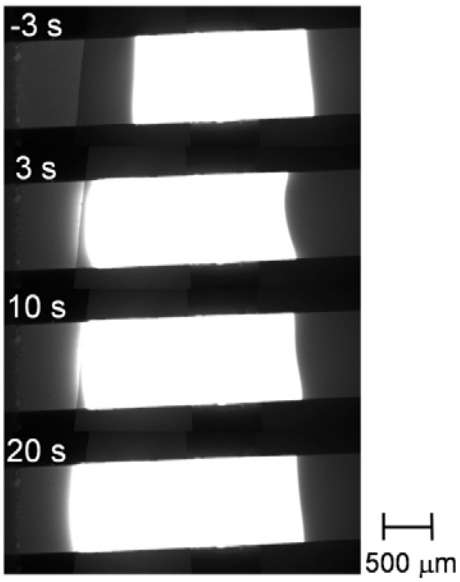

Figure 3.6: A sequence of fluorescence micrographs showing the electrochemical generation of a high pH plug (pH ~ 11.7) and its pressure driven motion as visualized using fluorescein as a pH sensitive dye. The region of high emission intensity corresponds to a high pH zone created in the vicinity of an embedded Pt working electrode. The edges of the plug assumed a parabolic shape when it is pushed by a syringe pump at a rate of 3 x 10^{-5} m/sec using a flow of 0.3 μl/min (here in the direction of the bead bed lying out of the view toward the left side of the image). The electrochemically driven fluid motion[6] is relatively small under the conditions used given the rather large cross sectional area of this device's channel system. The micrographs reveal that there is some hysteresis in the actuation of the pressure driven flow, one we believe to be related to a backpressure created by the bead plug. The time that the syringe pump was actuated was set as time zero.

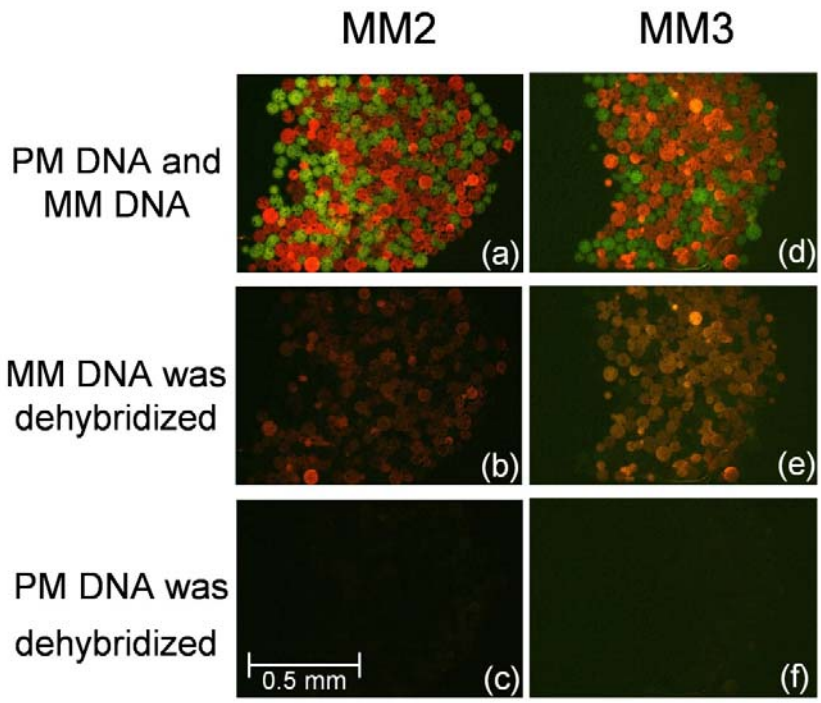

Figure 3.7: Fluorescence micrographs of a mixed plug of PM and MM conjugated magnetic core agarose beads bearing a covalently linked 21 base sequence. MM2 was used in the images (a)-(c) and MM3 was used in the images (d)-(f), respectively. The images in (a) and (d) correspond to the starting plugs, ones formed from the capture of an approximately equal mixture of beads bearing PM and MM duplexes. The images in (b) and (e) illustrate selectivity in the alkaline dehybridization of the ss- MM and PM targets using pulsatile infusions of high pH generated by the ORR. The images in (c) and (f) illustrates the exhaustive desorption of the ss-PM target via an exposure to a slightly higher pH.

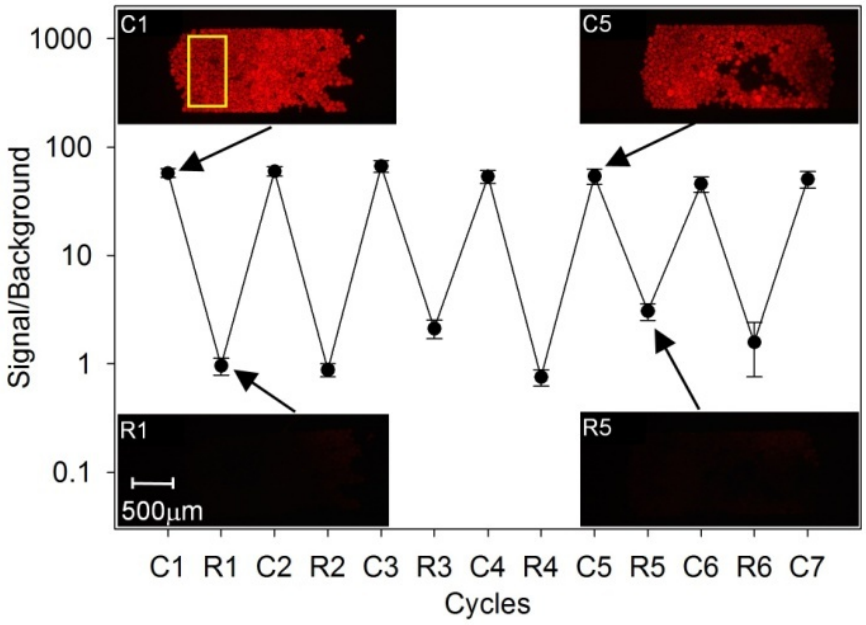

Figure 3.8: A plot of fluorescence intensity as a function of the number of PM-DNA capture (C1-C7) and release (R1-R6) cycles. The signal/background ratio was measured after each hybridization and dehybridization procedure over a common rectangular area residing at the leading edge of the agarose bead plug.

Table 3.1: Oligonucleotide sequence used in SNP analysis experiments

Name	Sequence
Probe	5'-CCT GGG AAA GT**C** CCC TCA ACA -C_6-NH_2-3'
PM Target	5'-Cal Fluo 610-TGT TGA GGG **G**AC TTT CCC AGG-3'
MM1 Target	5'-Oregon Green 488-TGT TGA GGG **T**AC TTT CCC AGG-3'
MM2 Target	5'-Oregon Green 488-TGT TGA GGG GAC TTT CC**T** AGG-3'
MM3 Target	5'-Oregon Green 488-TGT **G**GA GGG GAC TTT CCC AGG-3'

3.7. REFERENCES

(1) Sachidanandam, R.; Weissman, D.; Schmidt, S. C.; Kakol, J. M.; Stein, L. D. *et al* "A map of human genome sequence variation containing 1.42 million single nucleotide polymorphisms"; *Nature* **2001**, *409*, 928.

(2) Wang, D. G.; Fan, J.-B.; Siao, C.-J.; Berno, A.; Young, P. *et al* "Large-Scale Identification, Mapping, and Genotyping of Single-Nucleotide Polymorphisms in the Human Genome"; *Science* **1998**, *280*, 1077.

(3) Kruglyak, L. "Prospects for whole-genome linkage disequilibrium mapping of common disease genes"; *Nat. Genet.* **1999**, *22*, 139.

(4) McCarthy, J. J.; Hilfiker, R. "The use of single-nucleotide polymorphism maps in pharmacogenomics"; *Nat. Biotechnol.* **2000**, *18*, 505.

(5) Kassam, S.; Meyer, P.; Corfield, A.; Mikuz, G.; Sergi, C. "Single nucleotide polymorphisms (SNPs): History, biotechnological outlook and practical applications"; *Curr. Pharmacogenomics* **2005**, *3*, 237.

(6) Stoneking, M. "Single nucleotide polymorphisms: From the evolutionary past"; *Nature* **2001**, *409*, 821.

(7) Kruglyak, L. "The use of a genetic map of biallelic markers in linkage studies"; *Nat. Genet.* **1997**, *17*, 21.

(8) Hacia, J. G.; Fan, J. B.; Ryder, O.; Jin, L.; Edgemon, K. *et al* "Determination of ancestral alleles for human single-nucleotide polymorphisms using high-density oligonucleotide arrays"; *Nat. Genet.* **1999**, *22*, 164.

(9) Syvanen, A.-C. "Accessing genetic variation: genotyping single nucleotide polymorphisms"; *Nat. Rev. Genet.* **2001**, *2*, 930.

(10)Weber, J.; Barbier, V.; Pages-Berhouet, S.; Caux-Moncoutier, V.; Stoppa-Lyonnet, D. *et al* "A High-Throughput Mutation Detection Method Based on Heteroduplex Analysis Using Graft Copolymer Matrixes: Application to Brca1 and Brca2 Analysis"; *Anal. Chem.* **2004**, *76*, 4839.

(11) Handal, M. I.; Ugaz, V. M. "DNA mutation detection and analysis using miniaturized microfluidic systems"; *Expert Rev. Mol. Diagn.* **2006**, *6*, 29.

(12) Nataraj, A. J.; Olivos-Glander, I.; Kusukawa, N.; W. Edward Highsmith, J. "Single-strand conformation polymorphism and heteroduplex analysis for gel-based mutation detection"; *Electrophoresis* **1999**, *20*, 1177.

(13) Gelfi, C.; Righetti, S. C.; Zunino, F.; Torre, G. D.; Pierotti, M. A. *et al* "Detection of p53 point mutations by double-gradient, denaturing gradient gel electrophoresis"; *Electrophoresis* **1997**, *18*, 2921.

(14) Underhill, P. A.; Jin, L.; Lin, A. A.; Mehdi, S. Q.; Jenkins, T. *et al* "Detection of Numerous Y Chromosome Biallelic Polymorphisms by Denaturing High-Performance Liquid Chromatography"; *Genome Res.* **1997**, *7*, 996.

(15) Germer, S.; Higuchi, R. "Single-Tube Genotyping without Oligonucleotide Probes"; *Genome Res.* **1999**, *9*, 72.

(16) Kuppuswamy, M. N.; Hoffman, J. W.; Kasper, C. K.; Spitzer, S. G.; Groce, S. L. *et al* "Single Nucleotide Primer Extension to Detect Genetic Diseases: Experimental Application to Hemophilia B (Factor IX) and Cystic Fibrosis Genes"; *Proc. Natl. Acad. Sci. U.S.A.* **1991**, *88*, 1143.

(17) Barany, F. "Genetic Disease Detection and DNA Amplification Using Cloned Thermostable Ligase"; *Proc. Natl. Acad. Sci. U.S.A.* **1991**, *88*, 189.

(18) Okazaki, S. "Resolution limits of optical lithography"; *J. Vac. Sci. Technol. B* **1991**, *9*, 2829.

(19) Ronse, K. "Optical lithography-a historical perspective"; *C. R. Physique* **2006**, *7*, 844.

(20) Heller, M. J. "DNA microarray technology: Devices, systems, and applications"; *Annu. Rev. Biomed. Eng.* **2002**, *4*, 129.

(21) Ramsay, G. "DNA chips: State-of-the-art"; *Nat. Biotechnol.* **1998**, *16*, 40.

(22) Syvanen, A. C. "Toward genome-wide SNP genotyping"; *Nat. Genet.* **2005**, *37*,

S5.

(23) Schena, M.; Shalon, D.; Davis, R. W.; Brown, P. O. "Quantitative Monitoring of Gene Expression Patterns with a Complementary DNA Microarray"; *Science* **1995**, *270*, 467.

(24) Dufva, M. "Fabrication of high quality microarrays"; *Biomol. Eng.* **2005**, *22*, 173.

(25) Ng, J. K.-K.; Liu, W.-T. "Miniaturized platforms for the detection of single-nucleotide polymorphisms"; *Anal. Bioanal. Chem.* **2006**, *386*, 427.

(26) Whitesides, G. M. "The origins and the future of microfluidics"; *Nature* **2006**, *442*, 368.

(27) Reyes, D. R.; Iossifidis, D.; Auroux, P.-A.; Manz, A. "Micro Total Analysis Systems. 1. Introduction, Theory, and Technology"; *Anal. Chem.* **2002**, *74*, 2623.

(28) Auroux, P. A.; Iossifidis, D.; Reyes, D. R.; Manz, A. "Micro total analysis systems. 2. Analytical standard operations and applications"; *Anal. Chem.* **2002**, *74*, 2637.

(29) Hauptmann, P. R. "Selected examples of intelligent (micro) sensor systems: state-of-the-art and tendencies"; *Meas. Sci. Technol.* **2006**, *17*, 459.

(30) Pumera, M.; Merkoci, A.; Alegret, S. "New materials for electrochemical sensing VII. Microfluidic chip platforms"; *Trends Anal. Chem.* **2006**, *25*, 219.

(31) Xia, Y.; Whitesides, G. M. "Soft lithography"; *Angew. Chem. Int. Edit.* **1998**, *37*, 550.

(32) Verpoorte, E. "Microfluidic chips for clinical and forensic analysis"; *Electrophoresis* **2002**, *23*, 677.

(33) Sun, Y.; Kwok, Y. C. "Polymeric microfluidic system for DNA analysis"; *Anal. Chim. Acta* **2006**, *556*, 80.

(34) Vahedi, G.; Kaler, K.; Backhouse, C. J. "An integrated method for mutation detection using on-chip sample preparation, single-stranded conformation polymorphism,

and heteroduplex analysis"; *Electrophoresis* **2004**, *25*, 2346.

(35) Buch, J. S.; Rosenberger, F.; Highsmith, W. E., Jr.; Kimball, C.; DeVoe, D. L. *et al* "Denaturing gradient-based two-dimensional gene mutation scanning in a polymer microfluidic network"; *Lab Chip* **2005**, *5*, 392.

(36) Hashimoto, M.; Hupert, M. L.; Murphy, M. C.; Soper, S. A.; Cheng, Y. W. *et al* "Ligase Detection Reaction/Hybridization Assays Using Three-Dimensional Microfluidic Networks for the Detection of Low-Abundant DNA Point Mutations"; *Anal. Chem.* **2005**, *77*, 3243.

(37) Hebert, N. E.; Brazill, S. A. "Microchip capillary gel electrophoresis with electrochemical detection for the analysis of known SNPs"; *Lab Chip* **2003**, *3*, 241.

(38) Verpoorte, E. "Beads and chips: New recipes for analysis"; *Lab Chip* **2003**, *3*, 60N.

(39) Seong, G. H.; Zhan, W.; Crooks, R. M. "Fabrication of microchambers defined by photopolymerized hydrogels and weirs within microfluidic systems: Application to DNA hybridization"; *Anal. Chem.* **2002**, *74*, 3372.

(40) Kim, J.; Heo, J.; Crooks, R. M. "Hybridization of DNA to Bead-Immobilized Probes Confined within a Microfluidic Channel"; *Langmuir* **2006**, *22*, 10130.

(41) Fan, Z. H.; Mangru, S.; Granzow, R.; Heaney, P.; Ho, W. *et al* "Dynamic DNA hybridization on a chip using paramagnetic beads"; *Anal. Chem.* **1999**, *71*, 4851.

(42) Kohara, Y.; Noda, H.; Okano, K.; Kambara, H. "DNA probes on beads arrayed in a capillary, 'Bead-array', exhibited high hybridization performance"; *Nucl. Acids Res.* **2002**, *30*, e87.

(43) Ng, J. K.-K.; Feng, H.; Liu, W.-T. "Rapid discrimination of single-nucleotide mismatches using a microfluidic device with monolayered beads"; *Anal. Chim. Acta* **2007**, *582*, 295.

(44) Ali, M. F.; Kirby, R.; Goodey, A. P.; Rodriguez, M. D.; Ellington, A. D. *et al* "DNA Hybridization and Discrimination of Single-Nucleotide Mismatches Using

Chip-Based Microbead Arrays"; *Anal. Chem.* **2003**, *75*, 4732.

(45) Russom, A.; Ahmadian, A.; Andersson, H.; Nilsson, P.; Stemme, G. "Single-nucleotide polymorphism analysis by allele-specific extension of fluorescently labeled nucleotides in a microfluidic flow-through device"; *Electrophoresis* **2003**, *24*, 158.

(46) Taylor, J. D.; Briley, D.; Nguyen, Q.; Long, K.; Iannone, M. A. *et al* "Flow cytometric platform for high-throughput single nucleotide polymorphism analysis"; *BioTechniques* **2001**, *30*, 661.

(47) Iannone, M. A.; Taylor, J. D.; Chen, J.; Li, M.-S.; Rivers, P. *et al* "Multiplexed single nucleotide polymorphism genotyping by oligonucleotide ligation and flow cytometry"; *Cytometry* **2000**, *39*, 131.

(48) Barber, R. "Alkaline denaturation of DNA and the stability of the helix"; *Biochim. Biophys. Acta* **1971**, *238*, 60.

(49) Ageno, M.; Dore, E.; Frontali, C. "The Alkaline denaturation of DNA"; *Biophys. J.* **1969**, *9*, 1281.

(50) Luck, G.; Zimmer, C.; Snatzke, G.; Sondgerath, G. "Optical Rotatory Dispersion and Circular Dichroism of DNA from Various Sources at Alkaline pH"; *Eur. J. Biochem.* **1970**, *17*, 514.

(51) Birnboim, H. C.; Doly, J. "A rapid alkaline extraction procedure for screening recombinant plasmid DNA"; *Nucleic Acids Res.* **1979**, *7*, 1513.

(52) Mala, Z.; Kleparnik, K.; Bocek, P. "Highly alkaline electrolyte for single-stranded DNA separations by electrophoresis in bare silica capillaries"; *J. Chromatogr., A* **1999**, *853*, 371.

(53) Zimmer, C. "Alkaline denaturation of DNA's from various sources"; *Biochim. Biophys. Acta* **1968**, *161*, 584.

(54) Sosnowski, R. G.; Tu, E.; Butler, W. F.; O'Connell, J. P.; Heller, M. J. "Rapid determination of single base mismatch mutations in DNA hybrids by direct electric field

control"; *Proc. Natl. Acad. Sci. USA* **1997**, *94*, 1119.

(55) Mitrovski, S. M.; Nuzzo, R. G. "An electrochemically driven poly(dimethylsiloxane) microfluidic actuator: oxygen sensing and programmable flows and pH gradients"; *Lab Chip* **2005**, *5*, 634.

(56) Duffy, D. C.; McDonald, J. C.; Schueller, O. J. A.; Whitesides, G. M. "Rapid Prototyping of Microfluidic Systems in Poly(dimethylsiloxane)"; *Anal. Chem.* **1998**, *70*, 4974.

(57) Mitrovski, S. M.; Nuzzo Ralph, G. "A passive microfluidic hydrogen air fuel cell with exceptional stability and high performance "; *Lab Chip* **2006**, *6*, 353.

(58) Childs, W. R.; Nuzzo, R. G. "Decal transfer microlithography: A new soft-lithographic patterning method"; *J. Am. Chem. Soc.* **2002**, *124*, 13583.

(59) Monahan, J.; Gewirth, A. A.; Nuzzo, R. G. "A method for filling complex polymeric microfluidic devices and arrays"; *Anal. Chem.* **2001**, *73*, 3193.

(60) Peelen, D.; Smith, L. M. "Immobilization of amine-modified oligonucleotides on aldehyde-terminated alkanethiol monolayers on gold"; *Langmuir* **2005**, *21*, 266.

(61) Martin, M. M.; Lindqvist, L. "The pH dependence of fluorescein fluorescence"; *J. Lumin.* **1975**, *10*, 381.

(62) Pamme, N. "Magnetism and microfluidics"; *Lab Chip* **2006**, *6*, 24.

(63) Smistrup, K.; Hansen, O.; Bruus, H.; Hansen, M. F. "Magnetic separation in microfluidic systems using microfabricated electromagnets--experiments and simulations"; *J. Magn. Magn. Mater.* **2005**, *293*, 597.

(64) Pregibon, D. C.; Toner, M.; Doyle, P. S. "Magnetically and Biologically Active Bead-Patterned Hydrogels"; *Langmuir* **2006**, *22*, 5122.

(65) Polsky, F.; Edgell, M. H.; Seidman, J. G.; Leder, P. "High capacity gel preparative electrophoresis for purification of fragments of genomic DNA"; *Anal. Biochem.* **1978**, *87*, 397.

(66) Smith, S. S.; Gilroy, T. E.; Ferrari, F. A. "The influence of agarose-DNA affinity

on the electrophoretic separation of DNA fragments in agarose gels"; *Anal. Biochem.* **1983**, *128*, 138.

(67) Varilova, T.; Madera, M.; Pacakova, V.; Stulik, K. "Separation Media in Affinity Chromatography of Proteins - A Critical Review"; *Curr. Proteomics* **2006**, *3*, 55.

(68) Duro, G.; Izzo, V.; Barbieri, R. "Methods for recovering nucleic acid fragments from agarose gels"; *J. Chromatogr.: Biomed. Appl.* **1993**, *618*, 95.

(69) Peacock, A. C.; Dingman, C. W. "Molecular weight estimation and separation of ribonucleic acid by electrophoresis in agarose-acrylamide composite gels"; *Biochemistry* **1968**, *7*, 668.

(70) Shainoff, J. R. "Zonal immobilization of proteins"; *Biochem. Biophys. Res. Commun.* **1980**, *95*, 690.

(71) Mateo, C.; Palomo, J. M.; Fuentes, M.; Betancor, L.; Grazu, V. *et al* "Glyoxyl agarose: A fully inert and hydrophilic support for immobilization and high stabilization of proteins"; *Enzyme Microb. Technol.* **2006**, *39*, 274.

(72) In this particular case the pH value estimated by considering the buffer effect of the PBS was similar (to within ~ 0.1 pH units) to what we calculated using the simpler model based on pure water due to the fact that the pulse completely overwhelms its buffer capacity.

Chapter 4 Genotyping by Alkaline Dehybridization Using Graphically Encoded Particles

Note: This chapter is adapted from a manuscript that is in preparation for *Angew. Chem., Int. Ed.* as: Huaibin Zhang, Adam J. DeConinck, Scott C. Slimmer, Patrick S. Doyle, Jennifer A. Lewis, and Ralph G. Nuzzo, Genotyping by Alkaline Dehybridization Using Graphically Encoded Particles.

4.1. INTRODUCTION

Single-nucleotide polymorphisms (SNPs), a type of variation that involves one change in a single nucleotide, are the most commonly encountered and most important DNA sequence variation..[1-2] Point-of-Care (POC) diagnostic devices that discriminate SNP genotypes[3] have potential applications in global healthcare,[4-5] epidemic control,[6] and forensic analysis[7-8]. An ideal POC device should be portable, inexpensive to fabricate, easy to operate, and capable of rapid discrimination of multiple analytes.[9-10] Miniaturization of existing bench-top discrimination methods and assay formats has yet to adequately meet these requirements.[10-11] Enzyme-assisted genotyping methods[1] generally require expensive, and often chemically sensitive, reagents such as DNA ligases or polymerases that may not be ideal for POC applications. Recent studies, however, have shown impressive progress in developing novel non-enzymatic analysis methods[12-15], some of which show promise for the analysis of genomic DNA without PCR amplification.[16-17]

Most non-enzymatic genotyping methods are based on allele-specific oligonucleotide (ASO) probes which form either perfectly matched (PM) or single base mismatched (MM) duplexes with the target.[1,18] These duplexes are discriminated based on their stability under a certain discriminating condition, most often temperature.[1] One of the most widely used methods, the so called GeneChip (Affymetrix), requires careful optimization of the assay and reaction conditions so that a single temperature can discriminate many SNPs on an array.[19-20] Newer methods, such as Dynamic Allele-Specific Hybridization (DASH),[21-22] circumvent this challenge by monitoring the dehybridization process dynamically in a temporal[21] or spatial[23] temperature gradient, in which the optimal discrimination condition is achieved at one point of the gradient. These methods, however, require precise temperature control with dedicated instrumentation which may not be suitable for POC applications.

Herein, we report a non-enzymatic, isothermal, versatile, and potentially high-throughput genotyping approach that uses an alkaline discrimination method acting on a multiplexed particle array. SNP discrimination using alkaline dehybridization[24-27] has long been neglected because the pH range in which thermodynamic discrimination can be performed is quite narrow ($\Delta pH < 0.3$). We have previously reported, however, that SNPs can be discriminated by the kinetic differences exhibited in the dehybridization of PM and MM DNA duplexes in an alkaline solution using fluorescence microscopy.[28] The current work extends these observations and provides a means for implementing a

fully multiplexed analytical assay based on this mechanism of genotyping. We use an alkaline-based dehybridization that provides SNP discrimination isothermally using a gel bead sorting system that simplifies the device design, uses simple reagents (e.g., NaOH), and enables rapid analysis. We also enhance the versatility of this technique by using a graphically-encoded multifunctional hydrogel particle array for multiplexing.[29] This approach provides significant advantages over existing planar microarray technology,[30] as it allows for faster mass transfer, rapid probe-set modification, and potentially better quality control.[31]

4.2. RESULTS AND DISCUSSION

Multifunctional hydrogel particles incorporating ASO probes in distinct regions are fabricated using stop-flow lithography (SFL, Figure 4.1(a)).[29,32-37] Three monomer streams flow side-by-side in a microchannel (Figure 4.1(a)) in the laminar flow regime, minimizing mixing between the distinct streams. The central stream contains 60% polyethylene glycol diacrylate (PEGDA) loaded with an acrylate-modified dye; each side stream contains 20% PEGDA, 40% polyethylene glycol (PEG) and a selected acrylate-modified 21-base DNA probe. Exposing the monomer streams to a burst of UV light through a photomask produces 2D extruded particles where the shape and encoding of the particle (Figure 4.1(b) and (c)) are determined by the photomask. The DNA probe regions on the particle can be visualized after hybridizing fluorescently labeled target

DNA (Figure 4.1(d)). When several sets of particles are mixed and injected gently into a microfluidic channel with a PDMS dam (Figure 4.1(e)), they form a monolayer particle array for easy visualization (Figure 4.1(f)). These particles may then be ejected out the channel using a steep, pulsed increase of the fluid flow rate.

Using a hydrogel network as a solid support for co-polymerized DNA probes provides an ideal environment for quantitative DNA analysis with fast kinetics, low fluorescence background, and high target capacity.[29,38] The PEGDA/PEG mixture forms a semi-interpenetrating network[39] with tunable porosity, enabling control over mass transfer through the hydrogel-water interface.[38] Fabrication in the laminar flow regime allows immobilization of allele-specific probes in distinct regions for easy comparison, and SFL enables high-throughput fabrication with small variation between particles within a single batch. In this work numbers and letters are used as a graphical encoding for straightforward identification of particles, but more complex encodings such as barcodes may be used for machine-based identification.[29]

A schematic for genotyping using alkaline dehybridization and encoded particles is illustrated in Figure 4.1(g). When particles (labeled ":2") incorporating probes P3 and P1 are mixed with a fluorescently labeled homozygote (T1), both sides of the particle hybridize and fluoresce if a stringency condition is not applied ((i) in Figure 4.1(g)). The specific sequences for P3, P1, T1 and other DNAs used in this work are given in Table

4.1. The “colon” side of the :2 particle (i.e., P3) forms MM duplexes with a variant site in the center, while the “label” side (i.e., P1) forms PM duplexes. Increasing the pH of the surrounding medium results in dehybridization of the probe T1 from both sides, but the rate at which T1 dehybridizes is (as will be shown) faster for the MM case.[28] Within an appropriate time scale and pH range, the difference in dehybridization kinetics provides an easily measured temporal difference in the fluorescence intensity between the two sides ((ii) in Figure 4.1(g)), which evolves until both sides dehybridize completely ((iii) in Figure 4.1(g)). Dehybridization of the other homozygote, T3, provides a fluorescence difference with opposite sign, while a heterozygote sample (i.e., a mixture of hybridized T1 and T3) is expected to produce little or no difference between the two sides. The present work demonstrates that the temporal differences in fluorescence intensity between the two ends can be used effectively to discriminate genotypes.

To test this concept, three sets of P3/P1 particles labeled :2, :3 and :4 were fabricated, and hybridized with synthetic DNA targets T1, T3, and a 50/50 mixture of T1 and T3, respectively. These hybridized particles were then mixed together and injected into a microfluidic channel for assay. Phosphate buffer (pH 11.20) was injected into the channel at room temperature (22^{o}C), and the fluorescence intensity of the DNA duplexes during alkaline dehybridization was monitored using time-lapse fluorescence microscopy. The data was normalized and background corrected by calculating a time-dependent fluorescence retention ratio, $(I(t)-I_{min})/(I_{max}-I_{min})$, with maximum and minimum intensities

calculated for each probe region. Representative profiles of the fluorescence retention ratio are shown in Figure 4.2. As predicted, within a ~ 5 minutes dehybridization process, a significant intensity contrast is produced between either side of particles :2 and :3 (i.e., Figure 4.3(a) and Figure 4.3(b)) while particle :4 showed a much weaker intensity contrast (Figure 4.3(c)). To quantify the time-dependent intensity contrast for a given particle, we calculated the difference in the fluorescence retention ratio (Δ) between the "colon" and the "label" sides at all times and compared the different particle sets. The Δ curves of the three particles sets are distinctly different (Figure 4.3(d)). The negative peak in the Δ curve of particle set :2 reflects that the DNA duplexes at the "colon" side dehybridize faster than the "label" side, while the positive peak in particle set :3 indicates faster dehybridization on the "label" side.

In contrast to the single-peak behavior observed in each of the homozygous curves, the heterozygous curve shows a more complex double-peak behavior. The Δ curve for particle set :4 shows an initial positive peak followed by a negative peak, both with lower magnitude than the homozygous single-peak curves. This double-peak behavior appears to combine the behaviors observed in the two homozygous experiments, suggesting the presence of both PM and MM duplexes on each side (Figure 4.3(c)). It is interesting to note that the retention ratio observed on either side of the :4 particle set may be approximated by a linear combination of the observed retention ratios in the corresponding probe regions of the homozygous experiments(Figure 4.4). Further

quantitative studies are necessary to better interpret this behavior.

To simplify comparisons between the data sets we calculated the peak value Δ_m of each curve (i.e., Δ_{max} or Δ_{min} depending the absolute magnitude); for the "double-peak" heterozygous experiment we use the higher-magnitude negative peak. These Δ_m values for each particle in the array fall into three distinct groups corresponding to the three sets, as shown by the histogram in Figure 4.3(e). The use of Δ_m compensates to some extent for various types of system heterogeneity, and can be used autonomously as a single metric to make genotyping calls.

We performed similar experiments at 10^oC and 37^oC to evaluate the method's temperature sensitivity, and find the major difference to be in the time required to complete an experiment. The time required for the fluorescence intensity to fall to 5% of the initial value is approximately 60 minutes at 10 ^oC, 7 minutes at 22 ^oC, and 2 minutes at 37 ^oC (Figure 4.2). Our calculated Δ_m, however, is relatively insensitive to changes in temperature and remains a viable genotyping criterion. We verified statistical significance of this result using Welch's two-sample t-test, which showed the means of each Δ_m distribution to be significantly different from the other two in that experiment at 95 % confidence Figure 4.5(a)).

The sensitivity of the dehybridization rate to temperature presents some difficulties. At

higher temperatures the temporal resolution of the experiment may be insufficient for resolving the intensity contrast, while at lower temperatures the time required for experiments is greatly increased, reducing the utility in POC settings. This suggests that a multiplexed assay would require a detailed optimization for the different time scales involved. There exist modified procedures that could make such optimization unnecessary, however.

We therefore further tested this point by varying the mode of the dehybridization protocol, applying instead a temporal pH gradient to the particle assay so that an optimal stringency condition can be achieved for each SNP at any measurement temperature. To generate a temporal pH gradient, we injected a 0.02M NaOH solution at an increasing rate, mixing completely with a constant flow of water before reaching the particle assay (NaOH injection profile and estimated [OH-] and pH values are provided in Figure 4.6). Applying the same gradient at 10 ^{o}C, 22 ^{o}C and 37 ^{o}C for the three sets of P3/P1 particles shows similar discrimination to the constant pH buffer, with better discrimination at high temperature (Figure 4.5(b)). A standardized reaction condition not only minimizes the effort in optimization, but also generates better results.

The same protocols were applied to DNAs with the SNP site located three bases from the 5' end of the probe strand, rather than the center (as above). We fabricated three sets of particles incorporating probes P4 and P1 (Table 4.1), labeled :E, :F, and :K (Figure

4.1(f)), and hybridized separately with synthetic targets simulating three genotypes (Table 4.1, and key for Figure 4.5(d)). Both a constant pH 11.20 buffer (Figure 4.5(c)) and a pH gradient (Figure 4.5(d)) were applied to mixed sets of these particles, and Δ_m was calculated for each particle as previously described. As before, these values fall into clearly separated groups. In each of the twelve DNA/temperature/experiment combinations shown in Figure 4.5, the differences in distribution means are significant at the 95% confidence level. This result is most significant given that it is well known that SNPs located at the end of a DNA sequence are difficult to discriminate using thermal methods.[21] The clear discrimination shown here demonstrate the high sensitivity of this kinetic-based method even in this challenging context.

We further tested this genotyping approach using a "sandwich" tagging method (Figure 4.7(a)) on three clinically relevant mutations associated with thrombotic disorders, MTHFR (C→T), Factor II (G→A) and Factor V (G→A).[40] We fabricated three sets of particles, labeled :M, :FII, and :FV, each containing two 21-base ASO probes for the corresponding SNP. Probes for the wild-type sequence are always found on the "label" side, with the mutated sequence (mut) at the "colon" side. We prepared three mixtures of synthetic non-fluorescent target DNAs (~70 base long, Table 4.1) that simulate three combinations of homozygous or heterozygous samples. The target mixtures were hybridized with particle assays and rinsed ((i) in Figure 4.7(a)) before adding a mixture of three gene-specific, fluorescently labeled, secondary probes (30-base) ((ii) in Figure

4.7(a)). By carrying out an alkaline gradient experiment ((iii) in Figure 4.7(a)), we were able to straightforwardly determine the genotypes from the particle fluorescence at peak contrasts (Figure 4.7(b)). These results correspond correctly to the target composition. We believe this "sandwich" tagging scheme is useful for POC analysis of genomic DNA because it does not require labeling the target DNA and increases the specificity through two sequential hybridization steps of the sequence-specific probes. This specificity is necessary for analyzing highly complex genomic DNA.[16]

4.3. CONCLUSION

We herein demonstrate alkaline dehybridization as an effective alternative to temperature-based discrimination of SNPs. The kinetic difference of PM and MM duplexes dehybridization under alkaline conditions is effectively measured by the difference in fluorescence retention ratio, the peak value of which can serve as a simple metric for genotyping. We have demonstrated the utility of a pH gradient to discriminate target DNA sequences with different SNP insertion points over a range of temperatures, reducing optimization requirements. We combine this technique with the use of SFL-fabricated multifunctional encoded hydrogel particles to achieve high versatility. With the subattomole sensitivity of the hydrogel particle system demonstrated by the previous research,[38] the approach presented here may serve as a new route for analyzing unamplified genomic DNA.

4.4. EXPERIMENTAL

Microchannels for stop-flow lithography (SFL) and genotyping were fabricated by casting polydimethylsiloxane (PDMS, Sylgard 184, Dow Corning) off of photoresist masters. Single-layer masters for SFL channels were produced by spin-coating SU-8 50 (Microchem) at 2000 rpm for 30s, with a 5 min soft bake at 120 C, a 40 s 300 W UV exposure through a photomask, and a 5 min post-bake at 120 C. Two-layer masters incorporating a 40 um high dam for genotyping were similarly fabricated in two steps as above (spin-coat at 3500 rpm for 30 s for step), with an alignment step preceding the second exposure. PDMS elastomer and curing agent were mixed at a 10:1 ratio by weight and poured over masters, then baked at least 3 hours at 70^{o}C and peeled up to form the top surface of the channel. The bottom surface of the microchannel was fabricated by spin-coating PDMS at 1500 rpm onto a glass coverslip (Gold Seal) and baking for 6 hours at 70^{o}C. The two surfaces were bonded by exposure to UV/Ozone for 5 minutes.

Particles were fabricated by SFL[29] using three-inlet Y-junction channels in the laminar flow regime. Applied pressures were 1 psi in the central stream and 3 psi on either side. The central "label" stream consisted of a 60 vol% aqueous solution of poly(ethylene glycol) diacrylate (PEGDA, Sigma Aldrich, Mn = 700) with 5 vol% photoinitiator (Darocur 1173, Ciba) and 0.0005 wt% methacryloxyethyl thiocarbamoyl rhodamine B (PolyFluor 570, Polysciences) as the fluorescent dye. The "probe" streams on either side

consisted of an aqueous solution containing 20 vol% PEGDA, 40% poly(ethylene glycol) (Polysciences, Mn=200), 5 vol% photoinitiator and 30vol% of acrylate-modified single-strand DNA probe (IDT DNA) at 0.15 mM in TE buffer. Solid particles were produced by photopolymerization using UV light from an Hg lamp and a photomask incorporating the particle label at the microscope field stop. Fabrication was carried out with a flow time of 1 s, a pause after flow of 1 s, and an exposure time of 0.3 s. Particles were collected in a reservoir containing a mixture of 2/3 PEGDA and 1/3 TE buffer by volume and pipetted into microcentrifuge tubes. The particles were separated from solution by centrifugation at 5000 rpm for 1min. They were then rinsed three times by 0.05% TWEEN20 in PBS buffer (PBST), and stored in PBST at room temperature until use.

To carry out a genotyping experiment, standard assay particles were hybridized with Oregon Green-488 or Alex488-tagged target DNA overnight, while sandwich assay particles were first hybridized with a mixture of target DNA and then hybridized with fluorescently tagged secondary DNA probes. Particle samples were then mixed and injected gently into a microchannel (900um wide, 80um high) containing a PDMS dam (40um high) to form a monolayer assay.

In single-buffer experiments, alkaline dehybridization was carried out by flowing over the particles a pH 11.20 phosphate buffer at a rate of 10 ul/min. In a pH gradient

experiment, pH 7 deionized water was injected at a rate of 20 uL/min and allowed to mix completely with a time-varying stream of 0.02 M NaOH using a programmable syringe pump (PHD 22/2000, Harvard Apparatus, Holliston, MA, USA). The injection rate of NaOH and calculated [OH^-] and pH is given in Figure 4.6. Dehybridization was monitored by a Zeiss Axiovert 200M fluorescence microscope (Carl Zeiss, Thornwood, NY) with a home-build temperature control stage at 5x magnification and frame rates of 0.3-0.5 fps. The resulting images were analyzed using custom software in Matlab to locate the particles and determine the intensity in probe regions.

4.5. FIGURES AND TABLE

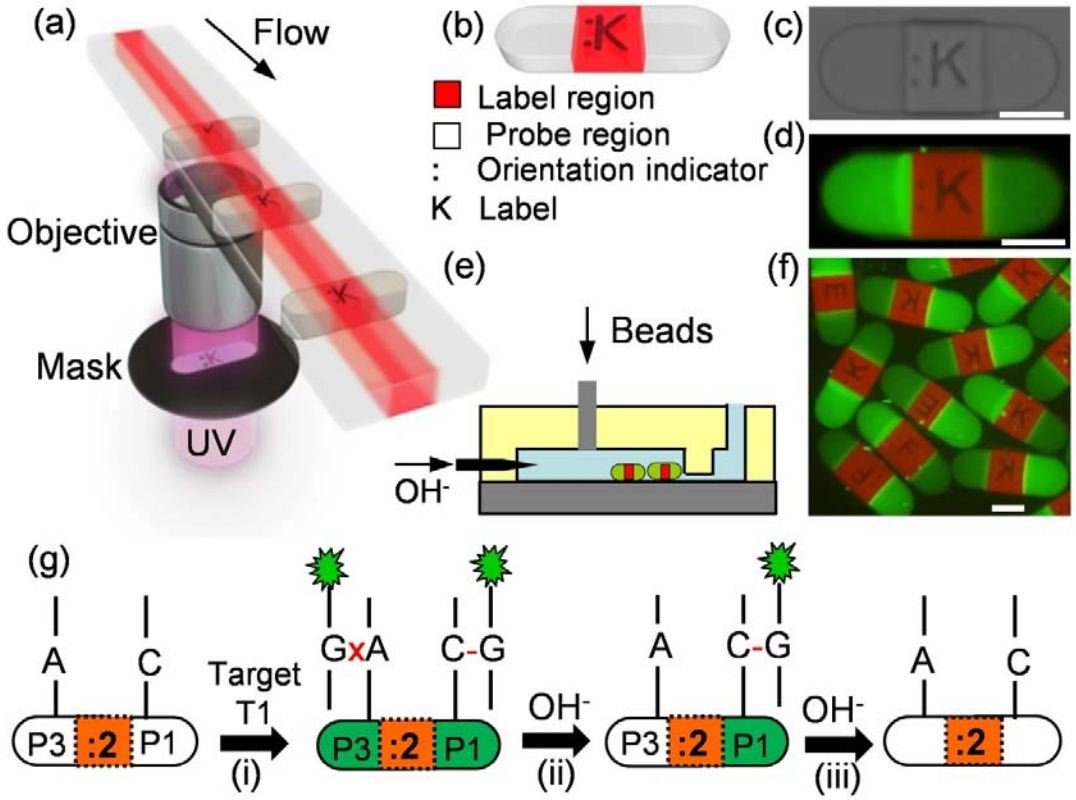

Figure 4.1: (a) Stop-flow lithography (SFL) is illustrated, in which we photocure co-flowing PEG-based monomer streams to produce multifunctional encoded hydrogel particles (b, c) which contain DNA probes on either side and a fluorescent dye in the center. Probe regions are visualized by fluoescence microscopy (d) after hybridization with Alex-488-labeled target DNA. Particles are immobilized by a dam in a microfluidic channel (e) to form a multiplexed particle assay (f). (g) illustrates a genotyping scheme using these particles in an alkaline dehybridization protocol.

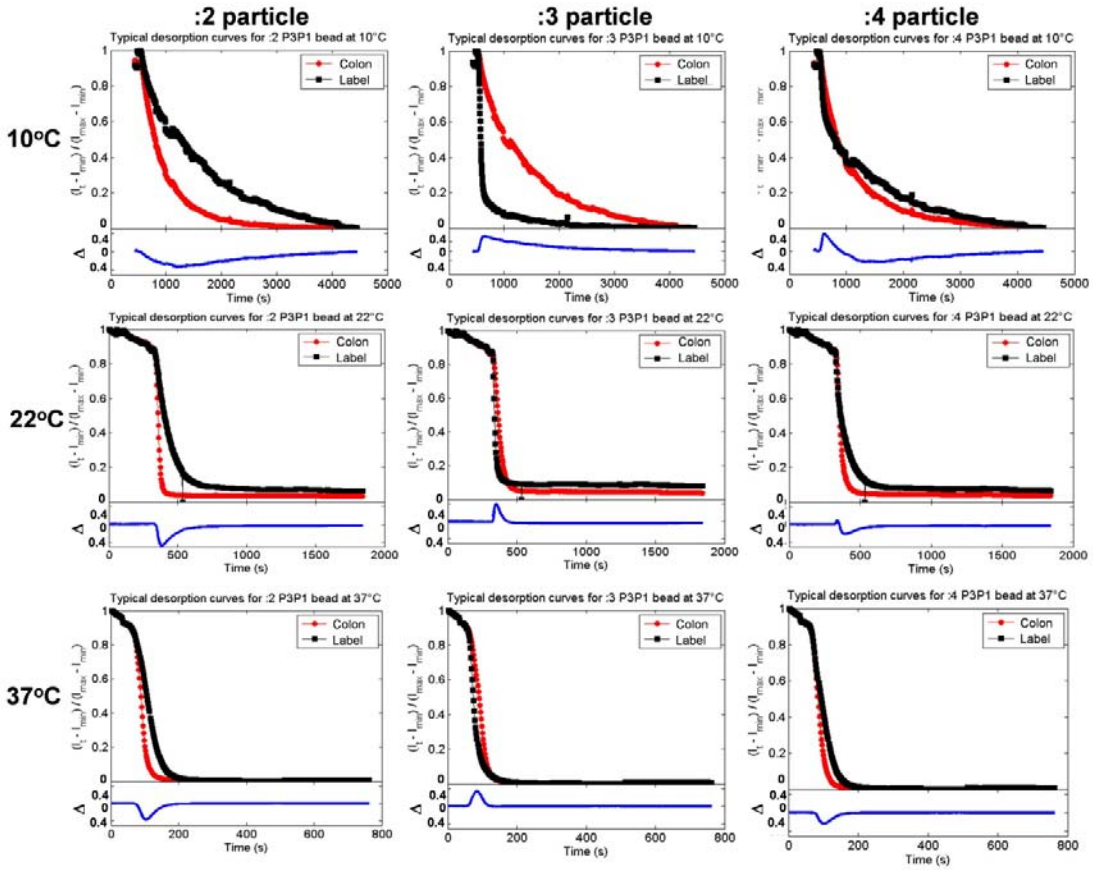

Figure 4.2: Retention ratio of each side and delta are plotted versus time for each type of P3/P1 particle, at increasing temperatures. Note that while the visible difference between the retention ratio curves becomes more difficult to discern at higher temperatures, the peak in delta remains a reliable indicator.

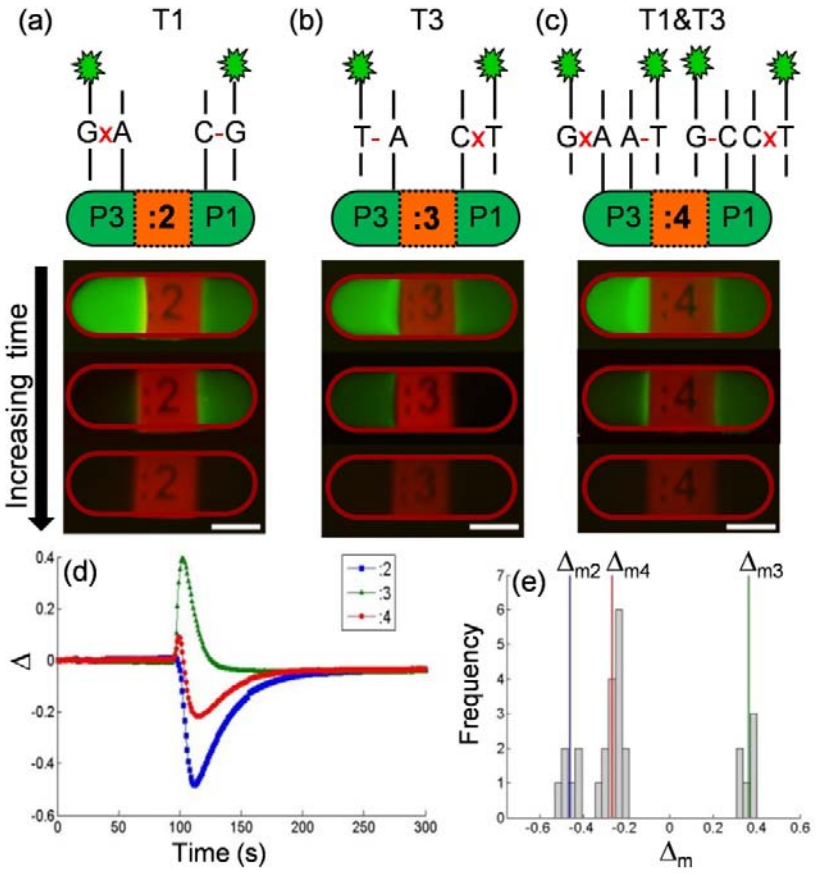

Figure 4.3: Three batches of particles containing allele-specific probes P1 and P3 (5'-CCTGGGAAAGT(C/A)CCCTCAACA-3', alternatives shown in parentheses) form PM or MM duplexes on either end of particle when they hybridize, respectively, with synthetic DNA targets T1 (a), T3 (b), and a 50/50 mixture of T1 andT3 (c), simulating three possible genotypes. A time-dependent difference in fluorescence retention ratio, Δ, across each particle is generated when subjected to an alkaline condition (pH 11.20 phosphate buffer). Δ curves for each particle type are shown in (d) and the peak values Δ_m are found for a mix of particles and plotted in a histogram (e). Δ_m fall into natural groups for each type of particle.

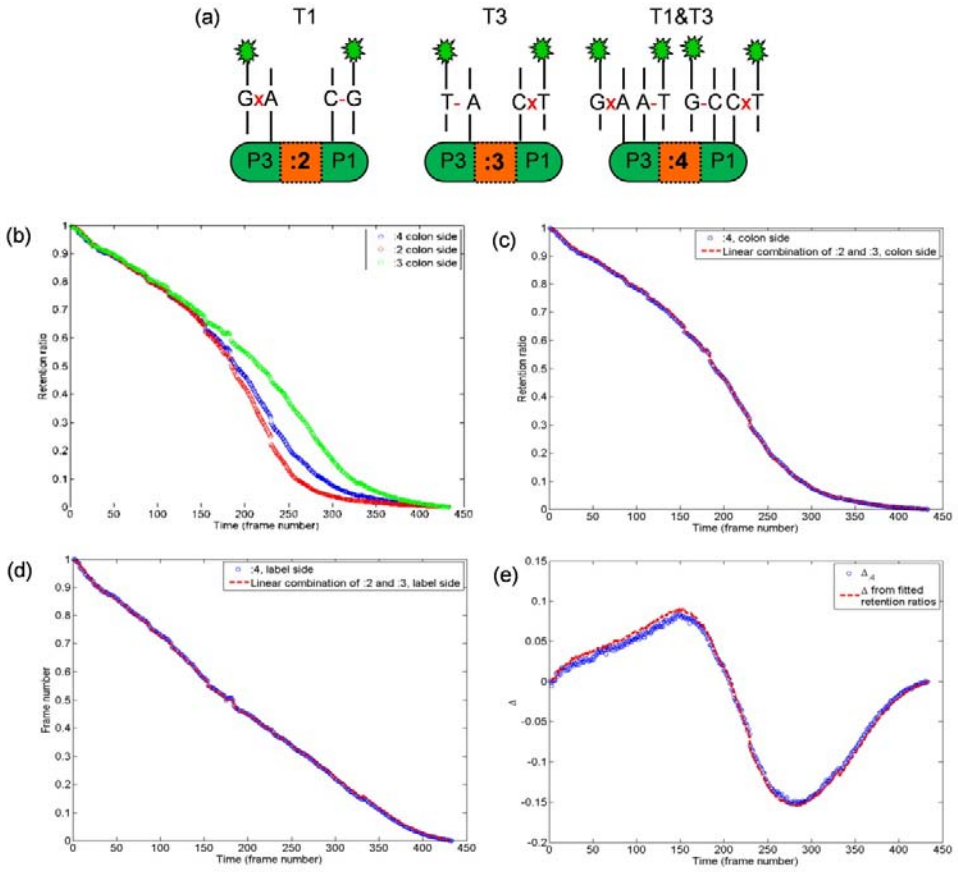

Figure 4.4: The hybridization schematic (a) shows the hybridized target strands in the two homozygous experiments, :2 and :3, and the heterozygous experiment, :4. Note that the PM and MM duplexes on either side of bead :4 are a combination of the duplexes on the corresponding sides of beads :2 and :3. In (b), we see the plotted retention ratios of :2, :3 and :4 on the colon side. The heterozygous colon-side signal (:4) can be expressed as a linear combination of the two homozygous colon-side signals (:2 and :3). As shown in Eq. 4.1, we calculate the linear combination using the relative fraction of R:2 as the fitting parameter (f1). Plotting this fitted colon-side data over the original colon-side :4 data (c) shows an extremely good fit (R2=0.9996). A similar procedure on

the label side (d; Eq. 4.2) also fits extremely well (R2=0.9998). Subtracting the fitted label side data from the fitted colon side data (Eq. 4.3) produces a delta curve (e) which closely reproduces (R2=0.9316) the Δ:4 from the experimental data.

$$R^{fit}_{:4,\,colon} = f_1 R_{:2,colon} + (1-f_1) R_{:3,colon} \qquad \text{Eq. 4.1}$$

$$R^{fit}_{:4,\,label} = f_2 R_{:2,\,label} + (1-f_2) R_{:3,\,label} \qquad \text{Eq. 4.2}$$

$$\Delta^{fit}_{:4,\,label} = R^{fit}_{:4,\,colon} - R^{fit}_{:4,\,label} \qquad \text{Eq. 4.3}$$

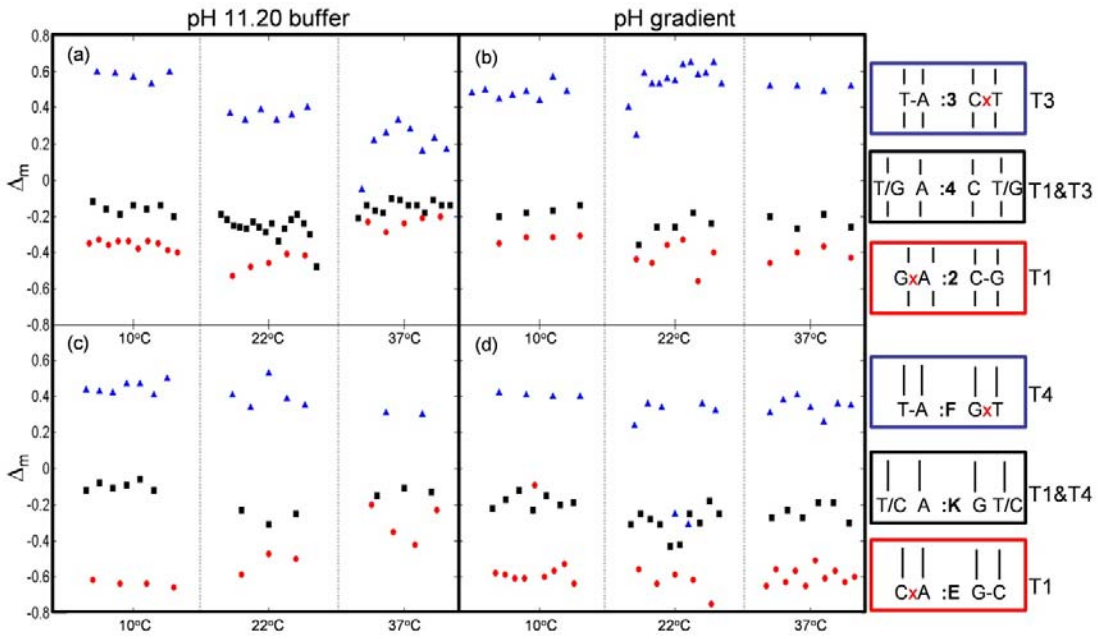

Figure 4.5: Genotyping is studied at different temperatures (10°C, 22°C, and 37°C) using a pH 11.20 buffer (a and c) or a pH gradient to drive dehybridization (b and d). (a) and (b) are for DNA with the variant base located in the center, while (c) and (d) show results when the variant base located at three base away from the end.

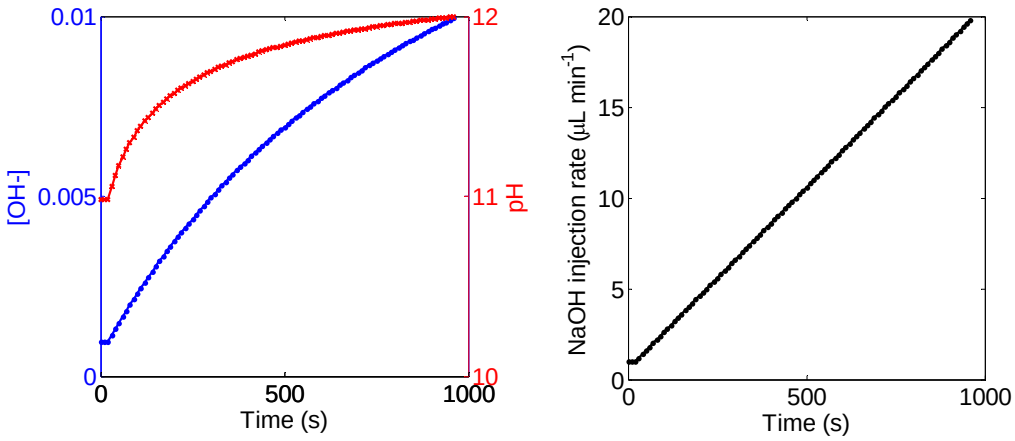

Figure 4.6: (a) shows the calculated values for the [OH^-] and pH during the first thousand seconds of a dynamic alkaline dehybridization experiment. (b) shows the injection rate of the NaOH solution; injection rate of water is constant at 20 uL/min.

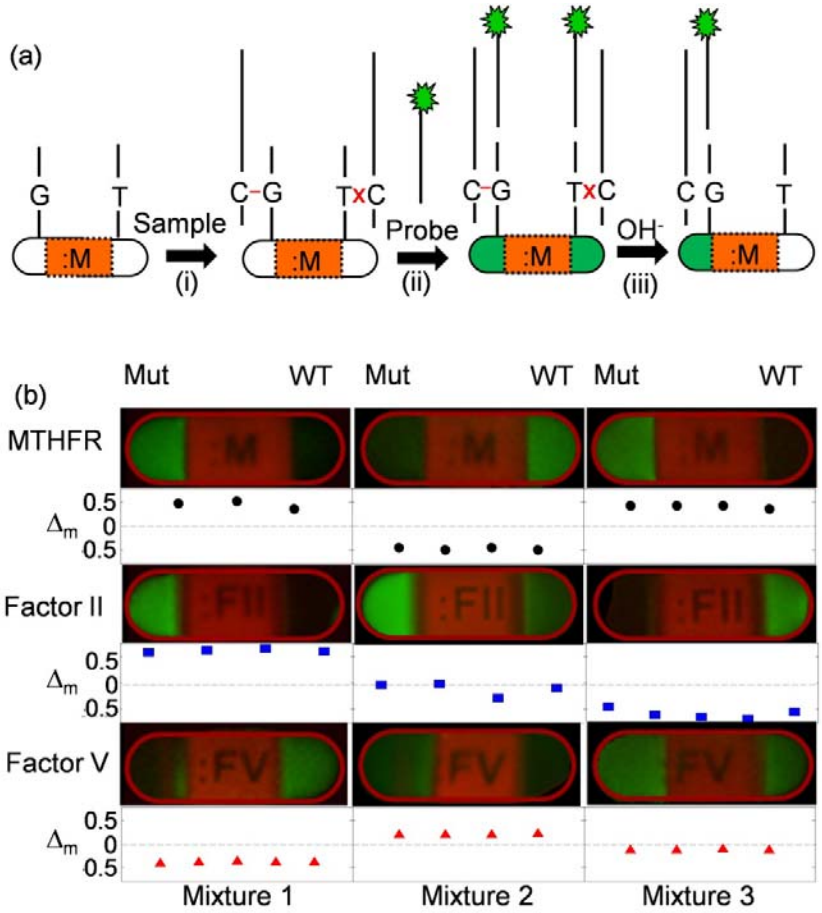

Figure 4.7: (a) Synthetic DNA targets of genes associated with thrombotic disorders (MTHFR, Factor II, and Factor V) and fluorescently labeled gene-specific secondary probes are sequentially hybridized to three types of particles containing allele-specific probes. Target mixture for test 1 contains MTHFR mutant, Factor II mutant and Factor V wild-type. Target mixture for test 2 contains MTHFR wild-type, 50/50 mixture of Factor II wild-type and mutant, and Factor V mutant. Target mixture for test 3 contains MTHFR mutant, Factor II wild-type, and 50/50 mixture of Factor V wild-type and mutant. (b) Representative images are shown for each test at the time of Δ_m. (Contrast in these images is enhanced.)

Table 4.1: DNA sequences

P1	5'-/Acryd/CCT GGG AAA GTC CCC TCA ACA /-3'
P3	5'-/Acryd/CCT GGG AAA GT**A** CCC TCA ACA / -3'
P4	5'-/Acryd/ CCT **A**GG AAA GTC CCC TCA ACA /-3'
T1	5'-Org488/TGT TGA GGG GAC TTT CCC AGG-3'
T3	5'-Org488/TGT TGA GGG **T**AC TTT CCC GGA-3'
T4	5'-Org488/TGT TGA GGG GAC TTT CC**T** GGA-3'
MTHFR 1st wild-type probe	5'-/Acryd/ ATG AAA TCG **G**CT CCC GCA GAC / -3'
MTHFR 1st Mutation probe	5'-/Acryd/ ATG AAA TCG ACT CCC GCA GAC / -3'
MTHFR wide-type target	5'-GAA GCA GGG AGC TTT GAG GCT GAC CTG AAG CAC TTG AAG GAG AAG GTG TCT GCG GGA G**C**C GAT TTC AT-3'
MTHFR mutation target	5'-GAA GCA GGG AGC TTT GAG GCT GAC CTG AAG CAC TTG AAG GAG AAG GTG TCT GCG GGA G**T**C GAT TTC AT-3'
MTHFR 2nd probe	5'-CAA GTG CTT CAG GTC AGC CTC AAA GCT CCC TGC TTC-Alex488-3
Factor II 1st wild-type probe	5'-/Acryd/ CTC AGC GAG CCT CAA TGC TCC / -3'
Factor II 1st Mutation probe	5'-/Acryd/ CTC AGC AAG CCT CAA TGC TCC / -3'
Factor II wide-type target	5'- TAG TAT TAC TGG CTC TTC CTG AGC CCA GAG AGC TGC CCA TGA ATA GCA CTG GGA GCA TTG AGG CT**C** GCT GAG -3'
Factor II mutation target	5'- TAG TAT TAC TGG CTC TTC CTG AGC CCA GAG AGC TGC CCA TGA ATA GCA CTG GGA GCA TTG AGG CT**T** GCT GAG -3'
Factor II 1st 2nd probe	5'- CTC TGG GCT CAG GAA GAG CCA GTA ATA CTA - Alex488-3'
Factor V 1st wild-type probe	5'-/Acryd/ TGG ACA GGC **G**AG GAA TAC AGG / -3'
Factor V 1st Mutation probe	5'-/Acryd/ TGG ACA GGC AAG GAA TAC AGG / -3'
Factor V wide-type target	5'- GAA GAA ATT CTC AGA ATT TCT GAA AGG TTA CTT CAA GGA CAA AAT ACC TGT ATT CCT CGC CTG TCC A -3'
Factor V mutation target	5'- GAA GAA ATT CTC AGA ATT TCT GAA AGG TTA CTT CAA GGA CAA AAT ACC TGT ATT CCT TGC CTG TCC A -3'
Factor V 2nd probe	5'- TAA CCT TTC AGA AAT TCT GAG AAT TTC TTC - Alex488-3

4.6. REFERENCES

(1) Syvanen, A.-C. "Accessing genetic variation: genotyping single nucleotide polymorphisms"; *Nat. Rev. Genet.* **2001**, *2*, 930.

(2) Syvanen, A. C. "Toward genome-wide SNP genotyping"; *Nat. Genet.* **2005**, *37*, S5.

(3) Holland, C. A.; Kiechle, F. L. "Point-of-care molecular diagnostic systems -- past, present and future"; *Curr. Opin. Microbiol.* **2005**, *8*, 504.

(4) Voisey, J.; Morris, C. P. "SNP Technologies for Drug Discovery: A Current Review"; *Curr. Drug Discovery Technol.* **2008**, *5*, 230.

(5) McCarthy, J. J.; Hilfiker, R. "The use of single-nucleotide polymorphism maps in pharmacogenomics"; *Nat. Biotechnol.* **2000**, *18*, 505.

(6) Schork, N. J.; Fallin, D.; Lanchbury, J. S. "Single nucleotide polymorphisms and the future of genetic epidemiology"; *Clin. Genet.* **2000**, *58*, 250.

(7) Sobrino, B.; Brión, M.; Carracedo, A. "SNPs in forensic genetics: a review on SNP typing methodologies"; *Forensic Sci. Int.* **2005**, *154*, 181.

(8) Budowle, B.; van, D. A. "Forensically relevant SNP classes"; *BioTechniques* **2008**, *44*, 603.

(9) Yager, P.; Edwards, T.; Fu, E.; Helton, K.; Nelson, K. *et al* "Microfluidic diagnostic technologies for global public health"; *Nature* **2006**, *442*, 412.

(10) Dobson, M. G.; Galvin, P.; Barton, D. E. "Emerging technologies for point-of-care genetic testing"; *Expert Rev. Mol. Diagn.* **2007**, *7*, 359.

(11) Ng, J. K.-K.; Liu, W.-T. "Miniaturized platforms for the detection of single-nucleotide polymorphisms"; *Anal. Bioanal. Chem.* **2006**, *386*, 427.

(12) Ogasawara, S.; Fujimoto, K. "SNP Genotyping by Using Photochemical Ligation"; *Angew. Chem., Int. Ed.* **2006**, *45*, 4512.

(13) Bowler, Frank R.; Diaz-Mochon, Juan J.; Swift, Michael D.; Bradley, M. "DNA Analysis by Dynamic Chemistry"; *Angew. Chem., Int. Ed.* **2010**, *49*, 1809.

(14) Taton, T. A.; Mirkin, C. A.; Letsinger, R. L. "Scanometric DNA Array Detection with Nanoparticle Probes"; *Science* **2000**, *289*, 1757.

(15) Sosnowski, R. G.; Tu, E.; Butler, W. F.; O'Connell, J. P.; Heller, M. J. "Rapid determination of single base mismatch mutations in DNA hybrids by direct electric field control"; *Proc. Natl. Acad. Sci. U.S.A.* **1997**, *94*, 1119.

(16) Bao, Y. P.; Huber, M.; Wei, T.-F.; Marla, S. S.; Storhoff, J. J. *et al* "SNP identification in unamplified human genomic DNA with gold nanoparticle probes"; *Nucl. Acids Res.* **2005**, *33*, e15.

(17) Castro, A.; Williams, J. G. K. "Single-Molecule Detection of Specific Nucleic Acid Sequences in Unamplified Genomic DNA"; *Anal. Chem.* **1997**, *69*, 3915.

(18) Kwok, P.-Y. "Methods for Genotyping single nucleotide polymorphisms"; *Annu. Rev. Genomics Hum. Genet.* **2001**, *2*, 235.

(19) Wang, D. G.; Fan, J.-B.; Siao, C.-J.; Berno, A.; Young, P. *et al* "Large-Scale Identification, Mapping, and Genotyping of Single-Nucleotide Polymorphisms in the Human Genome"; *Science* **1998**, *280*, 1077.

(20) Vainrub, A.; Pettitt, B. M. "Theoretical aspects of genomic variation screening using DNA microarrays"; *Biopolymers* **2004**, *73*, 614.

(21) Howell, W. M.; Job, M.; Gyllensten, U.; Brookes, A. J. "Dynamic allele-specific hybridization"; *Nat. Biotechnol.* **1999**, *17*, 87.

(22) Jobs, M.; Howell, W. M.; Stroemqvist, L.; Mayr, T.; Brookes, A. J. "DASH-2: Flexible, low-cost, and high-throughput SNP genotyping by dynamic allele-specific hybridization on membrane arrays"; *Genome Res.* **2003**, *13*, 916.

(23) Crews, N.; Wittwer, C. T.; Montgomery, J.; Pryor, R.; Gale, B. "Spatial DNA Melting Analysis for Genotyping and Variant Scanning"; *Anal. Chem.* **2009**, *81*, 2053.

(24) Frontali, C.; Ageno, M.; Dore, E. "Dynamics of the alkaline denaturation of DNA"; *Quaderni de La Ricerca Scientifica* **1968**, *No. 47*, 165.

(25) Ageno, M.; Dore, E.; Frontali, C. "The Alkaline denaturation of DNA"; *Biophys.*

J. **1969**, *9*, 1281.

(26) Crothers, D. M. "The kinetics of DNA denaturation"; *J. Mol. Biol.* **1964**, *9*, 712.

(27) Massie, H. R.; Zimm, B. H. "Kinetics of denaturation of DNA"; *Biopolymers* **1969**, *7*, 475.

(28) Zhang, H.; Mitrovski, S. M.; Nuzzo, R. G. "Microfluidic Device for the Discrimination of Single-Nucleotide Polymorphisms in DNA Oligomers Using Electrochemically Actuated Alkaline Dehybridization"; *Anal. Chem.* **2007**, *79*, 9014.

(29) Pregibon, D. C.; Toner, M.; Doyle, P. S. "Multifunctional Encoded Particles for High-Throughput Biomolecule Analysis"; *Science* **2007**, *315*, 1393.

(30) Heller, M. J. "DNA microarray technology: Devices, systems, and applications"; *Annu. Rev. Biomed. Eng.* **2002**, *4*, 129.

(31) Nolan, J. P.; Sklar, L. A. "Suspension array technology: evolution of the flat-array paradigm"; *Trends Biotechnol.* **2002**, *20*, 9.

(32) Jang, J.-H.; Dendukuri, D.; Hatton, T. A.; Thomas, E. L.; Doyle, P. S. "A route to three-dimensional structures in a microfluidic device: stop-flow interference lithography"; *Angew. Chem., Int. Ed.* **2007**, *46*, 9027.

(33) Panda, P.; Ali, S.; Lo, E.; Chung, B. G.; Hatton, T. A. *et al* "Stop-flow lithography to generate cell-laden microgel particles"; *Lab Chip* **2008**, *8*, 1056.

(34) Hwang, D. K.; Oakey, J.; Toner, M.; Arthur, J. A.; Anseth, K. S. *et al* "Stop-Flow Lithography for the Production of Shape-Evolving Degradable Microgel Particles"; *J. Am. Chem. Soc.* **2009**, *131*, 4499.

(35) Dendukuri, D.; Pregibon, D. C.; Collins, J.; Hatton, T. A.; Doyle, P. S. "Continuous-flow lithography for high-throughput microparticle synthesis"; *Nat. Mater.* **2006**, *5*, 365.

(36) Dendukuri, D.; Gu, S. S.; Pregibon, D. C.; Hatton, T. A.; Doyle, P. S. "Stop-flow lithography in a microfluidic device"; *Lab Chip* **2007**, *7*, 818.

(37) Shepherd, R. F.; Panda, P.; Bao, Z.; Sandhage, K. H.; Hatton, T. A. *et al*

"Stop-Flow Lithography of Colloidal, Glass, and Silicon Microcomponents"; *Adv. Mater.* **2008**, *20*, 1.

(38) Pregibon, D. C.; Doyle, P. S. "Optimization of Encoded Hydrogel Particles for Nucleic Acid Quantification"; *Anal. Chem.* **2009**, *81*, 4873.

(39) Witte, R. P.; Blake, A. J.; Palmer, C.; Kao, W. J. "Analysis of poly(ethylene glycol)-diacrylate macromer polymerization within a multicomponent semi-interpenetrating polymer network system"; *J. Biomed. Mater. Res., Part A* **2004**, *71A*, 508.

(40) Lefferts, J. A.; Jannetto, P.; Tsongalis, G. J. "Evaluation of the Nanosphere Verigene® System and the Verigene® F5/F2/MTHFR Nucleic Acid Tests"; *Exp. Mol. Pathol.* **2009**, *87*, 105.

Appendix A. Alkaline Dehybridization Using a Glass Slide Support

DNA immobilization and hybridization on a glass slide

The DNA immobilization was carried out on aldehyde-coated glass slides (5 ×10 mm) that were cut from a larger piece (Vantage Aldehyde Slides, CEL Associates, Pearland, TX) and rinsed with milli-Q water followed by drying in a stream of N_2.

The immobilization solution (24 μM probe ssDNA in pH 9 carbonate buffer) was heated by immersion in boiling water for 3 min and after it cooled down to room temperature, traces (~ 0.001%) of sodium dodecyl sulfate (SDS) surfactant were added to the solution to facilitate spreading onto the aldehyde-coated glass. Each slide was then used as a substrate onto which 5 μL of DNA immobilization solution was added. The glass slides were then placed in a dehumidifier and kept for at least 2 hours at room temperature to complete the Schiff base reaction. The DNA coated glass slide was then soaked in $NaBH_4$ solution (0.025 g $NaBH_4$ + 7 ml H_2O + 3 ml ethanol)[1] for 5 min in order to reduce the Schiff base and the remaining aldehyde group. In order to remove the non-specifically adsorbed DNA, the glass pieces were soaked in 2x SSPE/0.2 % SDS solution, which contained 2 mM EDTA, 7 mM SDS, 300 mM NaCl, and 20 mM NaH_2PO_4 the pH of which was adjusted to pH = 7.4 using 1 M NaOH,[2-3] for 5 min.

This procedure was followed by shaking in the same solution for 5 min and milli-Q water for 5 min after which the slide was soaked in boiling milli-Q water for 5 min. The final rinse was performed with milli-Q water after which the slide was dried in a stream of nitrogen.

The DNA hybridization was performed using a 2.5 μM complementary DNA solution which was prepared by diluting the stock DNA solution (described in Materials and Reagents section) with 2x SSPE/0.2 %SDS solution (pH = 7.4). The hybridization solution was heated by immersing in boiling water for 2 min before use. An 8 μL aliquot of hybridization solution was spread on the probe-coated glass slide after which it was kept in a humidity chamber (100 % RH) for 1 hr at 37 °C.[4] The slide was rinsed with water, and shaken in 2xSSPE/0.2%SDS solution twice for 5 min.

Device fabrication

Several methods were used to fabricate planar structures. Our best results came from a modification of a procedure taken from the literature.[1] In this method, a duplex coated glass slide was embedded in the device following a modification of the procedure described in the experimental section (i.e., Figure 3.1(a)). In brief, a duplex-coated glass slide and a WE array were placed into contact (duplex-side down) with a fully-cured PDMS flat (with a 5 mm distance from the center of the glass slide to the center of the WE array). Uncured PDMS prepolymer was poured over the setup and placed *in vacuo*

for 10 minutes. The prepolymer was then cured at 37 °C overnight. The entire "sandwich" was flipped over and the thin PDMS membrane was carefully peeled away to reveal the duplex-coated side of the glass slide and the WE. The latter assembly served as the bottom layer of the microfluidic device. A PDMS upper layer with microfluidic channels (width x separation x height = 0.2 mm x 0.2 mm x 0.05 mm) was treated with UV/ozone for 5 min and sealed conformally with the bottom layer. This protocol yields a modified glass surface active towards specific DNA capture/release albeit with an interfering (and generally high) non-specific background.

References

(1) Zammatteo, N.; Jeanmart, L.; Hamels, S.; Courtois, S.; Louette, P. *et al* "Comparison between Different Strategies of Covalent Attachment of DNA to Glass Surfaces to Build DNA Microarrays"; *Anal. Biochem.* **2000**, *280*, 143.

(2) Lin, Z.; Strother, T.; Cai, W.; Cao, X.; Smith, L. M. *et al* "DNA Attachment and Hybridization at the Silicon (100) Surface"; *Langmuir* **2002**, *18*, 788.

(3) Peelen, D.; Smith, L. M. "Immobilization of amine-modified oligonucleotides on aldehyde-terminated alkanethiol monolayers on gold"; *Langmuir* **2005**, *21*, 266.

(4) Dawson, E. D.; Reppert, A. E.; Rowlen, K. L.; Kuck, L. R. "Spotting optimization for oligo microarrays on aldehyde-glass"; *Anal. Biochem.* **2005**, *341*, 352.

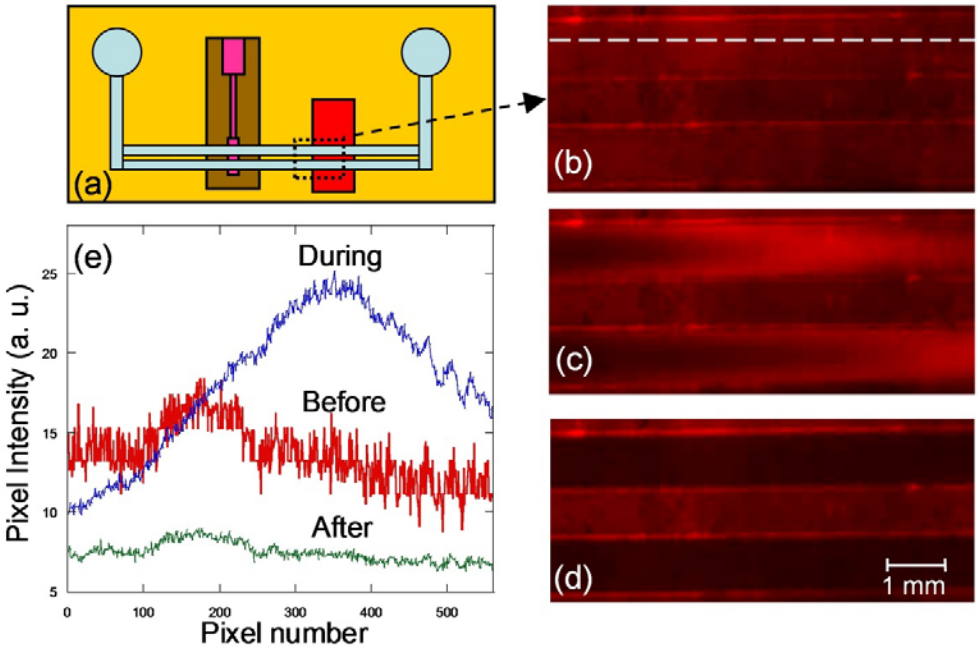

Figure A.1: (a) Schematic representation of the relative position of the Pt-WE and the ds-DNA coated glass slide. The distance between the center of the electrode and the slide is ~ 5 mm. (b) Fluorescence micrograph of the ds-DNA coated glass slide immediately prior to the beginning of the DNA dehybridization. (c)-(d) Fluorescence micrographs taken in the course of the DNA dehybridization. The image in (c) shows a laminar flow profile corresponding to the alkaline fluid flow from WE to CE.

Author's Biography

Huaibin Zhang was born in Yunnan, China on April 17, 1979. In the high school, he was selected as one of the three provincial representatives to compete in the National Chemistry Contest. After receiving the second-class honor in the contest, he was recruited by the Chemistry Department at the Nankai University. He joined Chemisoft Society there and participated in the production of two multi-media textbooks for general chemistry. In the summer of 2002 he entered the master program in chemistry at the University of Waterloo. Under the guidance of Professor Mónica Barra, Huaibin studied the mechanism of the thermal *cis*-to-*trans* isomerization of unsymmetrical 1,3-diaryltriazenes. After receiving a M. S. degree in 2004, Huaibin continued his chemistry studies by entering the doctoral program at the University of Illinois at Urbana-Champaign. He joined the research group of Professor Ralph G. Nuzzo and began exploring biological applications of microfluidic system. He discovered that alkaline dehybridization can be used to discriminate single nucleotide polymorphisms (SNP), and further developed a system to demonstrate the genotyping application of this technique. He also developed a membrane-based microfluidic contact printing technique to pattern biomolecules on soft materials. After receiving his Ph.D. in chemistry in 2010 Huaibin will be joining the laboratory of Professor David R. Walt at the Tufts University as a postdoctoral research fellow.